UNIVERSITY OF SOUTHERN CALIFORNIA
DEPARTMENT OF CIVIL ENGINEERING

PRELIMINARY EMPIRICAL MODELS FOR SCALING PSEUDO RELATIVE VELOCITY SPECTRA

by

Mihailo D. Trifunac and John G. Anderson

Report No. CE 78-04

A Report on the Research Conducted Under
a Contract from the U.S. Nuclear Regulatory Commission

Los Angeles, California

June, 1978

ABSTRACT

In this report, we present a method for direct scaling of Pseudo Relative Velocity Spectra (PSV) in terms of (i) earthquake magnitude, M, and epicentral distance, R, or (ii) Modified Mercalli Intensity (MMI) at a site. These models also depend directly on the geologic site conditions and are presented for horizontal and for vertical ground motions. This scaling is realized by means of "coefficient" functions which are determined through regression analysis of computed PSV spectra from recorded accelerograms. The resulting shapes and amplitudes of PSV spectra depend on all scaling parameters.

One of the principal advantages of the proposed method is that the ambiguities associated with the scaling of the fixed shape spectra by means of peak amplitudes of ground motion are now completely eliminated. The 91 direct regressions of 372 horizontal and 186 vertical spectra, at 91 periods, smoothed over all periods, lead to more complete and reliable sampling of the frequency-dependent characteristics of strong ground motion than the correlations of peak amplitudes alone.

INTRODUCTION

This is the fourth in a series of reports devoted to detailed characterization of strong earthquake ground motion. This series has been initiated with two reports which presented preliminary correlations of the duration of strong shaking in terms of (a) earthquake magnitude, M, epicentral distance, R, geological site conditions, s, and the component direction (Trifunac and Westermo, 1976a), and (b) in terms of Modified Mercalli Intensity (MMI) at the recording station, geologic site conditions, s, and component direction (Trifunac and Westermo, 1976b). The third report (Trifunac and Anderson, 1977) presents functions for scaling absolute acceleration spectra, SA, in terms of scaling parameters in (a) and (b) above. Together with the correlations of Fourier amplitude spectra with earthquake magnitude and epicentral distance (Trifunac, 1976a) and Modified Mercalli Intensity (Trifunac, 1978a) it showed that it is now becoming feasible to characterize all response spectrum amplitudes in terms of those simple scaling parameters which are often used in routine estimation of the effects of possible earthquake-induced shaking.

In this report, the methodology already applied to scaling of absolute acceleration, SA, will be used to develop analogous functionals for scaling of Pseudo Relative Velocity spectra, PSV. Detailed definitions of these spectra, their uses and other references on response spectrum approach can be found in the report by Hudson, et. al., 1972. For completeness in presentation, only the most general properties of these spectra are mentioned here briefly.

The functional called absolute acceleration spectrum, SA, represents the maxima of the absolute acceleration response of a single-degree-of-freedom viscously damped oscillator during transient excitation of its support by a single component of ground motion. It is plotted versus undamped natural frequency or period of the single-degree-of-freedom oscillator and usually for five fractions of critical damping ranging from 0.0 to 0.20. The Pseudo Relative Velocity spectrum, PSV, represents the maximum of relative displacement response multiplied by its natural circular frequency. PSV spectrum is often plotted on the Log-log scale because such presentation enables one to estimate from the same diagram not only the PSV amplitudes, but also the relative displacement spectra, SD, and approximately the absolute acceleration spectra, SA, for the same excitation.

As we noted in our previous report (Trifunac and Anderson, 1977) the availability of only very simple scaling parameters for scaling earthquake shaking like earthquake magnitude, M, and epicentral distance to the source, R, or the Modified Mercalli Intensity (or its equivalent) at the site, limits our ability to develop empirical scaling models which would be based on more direct and physical parameters describing the earthquake motions. Many recent studies have suggested that scaling of strong shaking, especially in the near-field, in terms of seismic moment, maximum dislocation and stress drop would be better than in terms of M and R, for example. However, the lack of enough of this data to permit statistical treatment in seismic risk studies suggests the use of M and R or MMI at the site and of s and v.

The data on PSV spectra have been extracted from Volume II tape (Trifunac and Lee, 1973) which contains all Fourier and response spectra for 381 uniformly processed strong-motion accelerograms (Hudson, et. al., 1972). Of these, 186 represent ground motion records in free field or in the basements of buildings and are suitable for this analysis. The distribution of these records among different magnitude and intensity levels, site conditions, distances and earthquakes which generated them have been summarized by Tables Ia and Ib in Trifunac and Anderson (1977).

The PSV spectra computed from hand-digitized accelerograms contain variable amounts of digitization and processing noise. The average amplitudes of this noise depend on frequency, fraction of critical damping and on the total duration of digitized accelerograms. The report by Trifunac (1978b) presents these noise spectra for all records used in this study and summarizes the procedures and assumptions employed to derive these estimates of PSV noise spectra. Here, it will be assumed that such approximate characterization of digitization noise is adequate for the purposes of this report and the average and average-plus one standard deviation of amplitudes of PSV spectra of noise will be used in an approximate way to reduce the contribution of noise to PSV spectral amplitudes used in regression analyses of this report.

EMPIRICAL MODELS FOR SCALING PSV SPECTRA

To scale empirically the PSV spectral amplitudes we employ two equations proposed by Trifunac (1976, 1977a) and by Trifunac and Anderson (1977), mutatis mutandis these equations become

$$\log_{10}[PSV(T)_{,p}] = M + \log_{10}A_o(R) - a(T)p - b(T)M - c(T) - d(T)s - e(T)v - f(T)M^2 - g(T)R \quad (1)$$

and

$$\log_{10}[PSV(T)_{,p}] = a(T)p + b(T)I_{MM} + c(T) + d(T)s + e(T)v \quad (2)$$

Here M is earthquake magnitude (for most data points, M is M_L, Richter, 1958), $\log_{10}A_o(R)$ (Table I) represents an empirical function (Richter, 1958) which determines the amplitude attenuation with distance, R (in km), from the reported earthquake epicenter. The "confidence level" p, between 0.1 and 0.9 approximates the probability that $PSV(T)_{,p}$ will not be exceeded. The term s represents geologic site conditions (s=0 for alluvium sites, s=2 for basement rock sites and s=1 for intermediate site conditions). Table 4 of Trifunac and Brady (1975) illustrates the rough nature of this classification which, in essence, represents a binary division of all recording sites into alluvium (s=0) and basement rock (s=2). s=1 has been used only for those cases where the geometry of a geologic setting is complicated or the knowledge about the site is incomplete to allow s=0 or s=2 classification. Clearly such classification is very rough since it neglects all geological characteristics of alluvium as well as the three-dimensional variations of the velocity and rigidity of materials through which earthquake waves propagate. A number of preliminary studies by the authors have shown, for example, that the

TABLE I

$\log_{10}A_o(R)$ Versus Epicentral Distance R*

R(km)	$-\log_{10}A_o(R)$	R (km)	$-\log_{10}A_o(R)$	R (km)	$-\log_{10}A_o(R)$
0	1.400	140	3.230	370	4.336
5	1.500	150	3.279	380	4.376
10	1.605	160	3.328	390	4.414
15	1.716	170	3.378	400	4.451
20	1.833	180	3.429	410	4.485
25	1.955	190	3.480	420	4.518
30	2.078	200	3.530	430	4.549
35	2.199	210	3.581	440	4.579
40	2.314	220	3.631	450	4.607
45	2.421	230	3.680	460	4.634
50	2.517	240	3.729	470	4.660
55	2.603	250	3.779	480	4.685
60	2.679	260	3.828	490	4.709
65	2.746	270	3.877	500	4.732
70	2.805	280	3.926	510	4.755
80	2.920	290	3.975	520	4.776
85	2.958	300	4.024	530	4.797
90	2.989	310	4.072	540	4.817
95	3.020	320	4.119	550	4.835
100	3.044	330	4.164	560	4.853
110	3.089	340	4.209	570	4.869
120	3.135	350	4.253	580	4.885
130	3.182	360	4.295	590	4.900

* Only the first two digits may be assumed to be significant.

overall depth of alluvium and sedimentary deposits beneath the site can be used to replace s and to refine equations (1) and (2). Such correlations will be presented in future reports.

From a practical viewpoint, however, it must be remembered that the details of the available knowledge on the geologic characteristics of a site will vary and that in some cases, information on the depth of alluvium may not be available. Thus, it appears useful to have available empirical correlations which are based on s=0, 1 and 2 classification as well. In equations (1) and (2), v designates vertical or horizontal components of PSV spectra (v=0 for horizontal and v=1 for vertical).

The amplitudes of functions a(T), b(T), ..., g(T) have been determined at selected periods, T, by regression analyses of the data equal to $\log_{10}[PSV,_p] - M - \log_{10}A_o(R)$ for equation (1) and $\log_{10}[PSV(T),_p]$ for equation (2). At each period, T, the details of regression analysis are then identical to those described by Trifunac (1976a). Other properties of equations (1) and (2) and the significance of $\log_{10}A_o(R)$ and g(T) have been discussed by Trifunac and Anderson (1977). Since all their procedures apply equally to PSV spectral amplitudes in this report, we will assume that equations (1) and (2) should represent suitable correlation functions for scaling PSV spectra as well.

a. Correlations in Terms of M, R, p, s, and v

Figure 1 and Table II contain the results of regression analysis in which equation (1) was fitted to computed PSV spectrum amplitudes. Following identical procedures as in Trifunac and Anderson (1977), functions a(T), b(T), ..., f(T) and g(T) were computed by a least

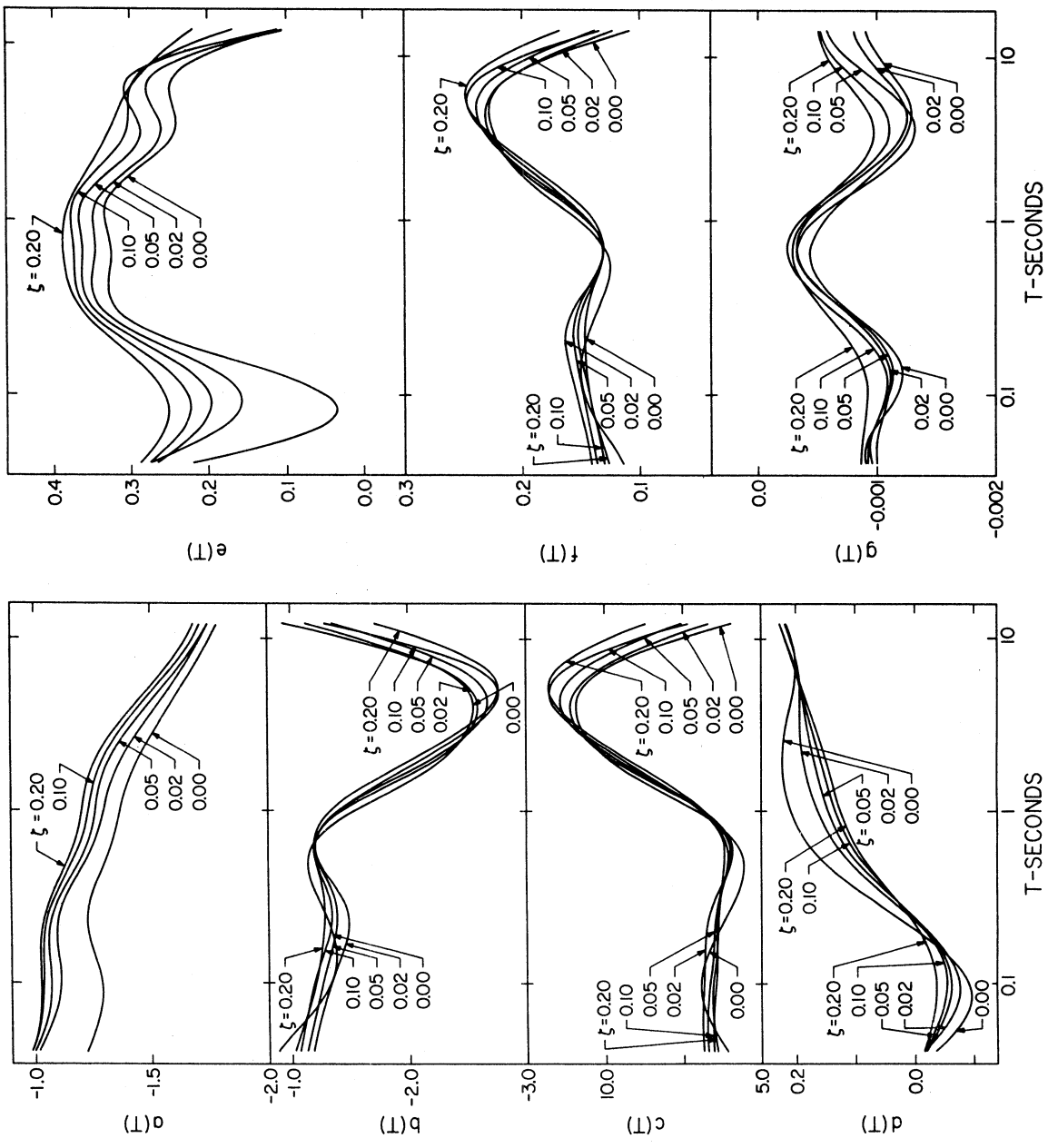

Figure 1

TABLE II

Regression Parameters for Equation (1) and $\alpha(T)$, $\beta(T)$ and $N(T)^*$ at Eleven Selected Periods

$\log_{10}T$(sec)	-1.398	-1.171	-0.943	-0.716	-0.489	-0.261	-0.034	0.193	0.420	0.648	0.875
ζ = 0.0											
a(T)	-1.218	-1.277	-1.275	-1.228	-1.241	-1.312	-1.361	-1.409	-1.498	-1.603	-1.705
b(T)	-0.883	-1.172	-1.364	-1.350	-1.217	-1.148	-1.461	-2.065	-2.468	-2.544	-2.083
c(T)	6.149	6.802	6.915	6.423	5.814	5.636	6.802	9.005	10.572	10.891	9.434
d(T)	-0.036	-0.090	-0.083	-0.013	0.082	0.162	0.205	0.221	0.221	0.207	0.202
e(T)	0.222	0.052	0.079	0.232	0.324	0.328	0.333	0.319	0.256	0.246	0.231
10f(T)	1.144	1.358	1.502	1.477	1.347	1.257	1.458	1.891	2.185	2.276	1.969
1000g(T)	-0.900	-0.998	-1.200	-1.097	-0.718	-0.451	-0.527	-0.839	-1.174	-1.279	-1.085
α(T)	0.765	0.815	0.897	1.057	1.258	1.500	1.707	2.032	2.665	3.909	4.018
β(T)	1.340	1.202	1.046	0.844	0.618	0.311	0.036	-0.413	-1.237	-2.599	-2.635
N(T)	162	96	57	33	20	11	7	4	2	1	1
ζ = 0.02											
a(T)	-1.013	-1.084	-1.108	-1.092	-1.132	-1.227	-1.289	-1.336	-1.430	-1.552	-1.664
b(T)	-1.186	-1.266	-1.373	-1.482	-1.419	-1.218	-1.370	-1.967	-2.475	-2.578	-2.115
c(T)	6.886	6.911	6.843	6.798	6.456	5.950	6.658	8.795	10.647	11.075	9.642
d(T)	-0.017	-0.067	-0.072	-0.025	0.049	0.117	0.159	0.181	0.193	0.194	0.201
e(T)	0.275	0.179	0.171	0.263	0.343	0.349	0.349	0.330	0.269	0.273	0.255
10f(T)	1.422	1.484	1.570	1.641	1.556	1.337	1.399	1.828	2.205	2.302	1.980
1000g(T)	-0.996	-1.030	-1.106	-1.004	-0.676	-0.367	-0.379	-0.737	-1.141	-1.234	-0.991
α(T)	0.782	0.838	0.915	1.064	1.267	1.537	1.756	2.066	2.658	3.846	3.930
β(T)	1.335	1.200	1.047	0.849	0.617	0.287	-0.002	-0.445	-1.243	-2.569	-2.585
N(T)	162	96	57	33	20	11	7	4	2	1	1
ζ = 0.05											
a(T)	-0.995	-1.056	-1.066	-1.058	-1.107	-1.202	-1.256	-1.288	-1.377	-1.513	-1.650
b(T)	-1.129	-1.212	-1.292	-1.375	-1.361	-1.218	-1.351	-1.902	-2.466	-2.680	-2.280
c(T)	6.731	6.761	6.624	6.534	6.348	6.021	6.664	8.629	10.644	11.436	10.241
d(T)	-0.020	-0.053	-0.060	-0.026	0.039	0.105	0.143	0.161	0.177	0.190	0.206
e(T)	0.267	0.208	0.208	0.282	0.353	0.364	0.368	0.350	0.294	0.301	0.281
10f(T)	1.371	1.439	1.510	1.567	1.521	1.347	1.391	1.789	2.210	2.387	2.102
1000g(T)	-0.954	-0.986	-1.119	-1.042	-0.684	-0.353	-0.426	-0.866	-1.266	-1.241	-0.852
α(T)	0.792	0.853	0.931	1.078	1.279	1.548	1.769	2.082	2.681	3.868	3.901
β(T)	1.327	1.194	1.042	0.842	0.610	0.284	-0.007	-0.455	-1.260	-2.585	-2.579
N(T)	162	96	57	33	20	11	7	4	2	1	1

TABLE II (Continued)

$\zeta = 0.10$

a(T)	-0.982	-1.029	-1.035	-1.038	-1.087	-1.172	-1.226	-1.261	-1.345	-1.480	-1.621
b(T)	-1.068	-1.137	-1.220	-1.325	-1.319	-1.205	-1.354	-1.848	-2.410	-2.768	-2.416
c(T)	6.562	6.550	6.449	6.457	6.315	6.078	6.767	8.530	10.511	11.757	10.705
d(T)	-0.016	-0.046	-0.054	-0.022	0.037	0.094	0.130	0.149	0.169	0.187	0.208
e(T)	0.277	0.230	0.236	0.301	0.362	0.375	0.378	0.363	0.316	0.304	0.278
10f(T)	1.309	1.374	1.451	1.526	1.488	1.337	1.394	1.750	2.173	2.460	2.209
1000g(T)	-0.923	-0.980	-1.080	-0.946	-0.588	-0.280	-0.313	-0.691	-1.056	-1.042	-0.725
α(T)	0.783	0.856	0.951	1.104	1.290	1.539	1.758	2.082	2.691	3.888	3.930
β(T)	1.337	1.192	1.031	0.829	0.605	0.287	-0.004	-0.460	-1.266	-2.587	-2.582
N(T)	162	96	57	33	20	11	7	4	2	1	1

$\zeta = 0.20$

a(T)	-0.983	-1.021	-1.023	-1.027	-1.072	-1.148	-1.196	-1.230	-1.316	-1.455	-1.597
b(T)	-1.023	-1.143	-1.227	-1.274	-1.277	-1.202	-1.297	-1.755	-2.344	-2.744	-2.553
c(T)	6.447	6.595	6.534	6.416	6.327	6.196	6.682	8.304	10.343	11.714	11.170
d(T)	-0.016	-0.033	-0.035	-0.011	0.037	0.088	0.122	0.141	0.160	0.184	0.207
e(T)	0.289	0.255	0.264	0.318	0.370	0.387	0.388	0.370	0.338	0.314	0.277
10f(T)	1.270	1.374	1.448	1.475	1.446	1.334	1.357	1.686	2.132	2.453	2.328
1000g(T)	-0.864	-0.894	-0.911	-0.783	-0.521	-0.370	-0.355	-0.669	-0.945	-0.902	-0.646
α(T)	0.793	0.870	0.970	1.119	1.291	1.538	1.761	2.101	2.741	3.979	4.036
β(T)	1.327	1.186	1.025	0.823	0.603	0.287	-0.007	-0.470	-1.288	-2.619	-2.605
N(T)	162	96	57	33	20	11	7	4	2	1	1

* See section entitled "Distribution of Spectral Amplitudes" for definition of α(T), β(T) and N(T).

squares fit at 91 periods and for ζ = 0.0, 0.02, 0.05, 0.10 and 0.20. These estimates displayed random fluctuations similar to those shown in Figure 2 of Trifunac (1976). The smoothed version of a(T), b(T), ..., g(T) shown in Figure 1 results from low-pass filtering of least squares fitted data with an Ormsby filter along $\log_{10}T$ axis.

It is seen that equation (1) represents a parabola in M for fixed values of T, s, p, v and R. Following the discussion of Trifunac and Anderson (1977) and for the reasons which apply to PSV amplitudes it is seen that equation (1) can be changed to become

$$\log_{10}A_o(R) - \log_{10}[PSV(T),_p]$$

$$= \begin{cases} -M_{max} + ap + bM_{max} + c + ds + ev + fM_{max}^2 + gR & M \geq M_{max} \\ -M + ap + bM + c + ds + ev + fM^2 + gR & M_{min} \leq M \leq M_{max} \\ -M + ap + bM_{min} + c + ds + ev + fM_{min}^2 + gR & M \leq M_{min} \end{cases}$$

where $M_{min} = b/2f$ and $M_{max} = (1-b)/2f$. Figure 2 presents M_{max} for different ζ and plotted versus T. Table III present M_{min} and M_{max} for ζ = 0.0, 0.02, 0.05, 0.10 and 0.20 and for eleven selected periods. It is seen that the magnitudes in this table are similar to the values in Table VI of Trifunac and Anderson (1977) and that M_{min} is in the range from about 4 to about 5.5 while M_{max} is generally between 7.5 and 8.5.

Since most earthquakes which contributed to the data used in this study fall in the range between M_{min} and M_{max}, strictly speaking, equation (1) could be considered valid only in that interval. The physical nature of simple theoretical models of earthquake

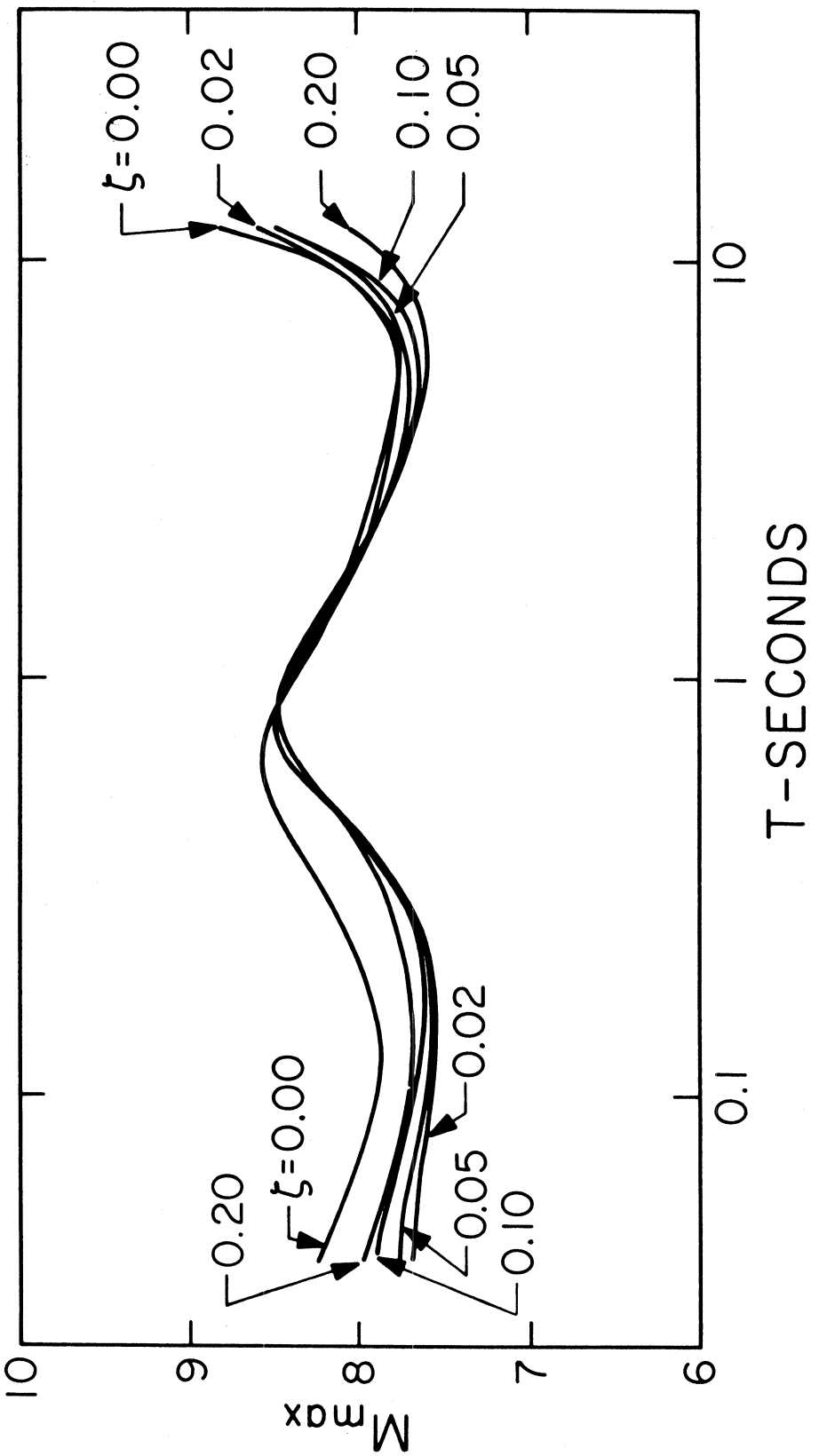
M_{max}
10
9
8
7
6
0.1
1
10
T-SECONDS
ζ=0.00
0.02
0.20
0.10
0.05
0.20
ζ=0.00
0.02
0.05
0.10

FIGURE 2

TABLE III

M_{min} and M_{max} Estimated from the Regression Based on Equation (1)

Period T		$\zeta = 0.0$		$\zeta = 0.02$		$\zeta = 0.05$		$\zeta = 0.10$		$\zeta = 0.20$	
$\log_{10}T$	(sec)	M^{*}_{min}	M^{**}_{max}	M_{min}	M_{max}	M_{min}	M_{max}	M_{min}	M_{max}	M_{min}	M_{max}
-1.398	0.04	3.86	8.23	4.17	7.69	4.12	7.76	4.08	7.90	4.03	7.96
-1.171	0.07	4.32	8.00	4.27	7.63	4.21	7.69	4.14	7.78	4.16	7.80
-0.943	0.11	4.54	7.87	4.37	7.56	4.28	7.59	4.20	7.65	4.24	7.69
-0.716	0.19	4.57	7.96	4.52	7.56	4.39	7.58	4.34	7.62	4.32	7.71
-0.489	0.32	4.52	8.23	4.56	7.77	4.47	7.76	4.43	7.79	4.42	7.87
-0.261	0.55	4.57	8.54	4.55	8.29	4.52	8.23	4.51	8.25	4.51	8.25
-0.034	0.92	5.01	8.44	4.90	8.47	4.86	8.45	4.86	8.44	4.78	8.46
0.193	1.56	5.46	8.10	5.38	8.12	5.32	8.11	5.28	8.14	5.20	8.17
0.420	2.63	5.65	7.94	5.61	7.88	5.58	7.84	5.55	7.85	5.50	7.84
0.648	4.45	5.59	7.79	5.60	7.77	5.61	7.71	5.63	7.66	5.59	7.63
0.875	7.50	5.29	7.83	5.34	7.87	5.42	7.80	5.47	7.73	5.48	7.63

* $M_{min} = \frac{-b(T)}{2f(T)}$

** $M_{max} = \frac{1-b(T)}{2f(T)}$

source then suggests approximate extension of (1) outside the interval between M_{min} and M_{max} as shown above. As we noted in our previous work, the parabolic dependence of amplitudes on M represents only a convenient and simple approximation to as yet unknown detailed dependence of these amplitudes on M.

The function a(T) in Figure 1 decreases from about -1 at T = 0.04 sec to approximately -1.75 near T = 10 sec. Very similar in shape and amplitudes to a(T) for scaling SA spectra (Trifunac and Anderson, 1977), this function shows that the distribution of spectral amplitudes about the mean level broadens in going from short to long periods. The ratio of spectral amplitudes which represent approximately the top and bottom boundaries of 8C confidence intervals then increase from about 6 for T = 0.04 sec to over 25 for T = 10 sec.

Functions b, c, d, e, f, and g in Figure 1 are similar to those we computed for scaling of SA spectra. Functions b(T), c(T), and f(T) reflect the differences in the units (in/sec and g's) which have been used for scaling of PSV amplitudes in this report and in the report for scaling of SA amplitudes and the fact that $SA \approx \frac{2\pi}{T} PSV$.

Figures 3 through 12 present examples of horizontal and vertical PSV spectral amplitudes for ζ = 0.00, 0.02, 0.05, 0.10 and 0.20, for p = 0.5 in equation (1) and for R = 0. To facilitate comparisons with the correlations based on equation (2) which will be discussed later in this report, we chose to plot spectra for R = 0. However, equation (1) can be considered to describe PSV amplitudes empirically only in the range of epicentral distances, R, for which the data is

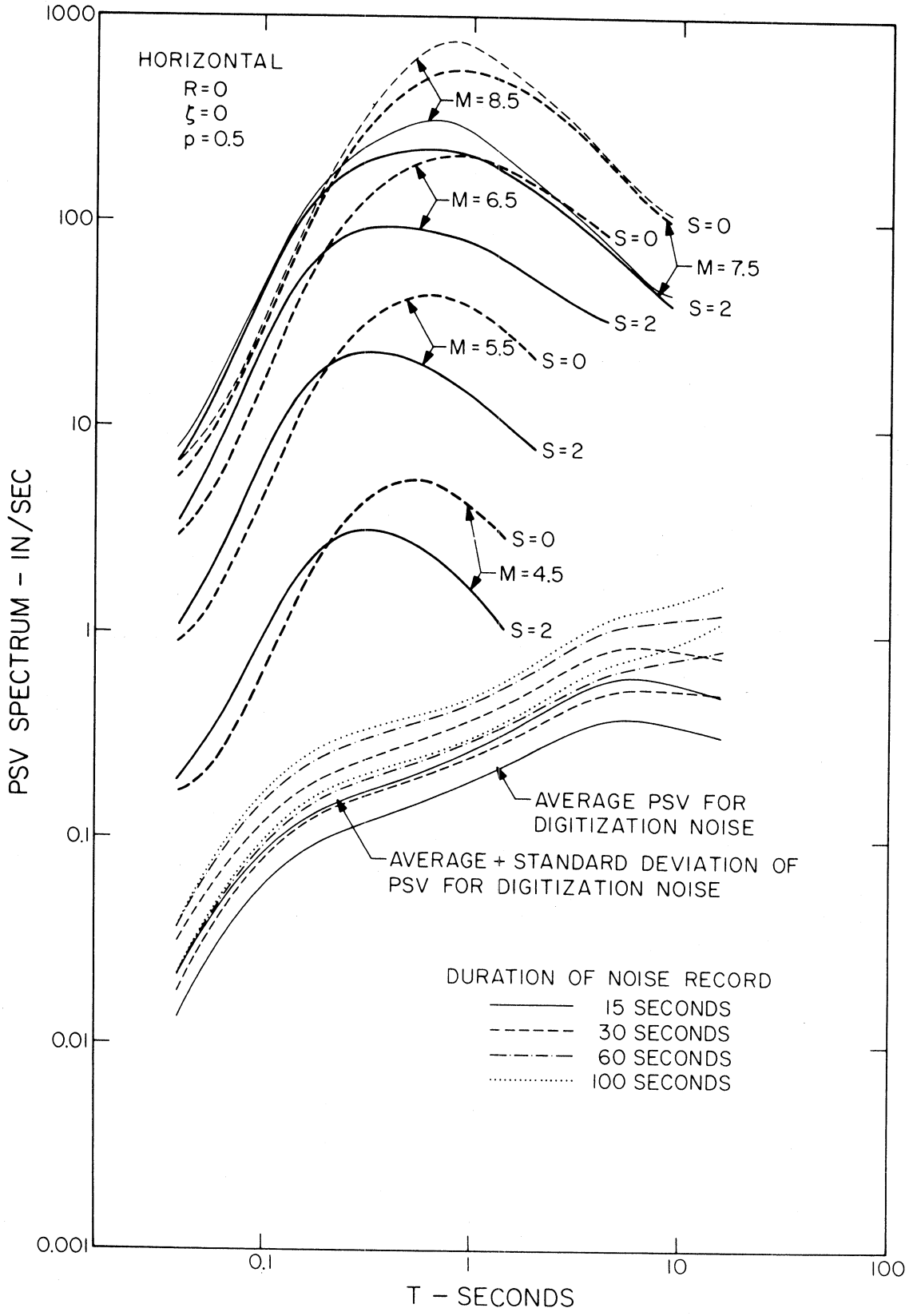
HORIZONTAL
R=0
ζ=0
p=0.5
M=8.5
M=6.5
M=7.5
M=5.5
M=4.5
S=0
S=2
AVERAGE PSV FOR DIGITIZATION NOISE
AVERAGE + STANDARD DEVIATION OF PSV FOR DIGITIZATION NOISE
DURATION OF NOISE RECORD
15 SECONDS
30 SECONDS
60 SECONDS
100 SECONDS
PSV SPECTRUM - IN/SEC
T - SECONDS
1000
100
10
1
0.1
0.01
0.001
0.1
1
10
100

FIGURE 3

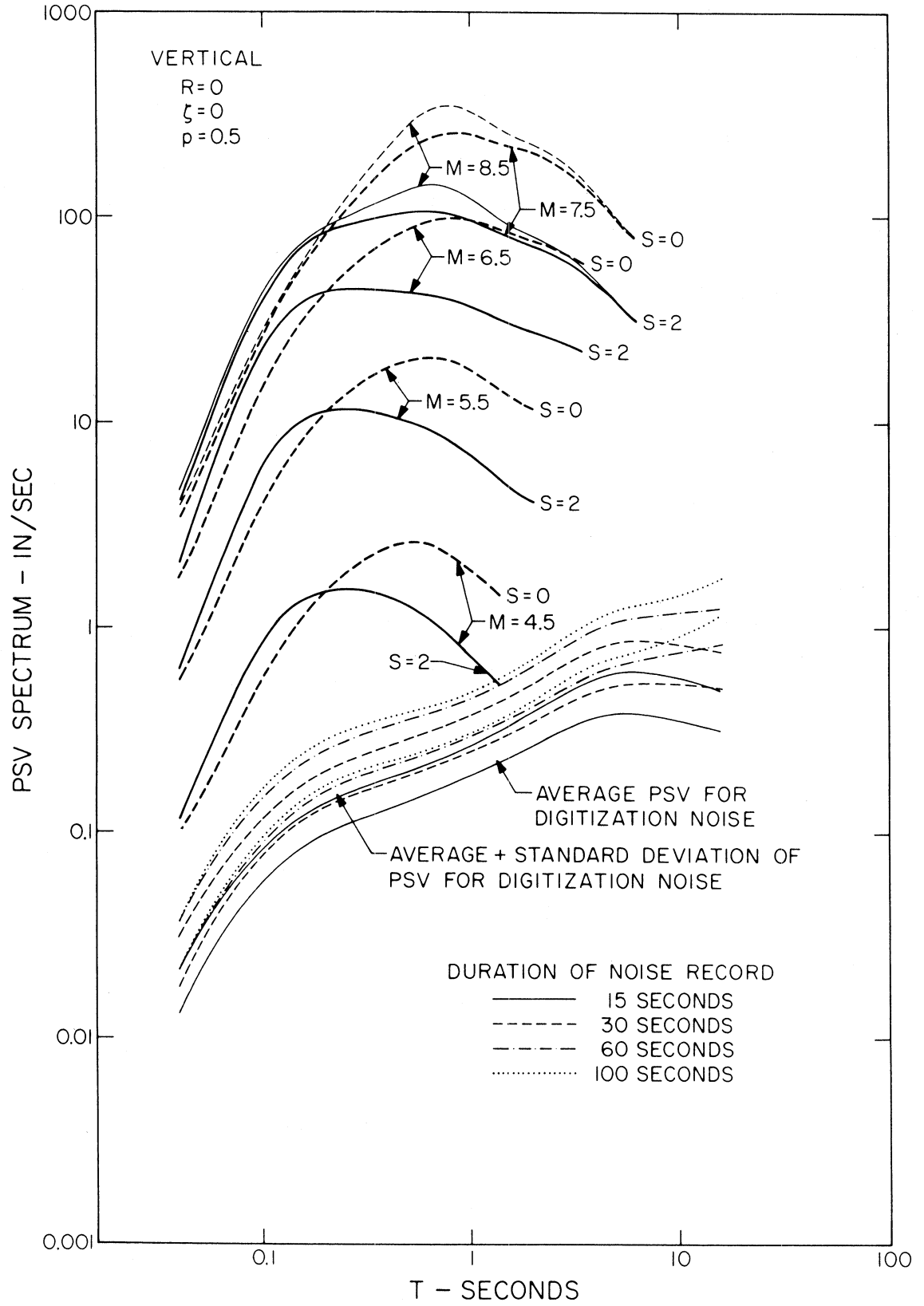
VERTICAL
R=0
ζ=0
p=0.5
M=8.5
M=7.5
S=0
M=6.5
S=0
S=2
S=2
M=5.5
S=0
S=2
S=0
M=4.5
S=2
AVERAGE PSV FOR DIGITIZATION NOISE
AVERAGE + STANDARD DEVIATION OF PSV FOR DIGITIZATION NOISE
DURATION OF NOISE RECORD
15 SECONDS
30 SECONDS
60 SECONDS
100 SECONDS
PSV SPECTRUM - IN/SEC
T - SECONDS
1000
100
10
1
0.1
0.01
0.001
0.1
1
10
100

FIGURE 4

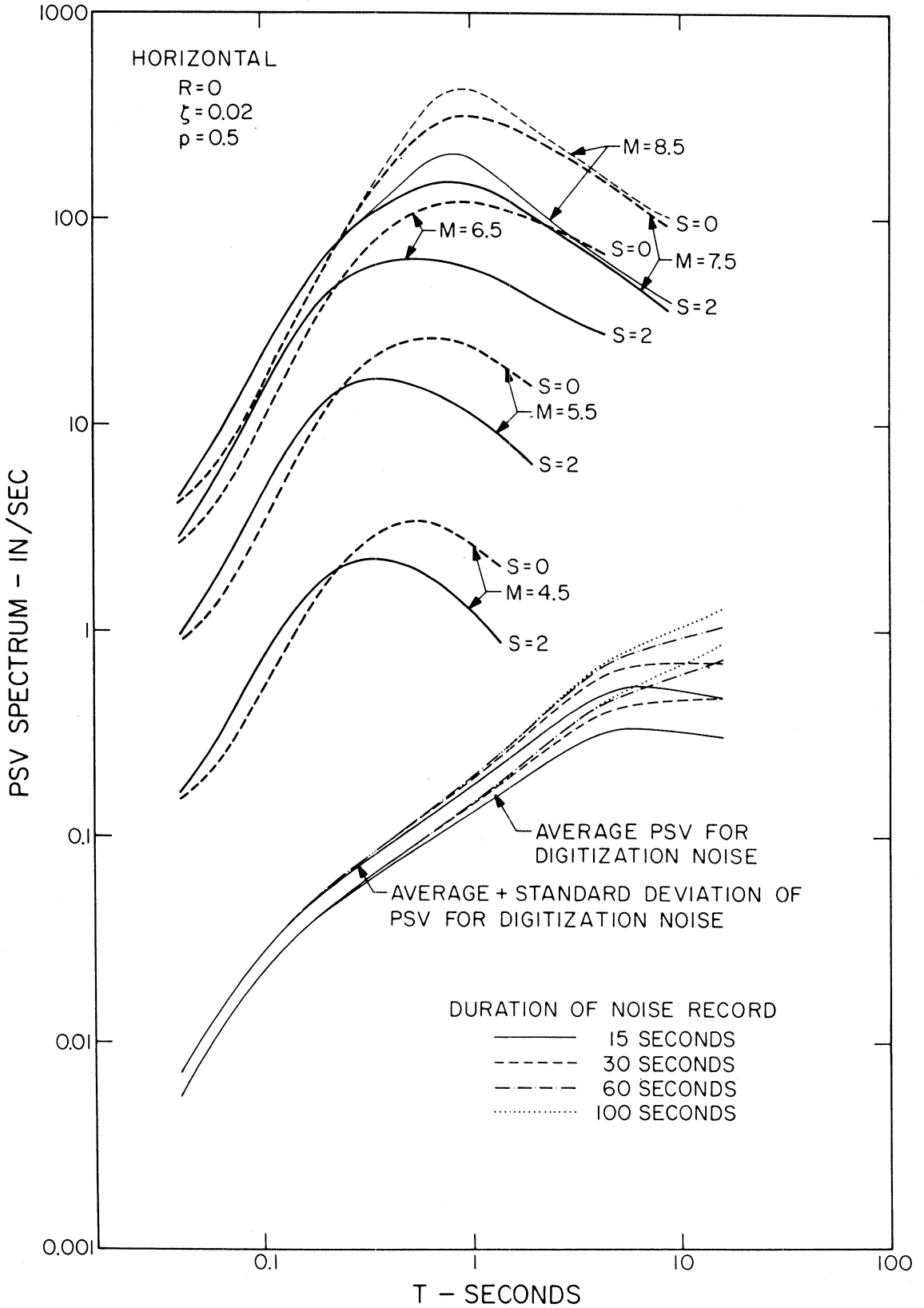
HORIZONTAL
R=0
ζ=0.02
p=0.5
M=8.5
S=0
S=0
M=7.5
S=2
M=6.5
S=2
S=0
M=5.5
S=2
S=0
M=4.5
S=2
AVERAGE PSV FOR DIGITIZATION NOISE
AVERAGE + STANDARD DEVIATION OF PSV FOR DIGITIZATION NOISE
DURATION OF NOISE RECORD
15 SECONDS
30 SECONDS
60 SECONDS
100 SECONDS
PSV SPECTRUM - IN/SEC
1000
100
10
1
0.1
0.01
0.001
0.1
1
10
100
T - SECONDS

FIGURE 5

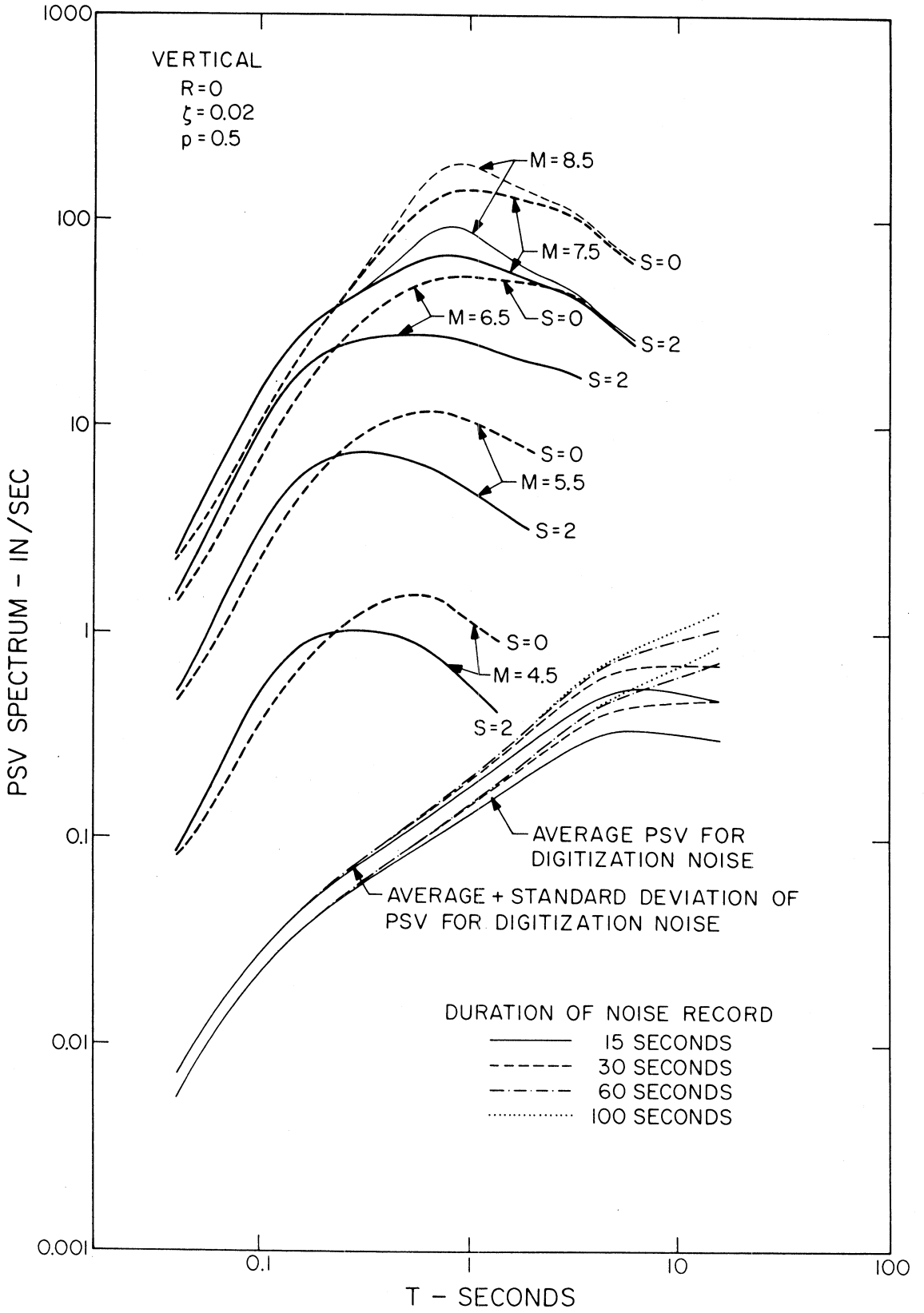
VERTICAL
R=0
ζ=0.02
p=0.5
M=8.5
M=7.5
S=0
M=6.5
S=0
S=2
S=2
S=0
M=5.5
S=2
S=0
M=4.5
S=2
AVERAGE PSV FOR DIGITIZATION NOISE
AVERAGE + STANDARD DEVIATION OF PSV FOR DIGITIZATION NOISE
DURATION OF NOISE RECORD
15 SECONDS
30 SECONDS
60 SECONDS
100 SECONDS
PSV SPECTRUM - IN/SEC
T - SECONDS
1000
100
10
1
0.1
0.01
0.001
0.1
1
10
100

FIGURE 6

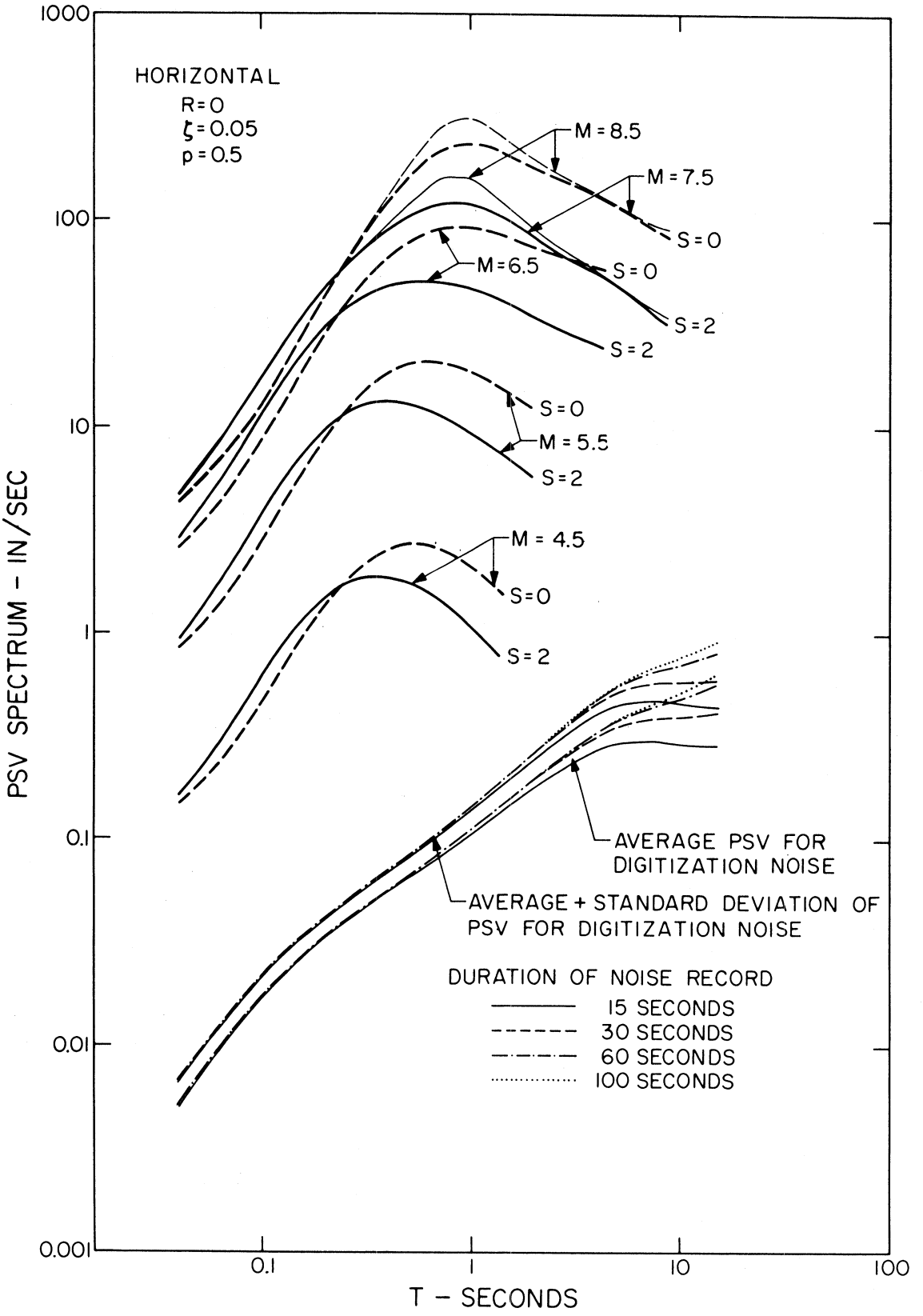
HORIZONTAL
R=0
ζ=0.05
p=0.5
M = 8.5
M = 7.5
S=0
S=0
M=6.5
S=2
S=2
S=0
M = 5.5
S=2
M = 4.5
S=0
S=2
AVERAGE PSV FOR DIGITIZATION NOISE
AVERAGE + STANDARD DEVIATION OF PSV FOR DIGITIZATION NOISE
DURATION OF NOISE RECORD
15 SECONDS
30 SECONDS
60 SECONDS
100 SECONDS
PSV SPECTRUM - IN/SEC
1000
100
10
1
0.1
0.01
0.001
0.1
1
10
100
T - SECONDS

FIGURE 7

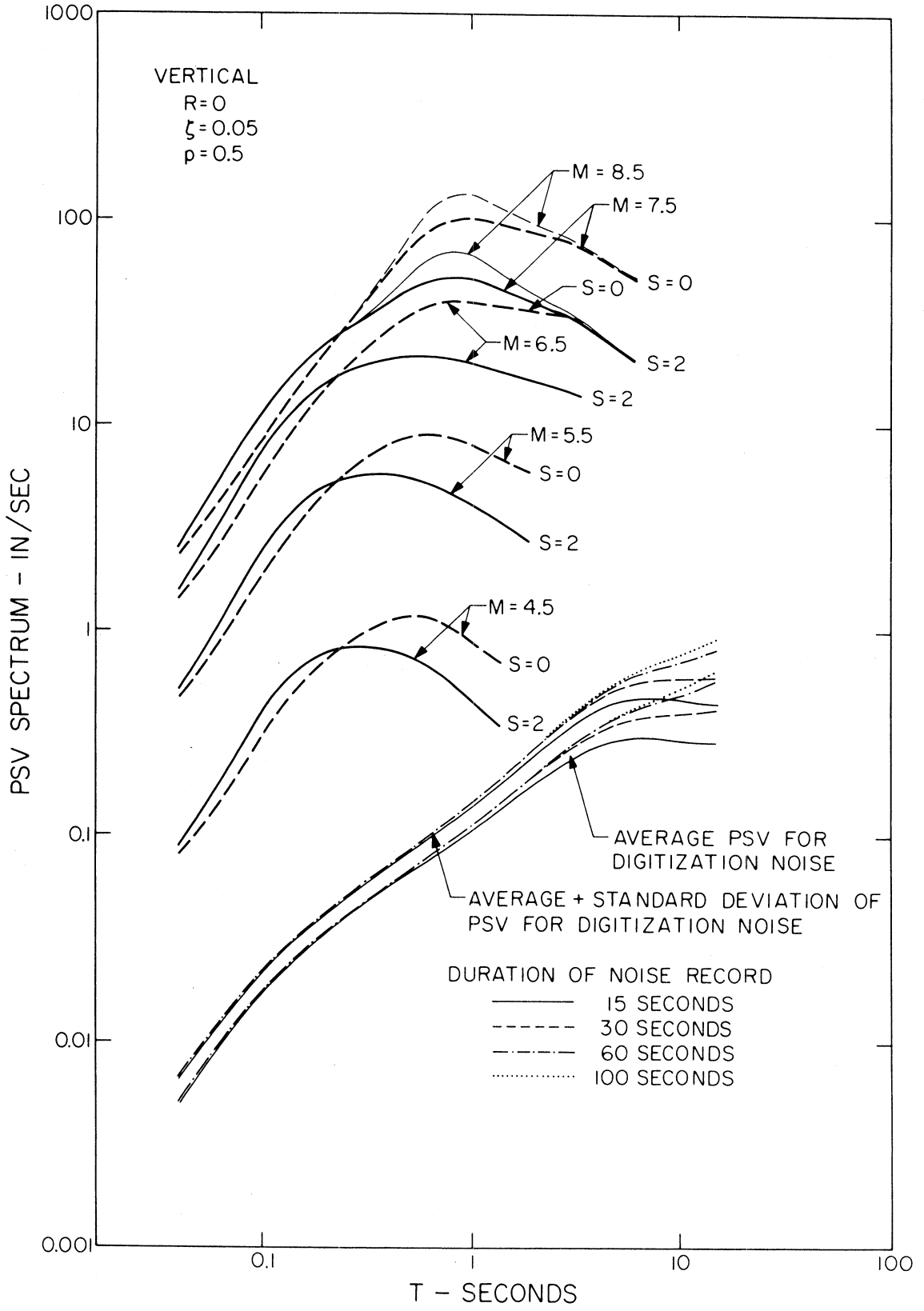
VERTICAL
R=0
ζ=0.05
p=0.5
M = 8.5
M = 7.5
S=0
S=0
M=6.5
S=2
S=2
M=5.5
S=0
S=2
M=4.5
S=0
S=2
AVERAGE PSV FOR DIGITIZATION NOISE
AVERAGE + STANDARD DEVIATION OF PSV FOR DIGITIZATION NOISE
DURATION OF NOISE RECORD
15 SECONDS
30 SECONDS
60 SECONDS
100 SECONDS
PSV SPECTRUM - IN/SEC
T - SECONDS
1000
100
10
1
0.1
0.01
0.001
0.1
1
10
100

FIGURE 8

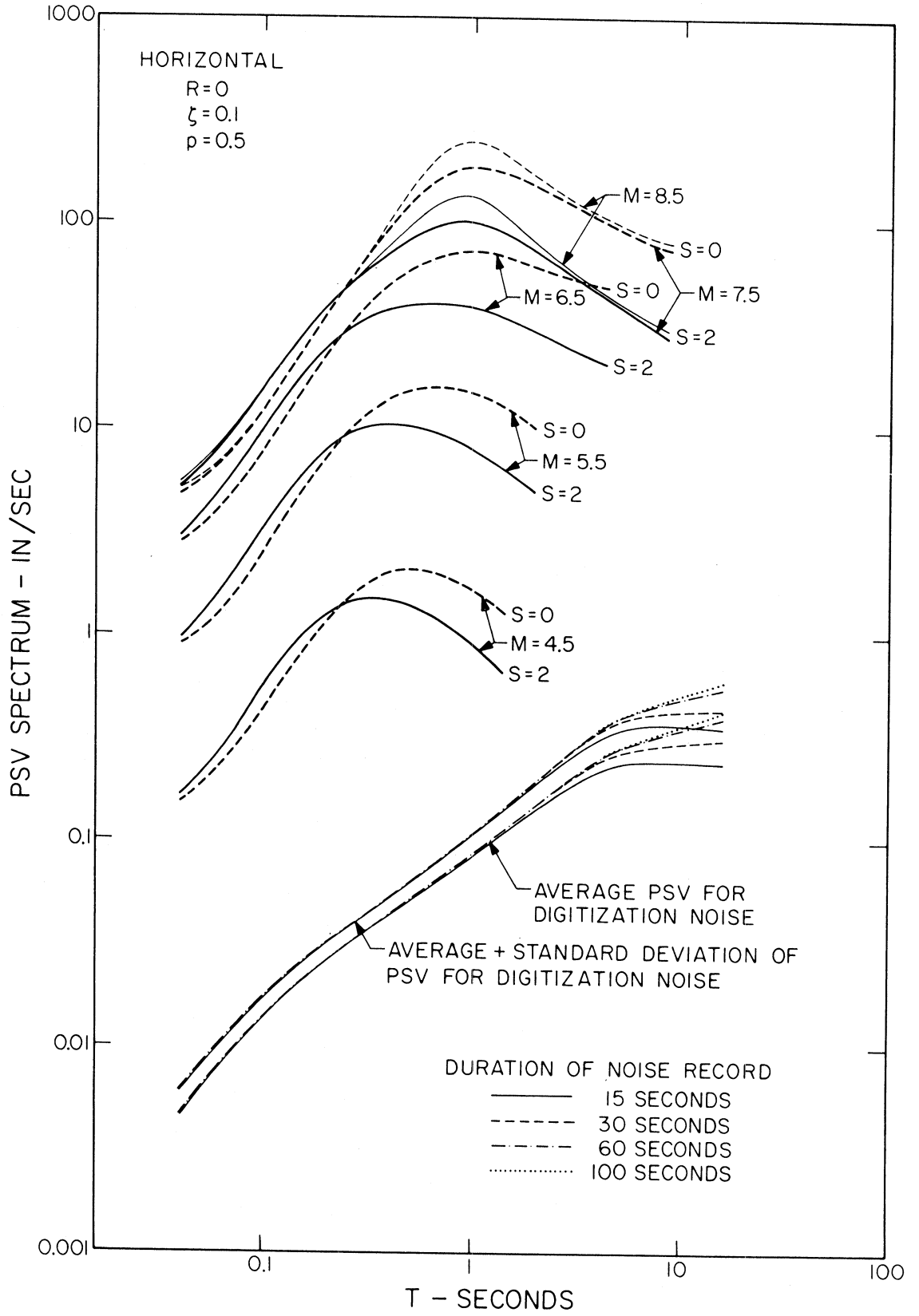
HORIZONTAL
R=0
ζ=0.1
p=0.5
M=8.5
S=0
M=6.5
S=0
M=7.5
S=2
S=2
S=0
M=5.5
S=2
S=0
M=4.5
S=2
AVERAGE PSV FOR DIGITIZATION NOISE
AVERAGE + STANDARD DEVIATION OF PSV FOR DIGITIZATION NOISE
DURATION OF NOISE RECORD
15 SECONDS
30 SECONDS
60 SECONDS
100 SECONDS
PSV SPECTRUM - IN/SEC
T - SECONDS
1000
100
10
1
0.1
0.01
0.001
0.1
1
10
100

FIGURE 9

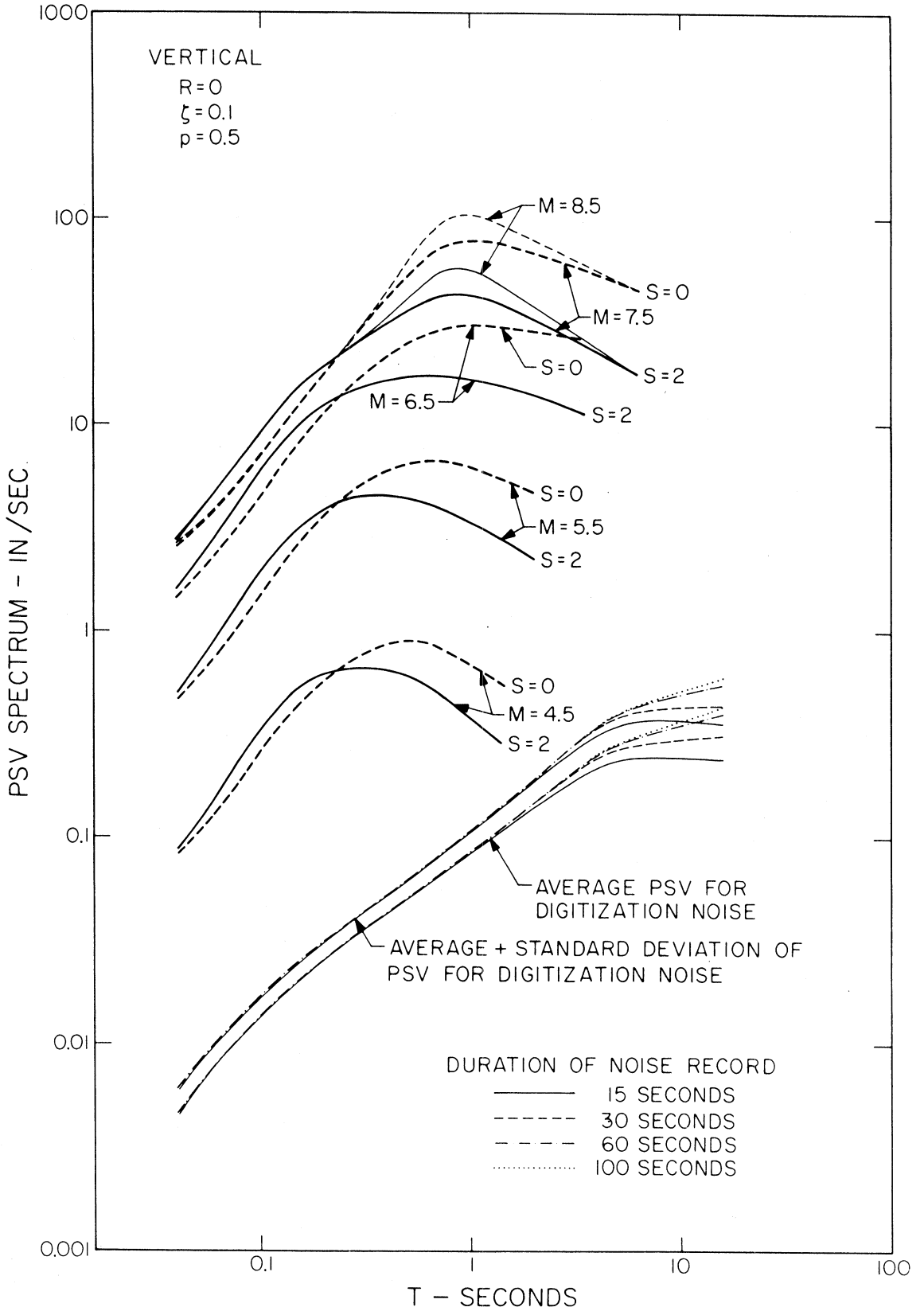
VERTICAL
R=0
ζ=0.1
p=0.5
M=8.5
S=0
M=7.5
S=2
S=0
M=6.5
S=2
S=0
M=5.5
S=2
S=0
M=4.5
S=2
AVERAGE PSV FOR DIGITIZATION NOISE
AVERAGE + STANDARD DEVIATION OF PSV FOR DIGITIZATION NOISE
DURATION OF NOISE RECORD
15 SECONDS
30 SECONDS
60 SECONDS
100 SECONDS
PSV SPECTRUM - IN/SEC
T - SECONDS
1000
100
10
1
0.1
0.01
0.001
0.1
1
10
100

FIGURE 10

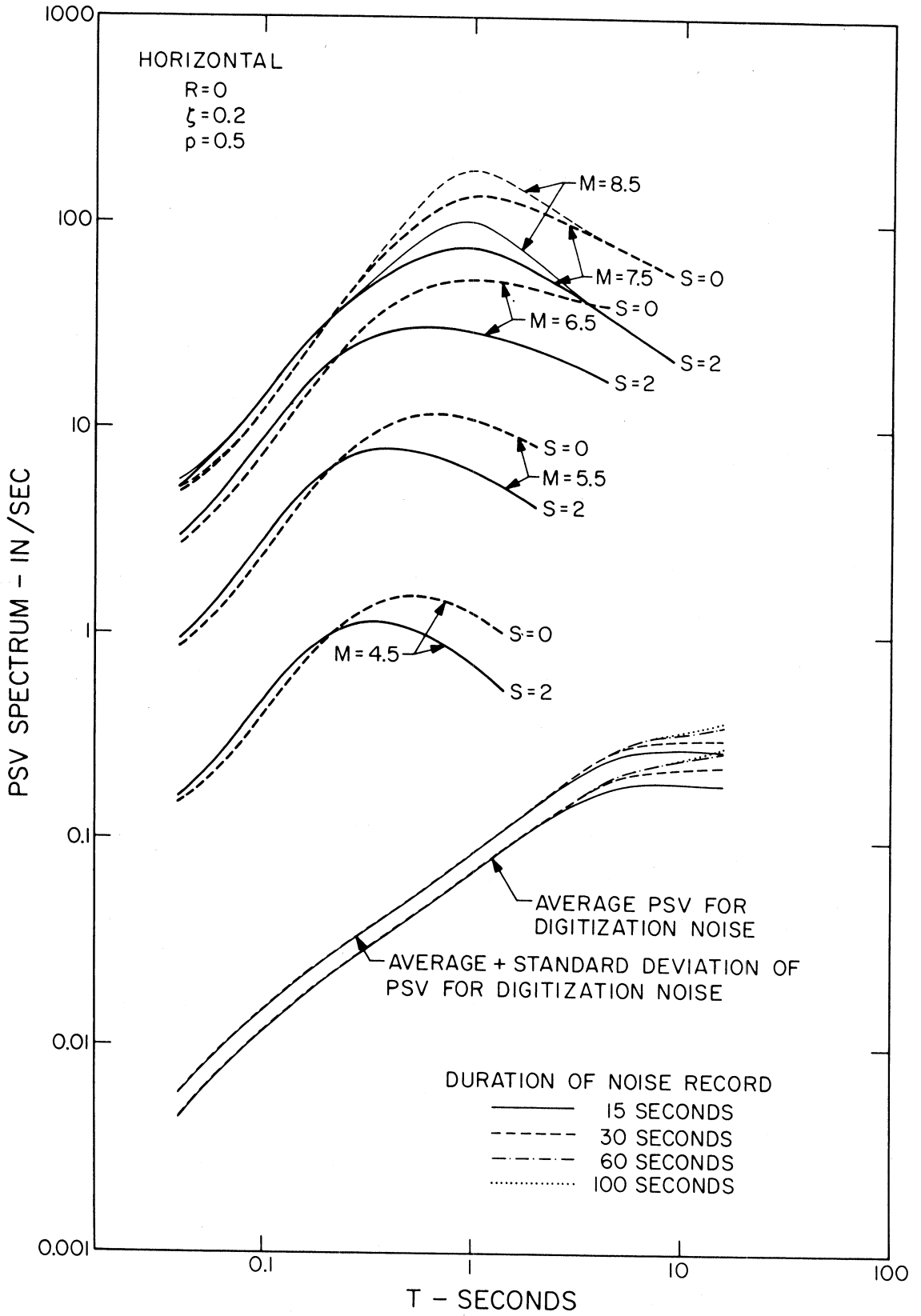
HORIZONTAL
R=0
ζ=0.2
p=0.5
M=8.5
M=7.5
S=0
S=0
M=6.5
S=2
S=2
S=0
M=5.5
S=2
S=0
M=4.5
S=2
AVERAGE PSV FOR DIGITIZATION NOISE
AVERAGE + STANDARD DEVIATION OF PSV FOR DIGITIZATION NOISE
DURATION OF NOISE RECORD
15 SECONDS
30 SECONDS
60 SECONDS
100 SECONDS
PSV SPECTRUM - IN/SEC
T - SECONDS
1000
100
10
1
0.1
0.01
0.001
0.1
1
10
100

FIGURE 11

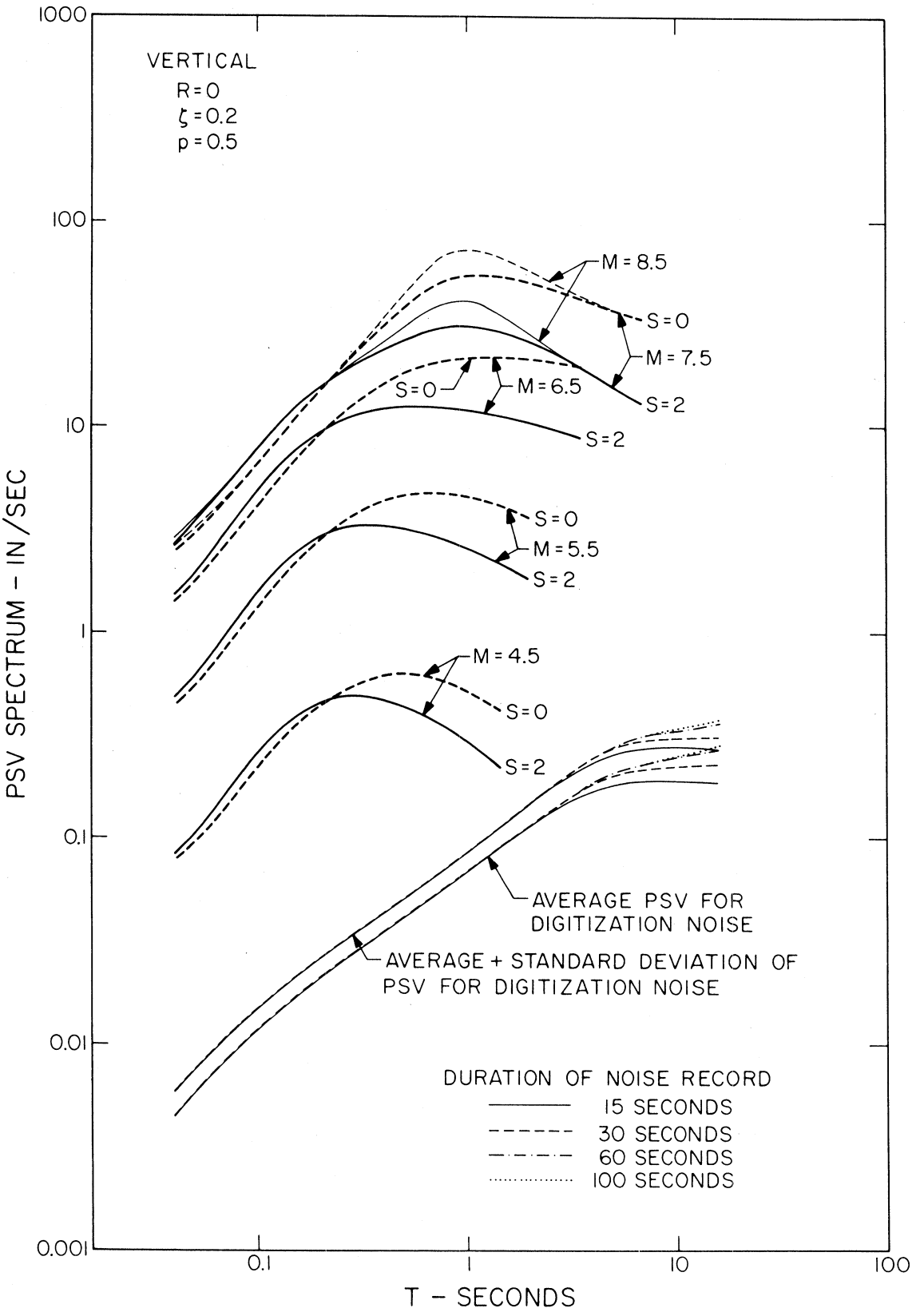
VERTICAL
R=0
ζ=0.2
p=0.5
M=8.5
S=0
M=7.5
S=2
S=0
M=6.5
S=2
S=0
M=5.5
S=2
M=4.5
S=0
S=2
AVERAGE PSV FOR DIGITIZATION NOISE
AVERAGE + STANDARD DEVIATION OF PSV FOR DIGITIZATION NOISE
DURATION OF NOISE RECORD
15 SECONDS
30 SECONDS
60 SECONDS
100 SECONDS
PSV SPECTRUM - IN/SEC
T - SECONDS
1000
100
10
1
0.1
0.01
0.001
0.1
1
10
100

FIGURE 12

available (from about 20 km to about 200 km). Figures 3 through 12 also present spectra for alluvium sites (dashed lines, s=0) and for basement rock sites (full lines, s=2). The spectra for M = 8.5 have been drawn with lighter lines to emphasize that data are available now only for magnitudes less than 7.0 to 7.5, and that spectra for M = 8.5 represents an extrapolation based on equation (1). These figures further show the average and average plus one standard deviation of PSV amplitudes that would result from processing and digitization noise that are present in all records used in this report. These PSV spectra of noise have been presented as functions of ζ and the length of digitized records.

The spectra in Figures 3 through 12 illustrate the rate at which spectral amplitudes increase with magnitude and show that beyond M = 7.5, PSV amplitudes as modeled by the above equations essentially cease to grow. Such behavior is a direct consequence of the assumed functional dependence of PSV spectra on M but its plausibility seems to be supported by simple theoretical models (Trifunac, 1973) and by a direct scaling of peak acceleration, peak velocity and peak displacement data with respect to magnitude (see Figures 5, 6 and 7 in Trifunac and Brady, 1976). Current research by the authors which deals with similar scaling of spectral amplitudes supports this trend by showing that the function f(T) is significantly different from zero for essentially all periods T considered in this study.

Spectra in Figures 3 through 12 and for M = 4.5 have been plotted only for periods T less than about 2 sec, the period range where equation (1) may be essentially unaffected by the noise. Even though the

approximate noise elimination scheme of Trifunac and Anderson (1977) has also been applied in this work, the quality of available data for T longer than about 2 sec is such that the functions a(T) through g(T) still reflect some noise content for $T \gtrsim 2$ sec.

Figures 13 and 14 show the changes of PSV spectra with epicentral distance, $R \leq 200$ km. It can be seen from these figures that equation (1) predicts only minor changes in the shape of spectral amplitudes with increasing R, since $|g(T)|$ is less than 0.001 for all T considered in this study. The amplitude attenuation with distance is thus dominated by the terms $\log_{10}A_o(R)$ in equation (1). For distances less than approximately 200 km, $\log_{10}A_o(R)$ and g(T)R can be combined as $\log_{10}A_o(R) + R/1000$ to describe complete dependence of amplitudes with epicentral distance.

In many simplified methods for scaling response spectrum amplitudes in terms of peak acceleration it is customary (Housner, 1970; Seed, et. al., 1974; Newmark and Rosenblueth, 1971) to use a fixed shape response spectrum and to determine its amplitudes so that for $T \to 0$, $\frac{2\pi}{T}$ PSV spectrum approaches the amplitude of absolute peak acceleration. In our earlier work we showed how this approach compares with the normalized absolute acceleration spectra when the changes of spectrum shape are related to magnitude and geologic site conditions (Trifunac and Anderson, 1977). In this report, we present the corresponding comparison for PSV spectra normalized so that [normalized PSV(T)] = [0.04 PSV(T)]/[T PSV(0.04)]. Since $SA \approx \frac{2\pi}{T}$ PSV this normalization approximates [normalized SA(T)] = SA(T)/SA(0.04) so that Figures 15 through 24 should resemble

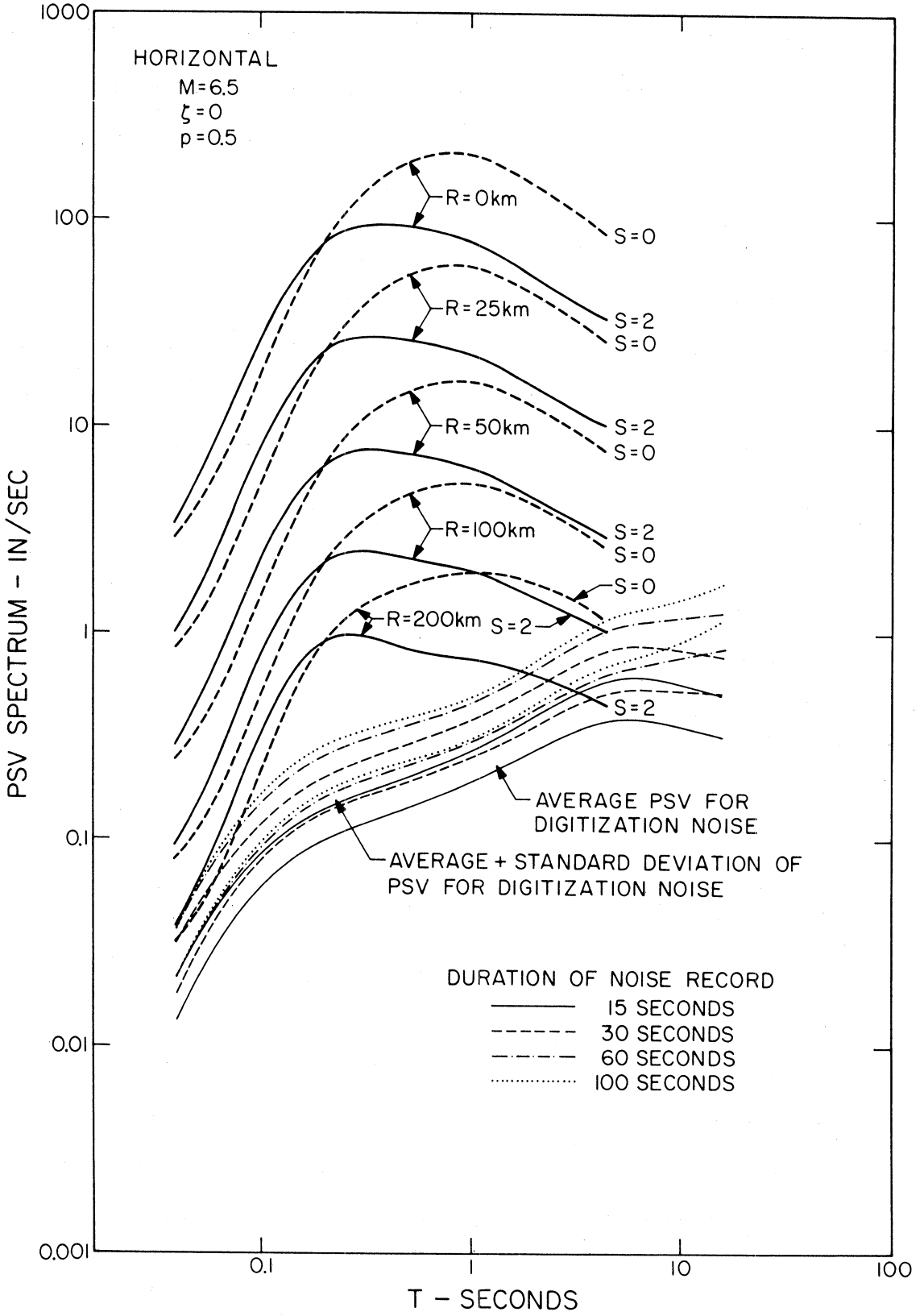
HORIZONTAL
M=6.5
ζ=0
p=0.5
R=0km
S=0
R=25km
S=2
S=0
R=50km
S=2
S=0
R=100km
S=2
S=0
R=200km
S=0
S=2
S=2
AVERAGE PSV FOR DIGITIZATION NOISE
AVERAGE + STANDARD DEVIATION OF PSV FOR DIGITIZATION NOISE
DURATION OF NOISE RECORD
15 SECONDS
30 SECONDS
60 SECONDS
100 SECONDS
PSV SPECTRUM - IN/SEC
1000
100
10
1
0.1
0.01
0.001
0.1
1
10
100
T - SECONDS

FIGURE 13

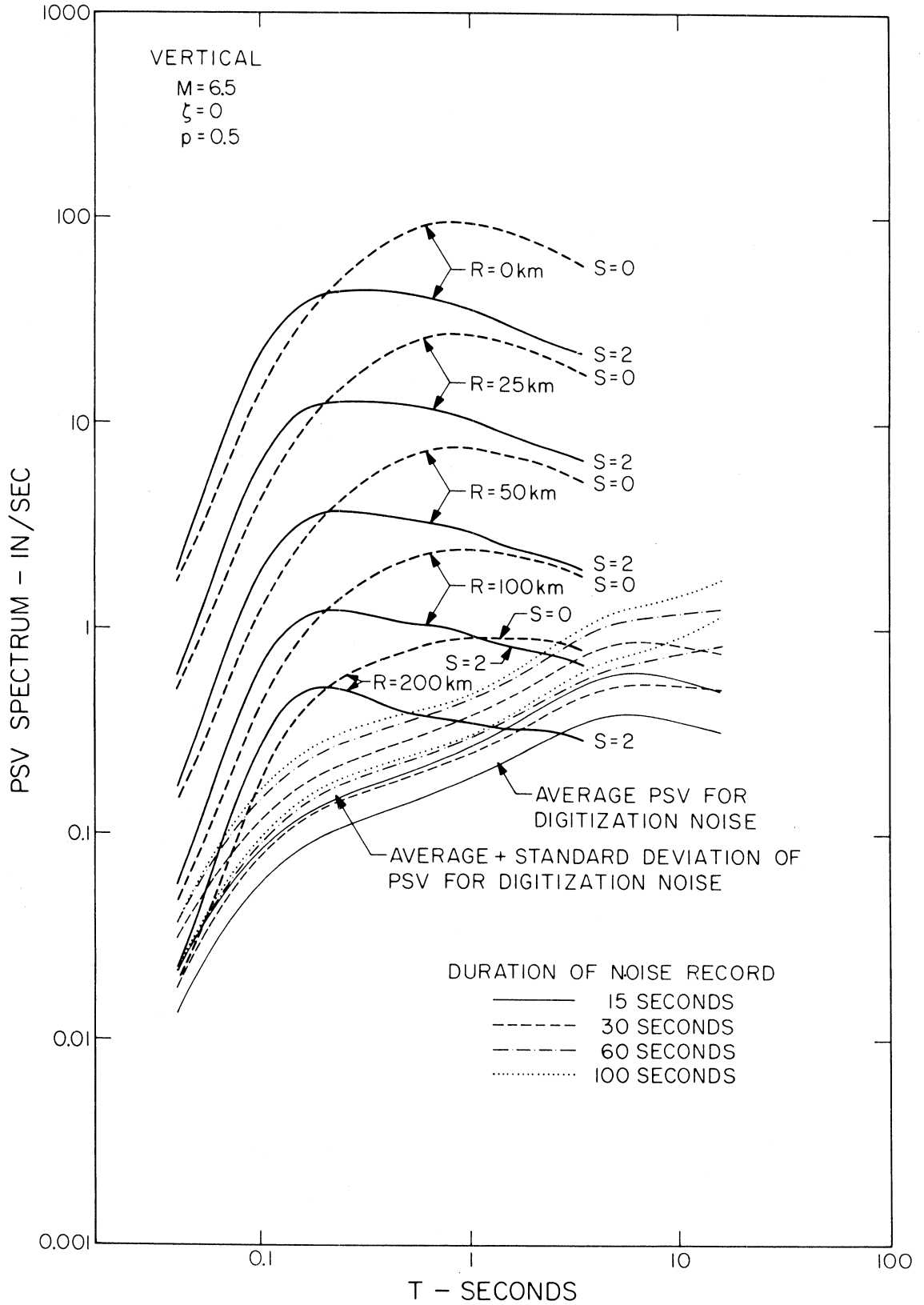
VERTICAL
M=6.5
ζ=0
p=0.5
R=0km
S=0
S=2
S=0
R=25km
S=2
S=0
R=50km
S=2
S=0
R=100km
S=0
S=2
R=200km
S=2
AVERAGE PSV FOR DIGITIZATION NOISE
AVERAGE + STANDARD DEVIATION OF PSV FOR DIGITIZATION NOISE
DURATION OF NOISE RECORD
15 SECONDS
30 SECONDS
60 SECONDS
100 SECONDS
PSV SPECTRUM - IN/SEC
1000
100
10
1
0.1
0.01
0.001
0.1
1
10
100
T - SECONDS

FIGURE 14

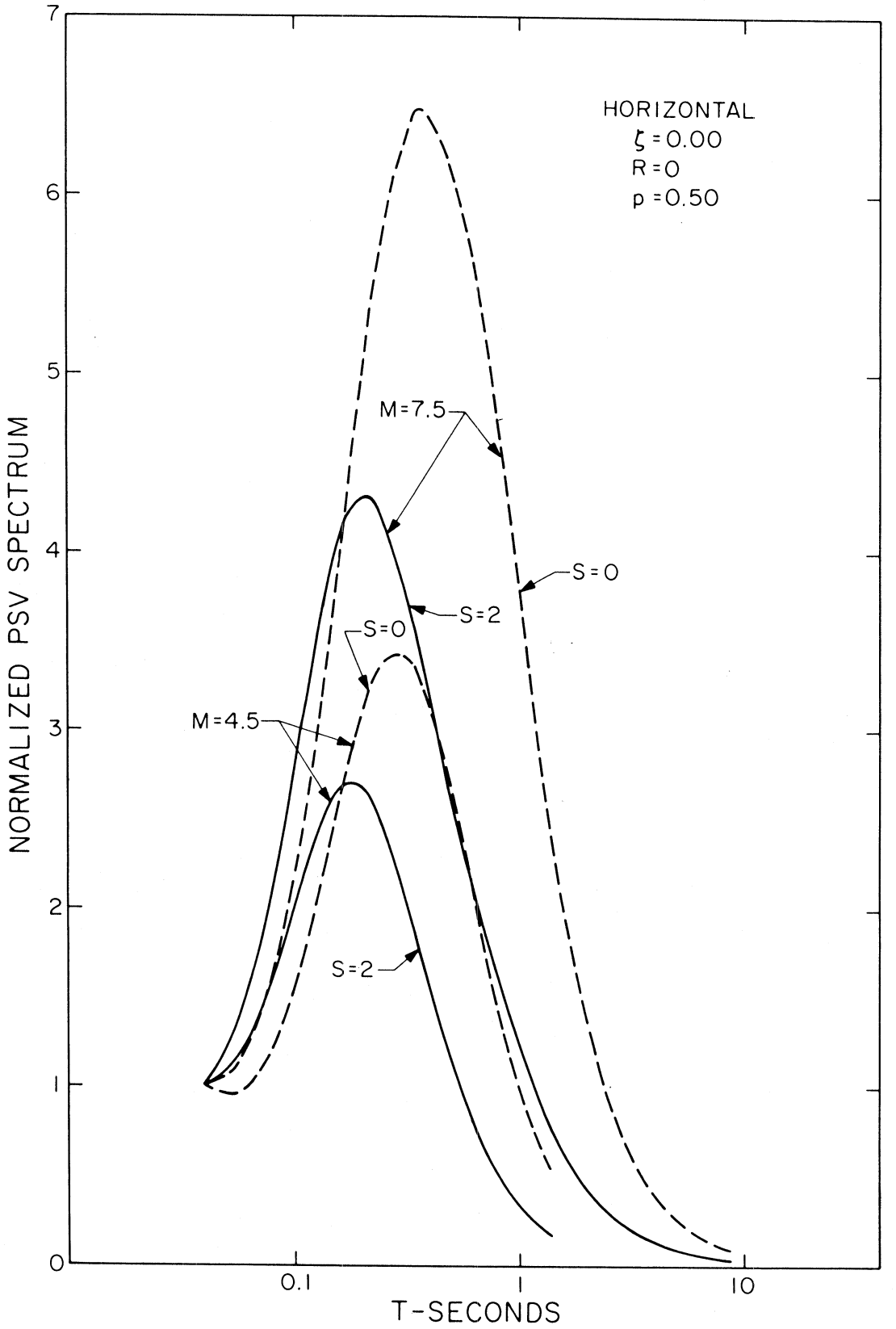
HORIZONTAL
ζ = 0.00
R = 0
p = 0.50
M=7.5
S=0
S=2
S=0
M=4.5
S=2
NORMALIZED PSV SPECTRUM
T-SECONDS
0
1
2
3
4
5
6
7
0.1
10

FIGURE 15

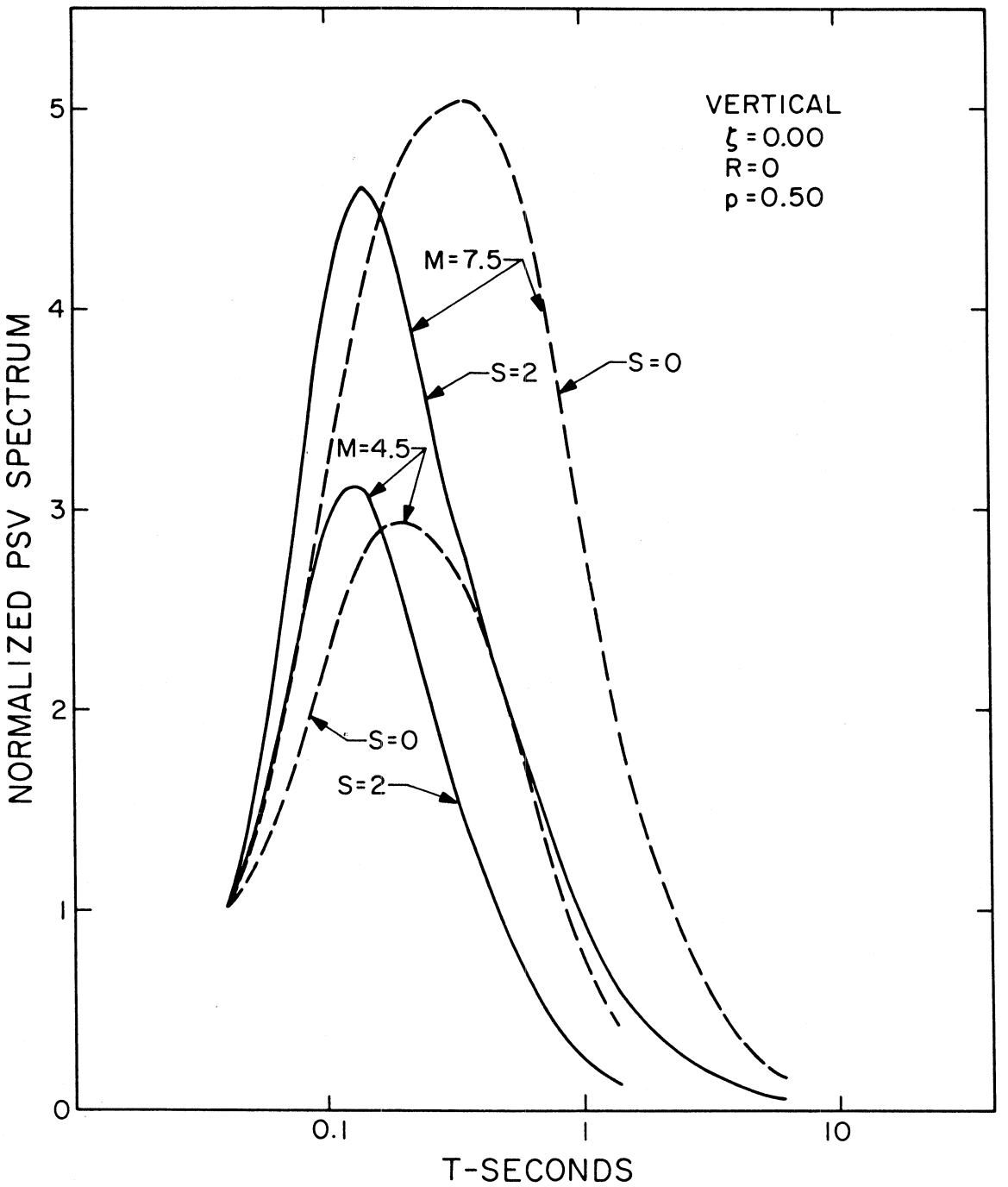
VERTICAL
ζ = 0.00
R = 0
p = 0.50
M=7.5
S=2
S=0
M=4.5
S=0
S=2
NORMALIZED PSV SPECTRUM
T-SECONDS
0
1
2
3
4
5
0.1
1
10

FIGURE 16

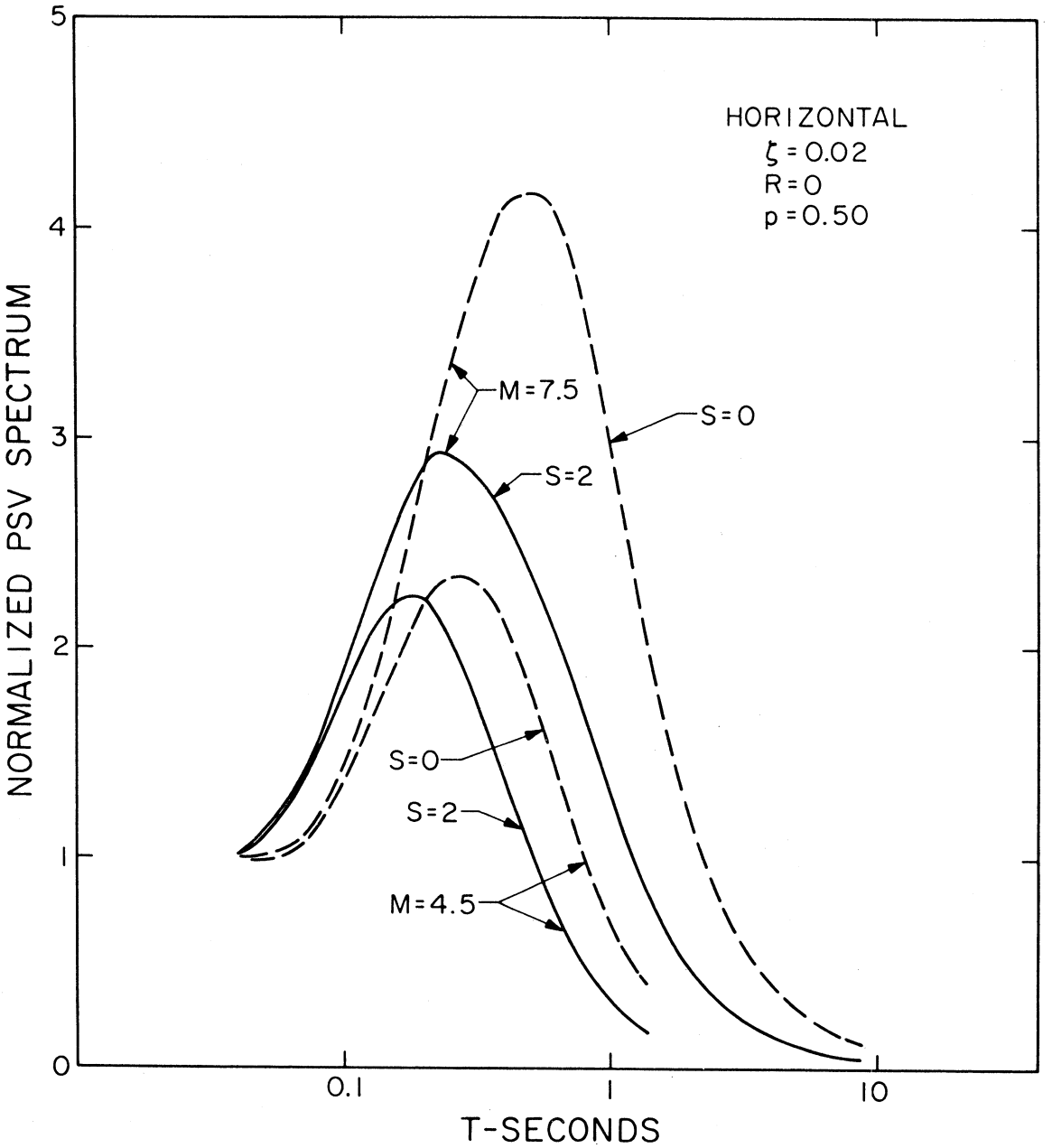
HORIZONTAL
ζ = 0.02
R = 0
p = 0.50
M=7.5
S=0
S=2
S=0
S=2
M=4.5
NORMALIZED PSV SPECTRUM
T-SECONDS
0
1
2
3
4
5
0.1
1
10

FIGURE 17

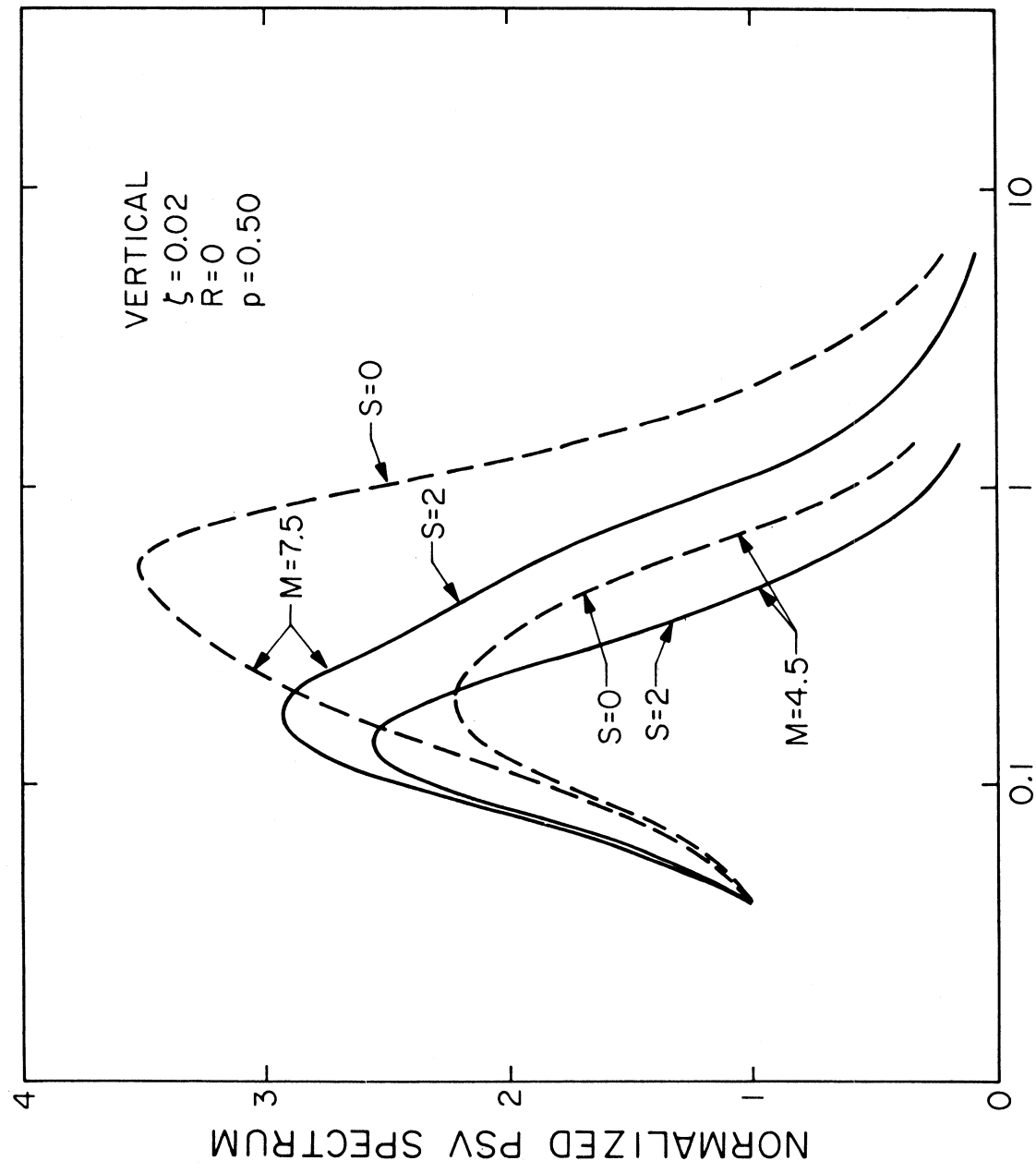
VERTICAL
ζ = 0.02
R = 0
p = 0.50
S=0
S=2
M=7.5
S=0
S=2
M=4.5
NORMALIZED PSV SPECTRUM
T-SECONDS
0
1
2
3
4
0.1
1
10

FIGURE 18

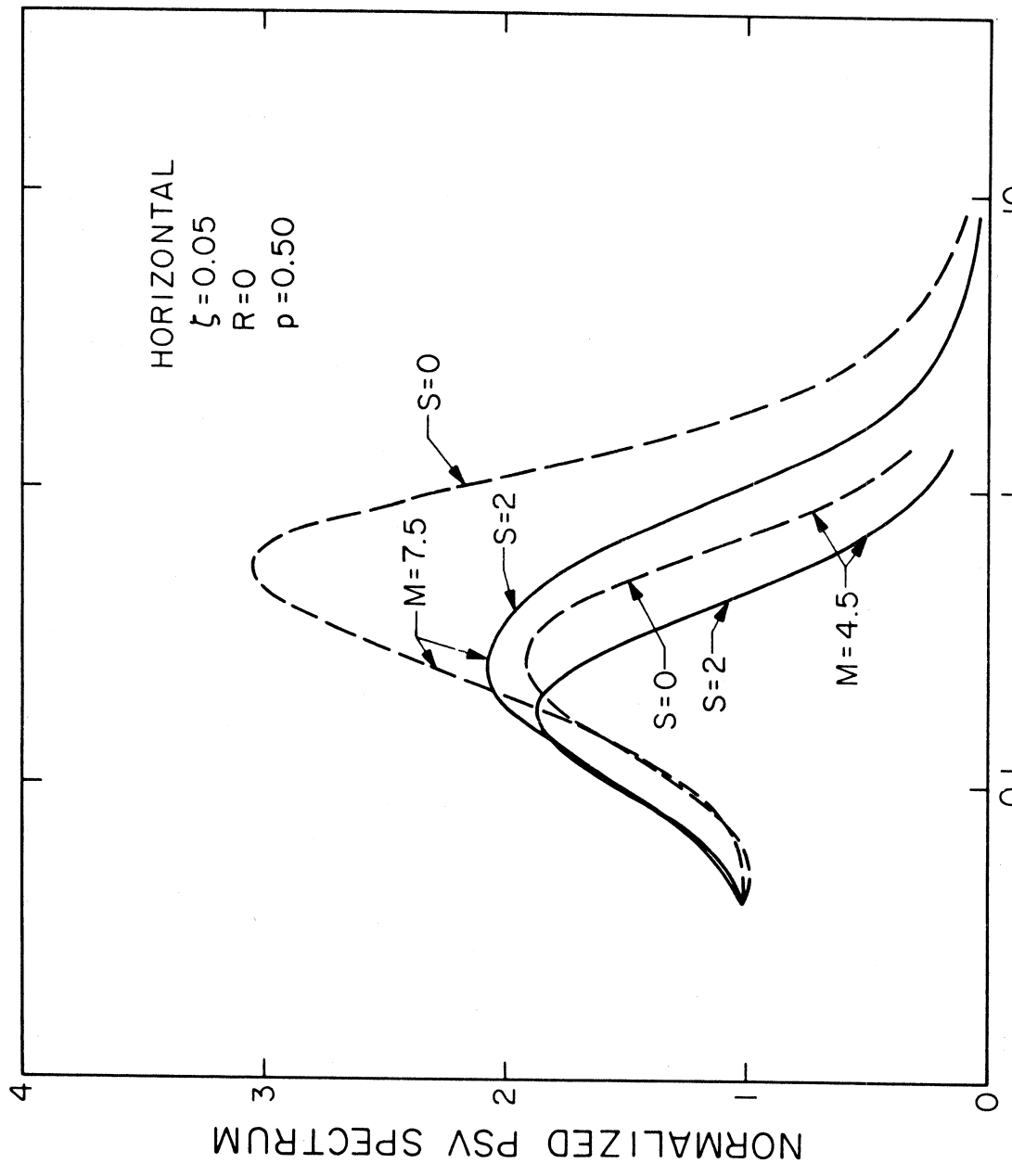
HORIZONTAL
ζ=0.05
R=0
p=0.50
S=0
S=2
M=7.5
S=0
S=2
M=4.5
NORMALIZED PSV SPECTRUM
T-SECONDS
0
1
2
3
4
0.1
10

FIGURE 19

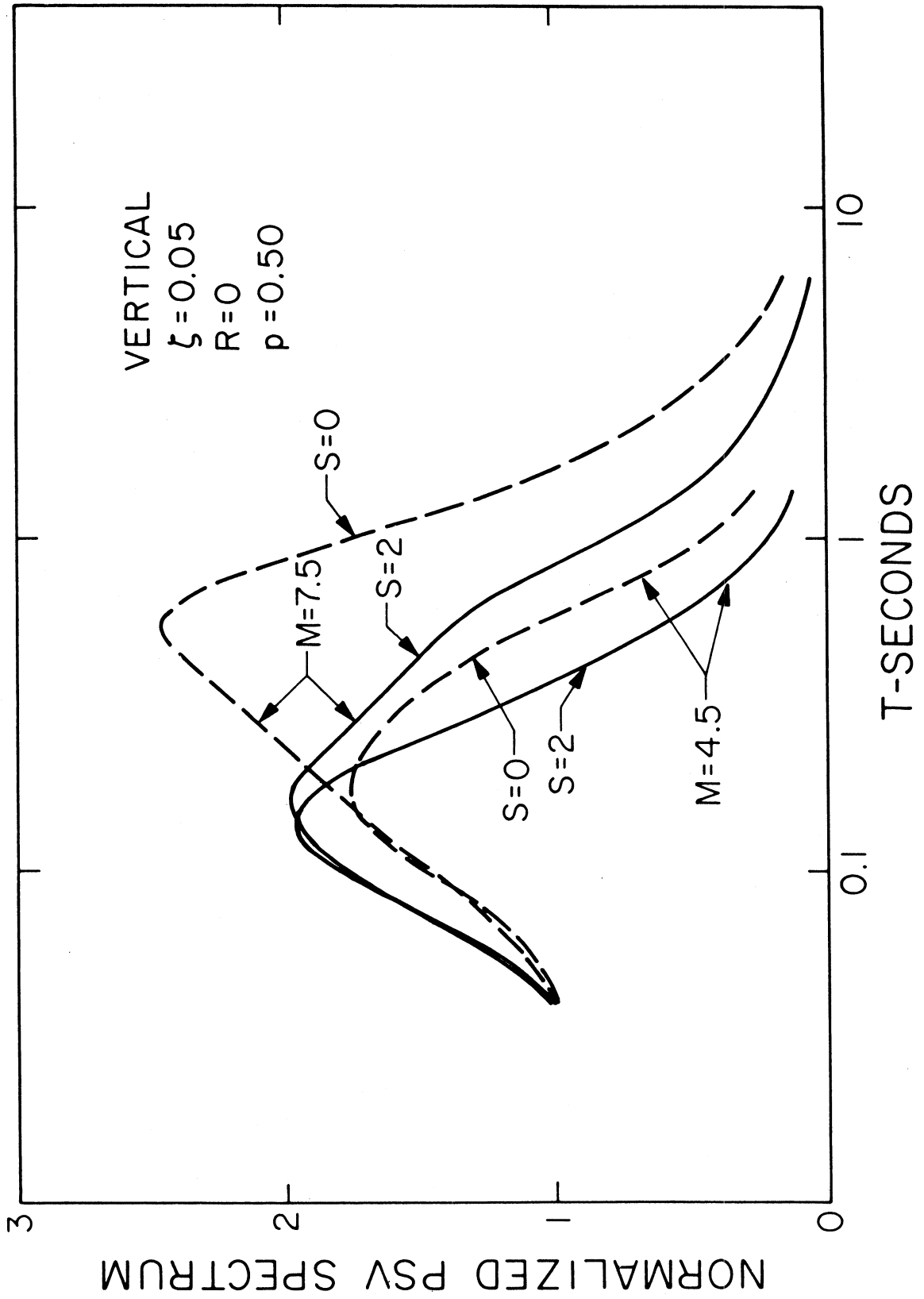
VERTICAL
ζ=0.05
R=0
p=0.50
S=0
M=7.5
S=2
S=0
S=2
M=4.5
NORMALIZED PSV SPECTRUM
T-SECONDS
0
1
2
3
0.1
10

FIGURE 20

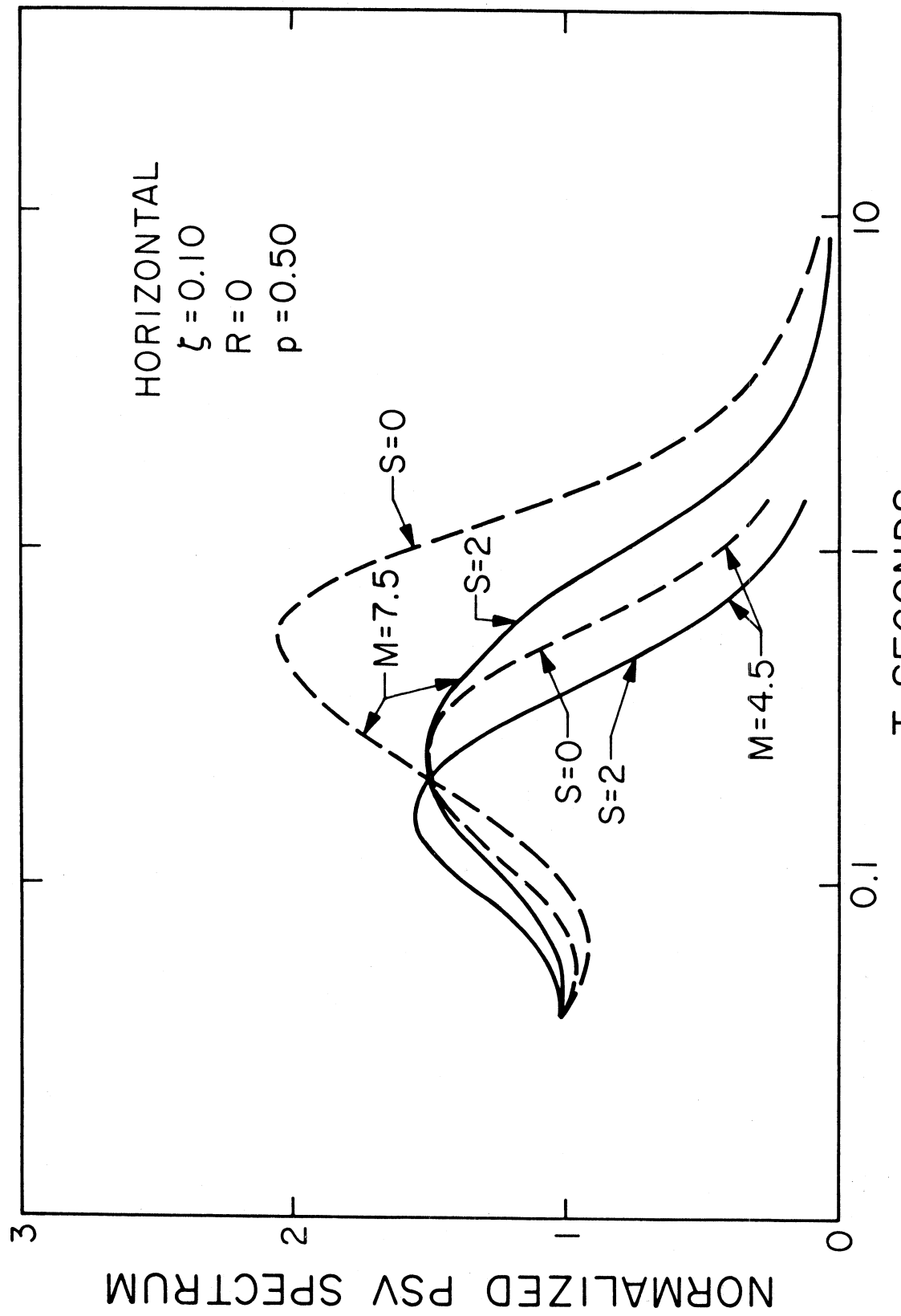
HORIZONTAL
ζ = 0.10
R = 0
p = 0.50
S=0
M=7.5
S=2
S=0
S=2
M=4.5
NORMALIZED PSV SPECTRUM
T-SECONDS
0
1
2
3
0.1
10

FIGURE 21

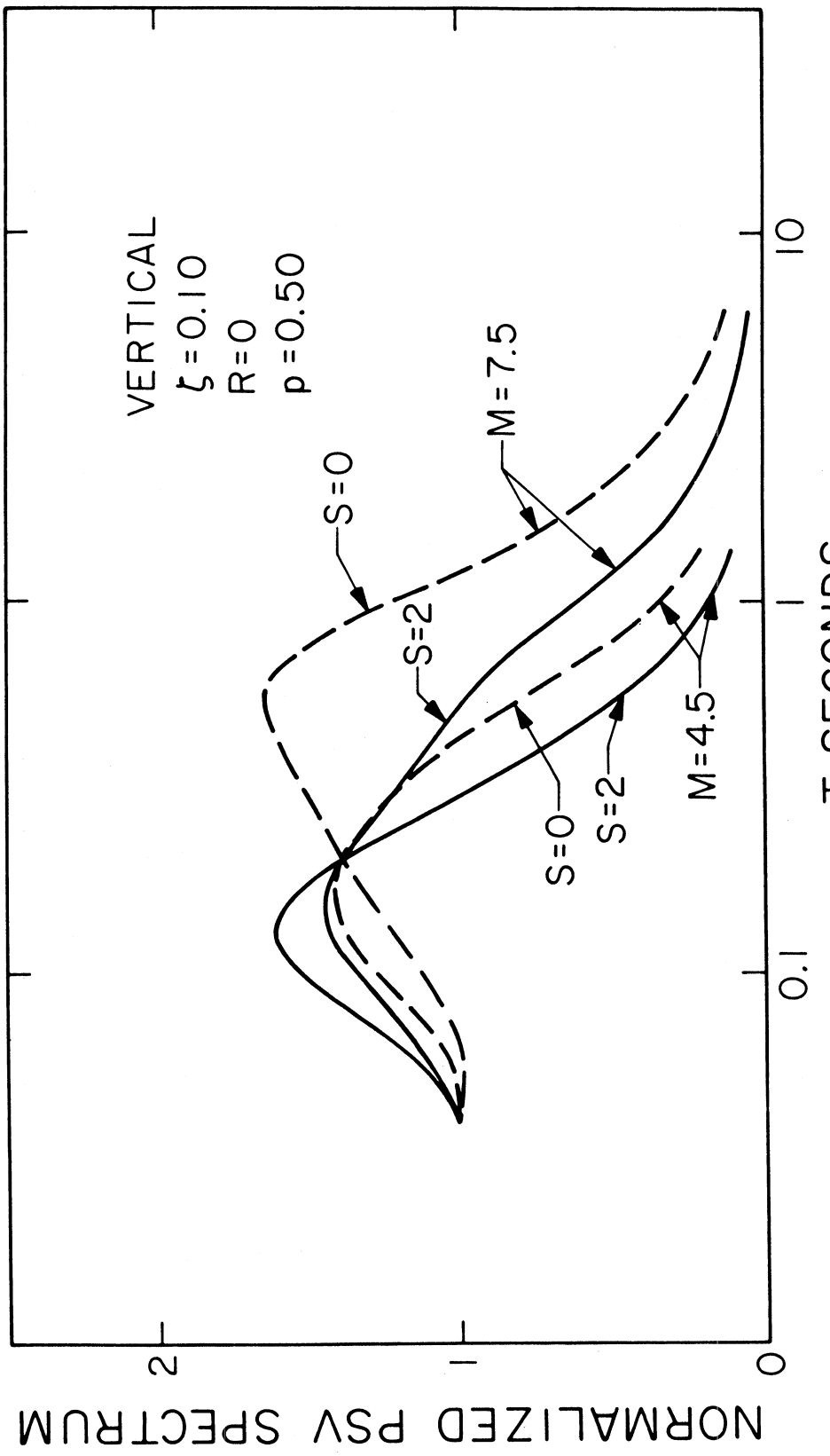
NORMALIZED PSV SPECTRUM
2
1
0
0.1
1
10
T-SECONDS
VERTICAL
ζ=0.10
R=0
p=0.50
M=7.5
S=0
S=2
M=4.5
S=0
S=2

FIGURE 22

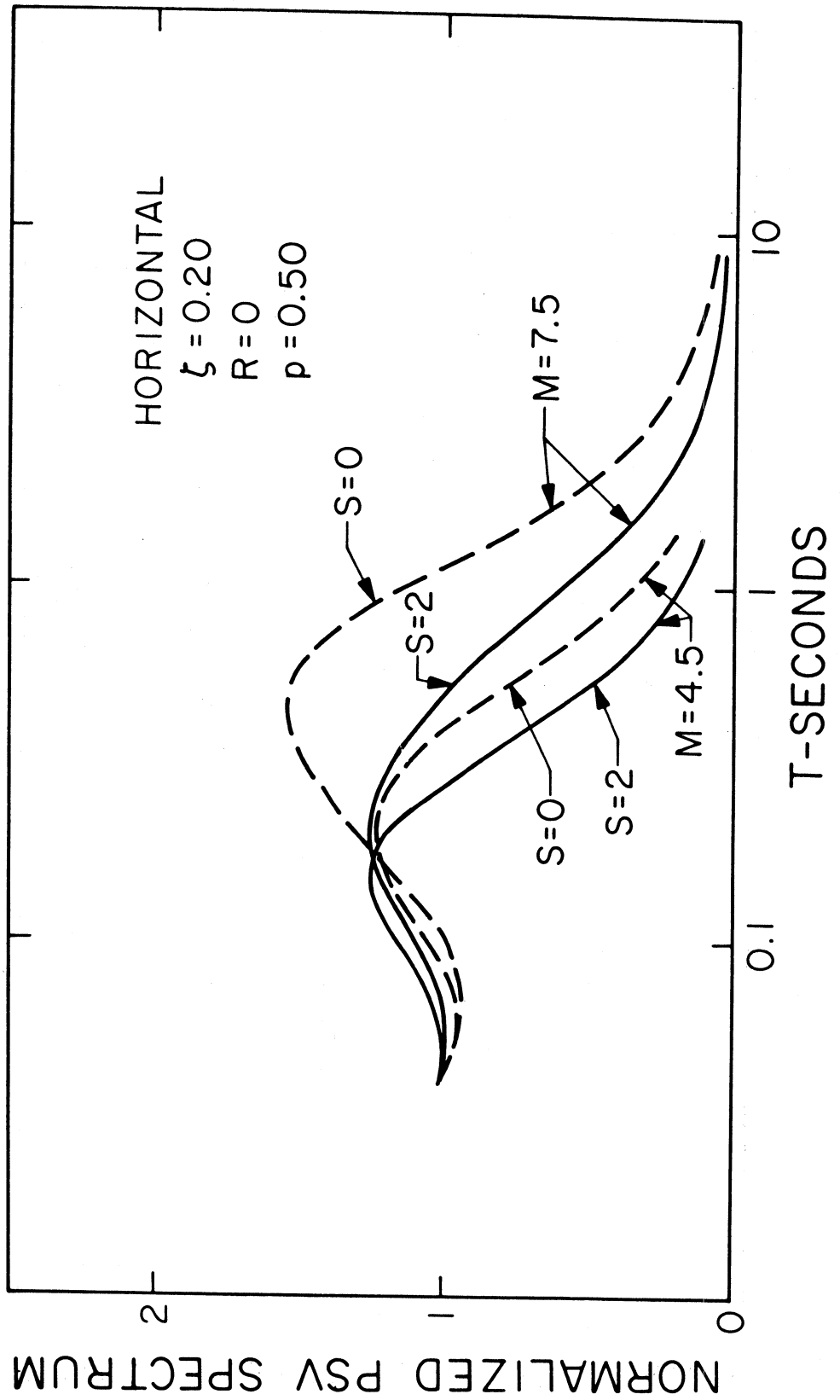
HORIZONTAL
ζ = 0.20
R = 0
p = 0.50
S=0
S=2
M=7.5
M=4.5
S=0
S=2
NORMALIZED PSV SPECTRUM
T-SECONDS
0
1
2
0.1
10

FIGURE 23

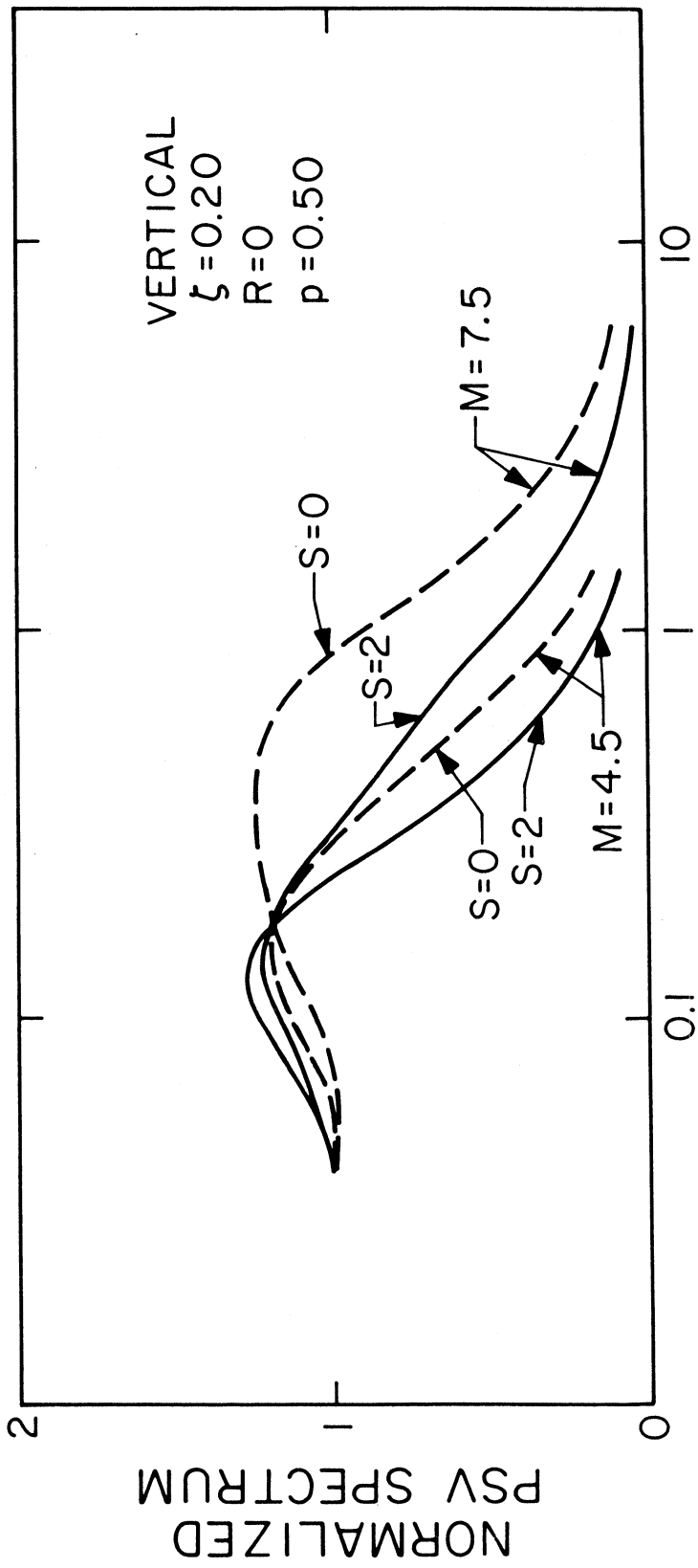
VERTICAL
ζ=0.20
R=0
p=0.50
M=7.5
S=0
S=2
M=4.5
S=0
S=2
NORMALIZED
PSV SPECTRUM
2
1
0
0.1
1
10
T-SECONDS

FIGURE 24

Figures 18 through 27 of Trifunac and Anderson (1977). Detailed comparison of these figures shows that this is indeed the case. Figures 15 through 24 show such normalized spectra for M = 4.5 and 7.5, for s=0 and 2, horizontal and vertical ground motion and for p = 0.5 to facilitate comparison with the previous reports dealing with SA spectra.

Figures 25 through 30 show the comparison of PSV spectra computed from Pacoima dam accelerogram and El Centro accelerogram with the spectra for p = 0.1 and 0.9 computed from equation (1). The PSV spectra in Figures 25, 26 and 27 have been computed for M = 6.4, R = 9.1 km and s=2. These parameters approximate the conditions at the Pacoima Dam site during the San Fernando, California, earthquake of 1971. The spectra in Figures 28, 29 and 30 have been computed for M = 6.4, R = 15 km and s=0, the conditions during the Imperial Valley, California, earthquake of 1940. The interval between the computed spectra for p = 0.1 and 0.9 and for a chosen value of ζ then represents approximately the 80% confidence interval where spectra of recorded motions would be expected to lie. As can be seen from Figures 25 through 30, the agreement between the spectra of recorded motions and the spectra from equation (1) is good. Figure 30 shows an example of worse than typical agreement between the spectra of recorded motion at El Centro and the scaling with equation (1).

b. Correlations in Terms of I_{MM}, p, s, and v

Figure 31 and Table IV contain the results of the regression

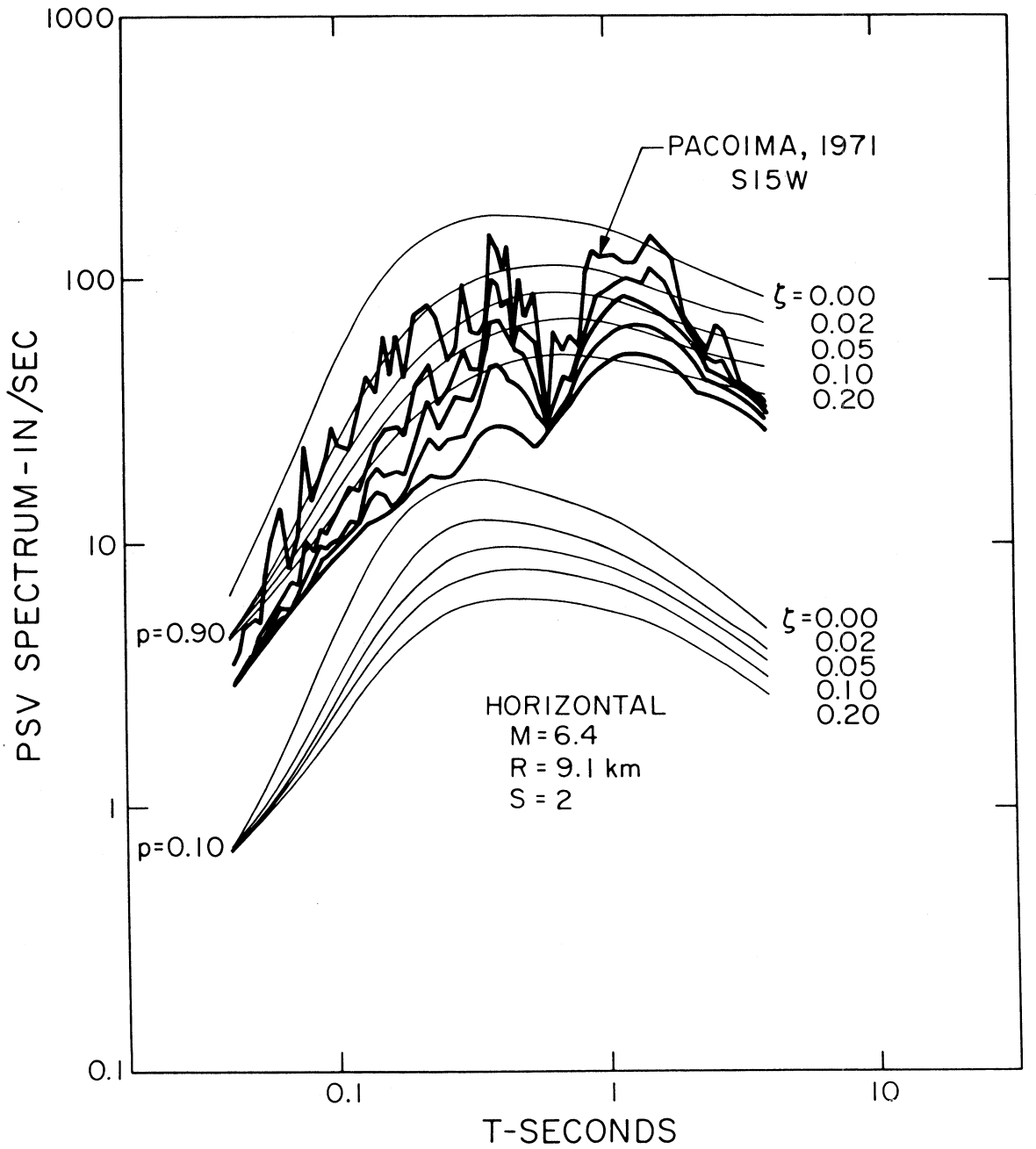
1000
100
10
1
0.1
PSV SPECTRUM-IN/SEC
PACOIMA, 1971
S15W
ζ=0.00
0.02
0.05
0.10
0.20
p=0.90
p=0.10
HORIZONTAL
M=6.4
R=9.1 km
S=2
0.1
1
10
T-SECONDS

FIGURE 25

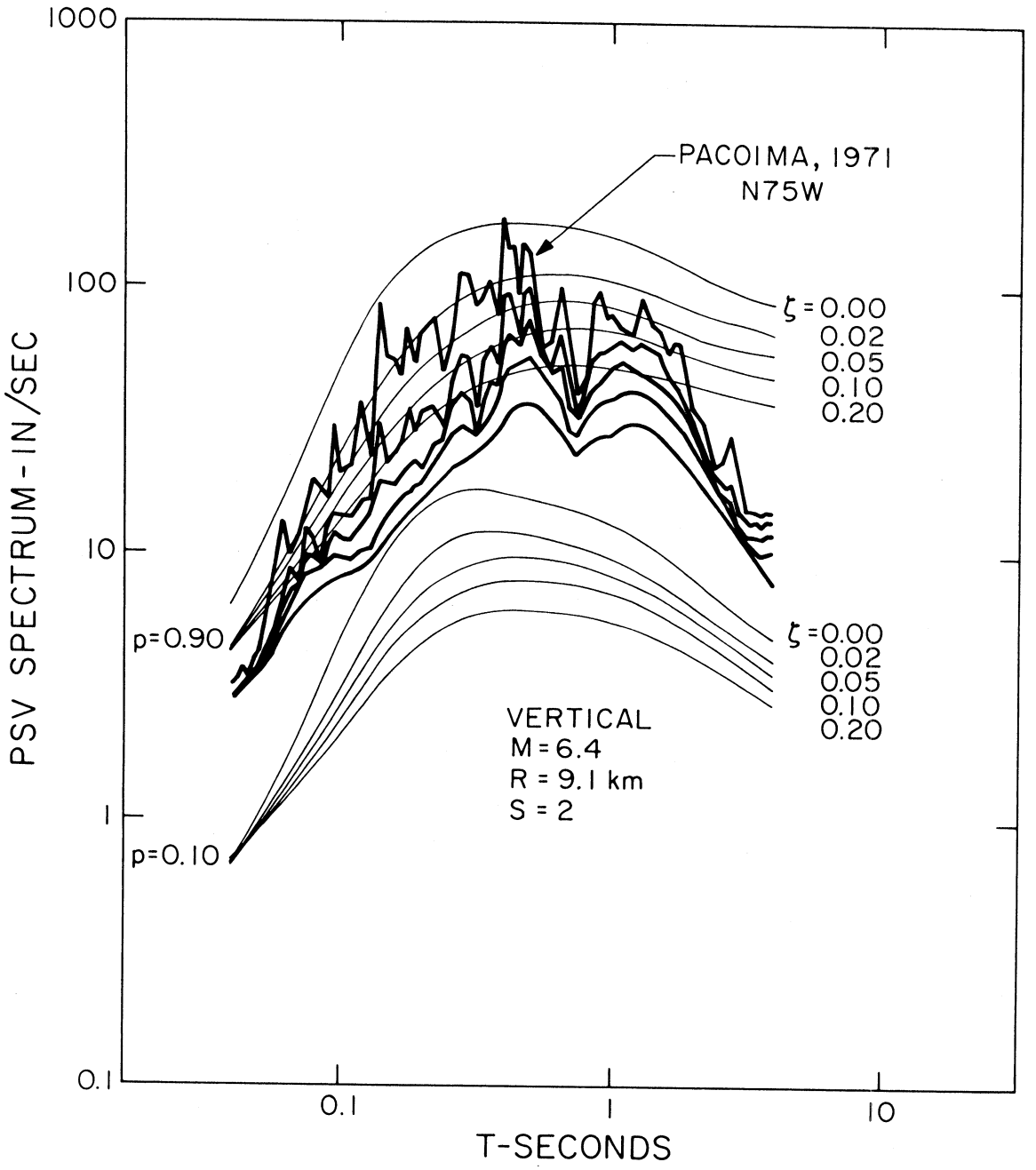
1000
100
10
1
0.1
PSV SPECTRUM-IN/SEC
PACOIMA, 1971
N75W
ζ = 0.00
0.02
0.05
0.10
0.20
p=0.90
ζ = 0.00
0.02
0.05
0.10
0.20
VERTICAL
M = 6.4
R = 9.1 km
S = 2
p=0.10
0.1
1
10
T-SECONDS

FIGURE 26

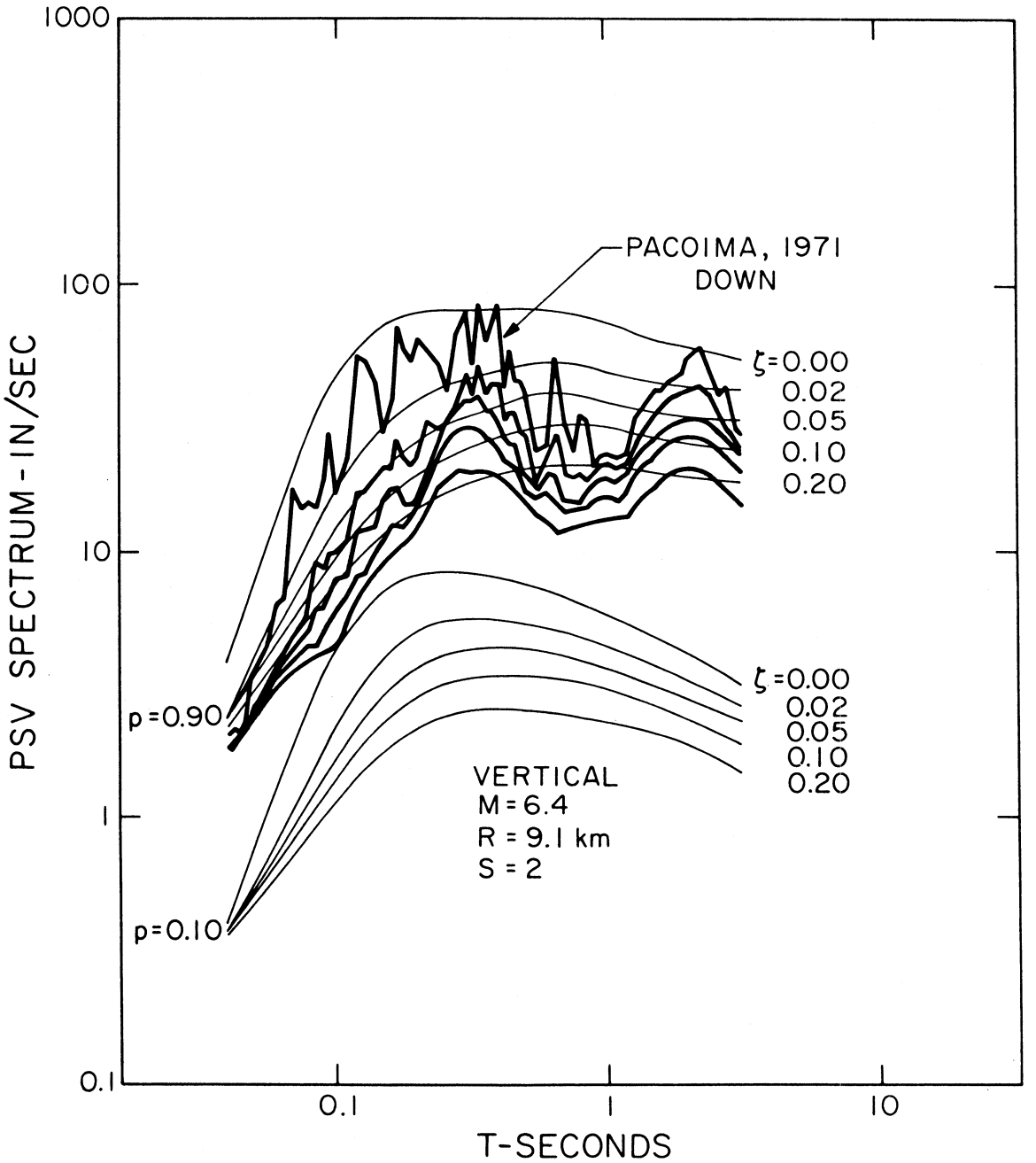
1000
100
10
1
0.1
PSV SPECTRUM - IN/SEC
PACOIMA, 1971
DOWN
ζ=0.00
0.02
0.05
0.10
0.20
p=0.90
ζ=0.00
0.02
0.05
0.10
0.20
p=0.10
VERTICAL
M=6.4
R=9.1 km
S=2
0.1
1
10
T-SECONDS

FIGURE 27

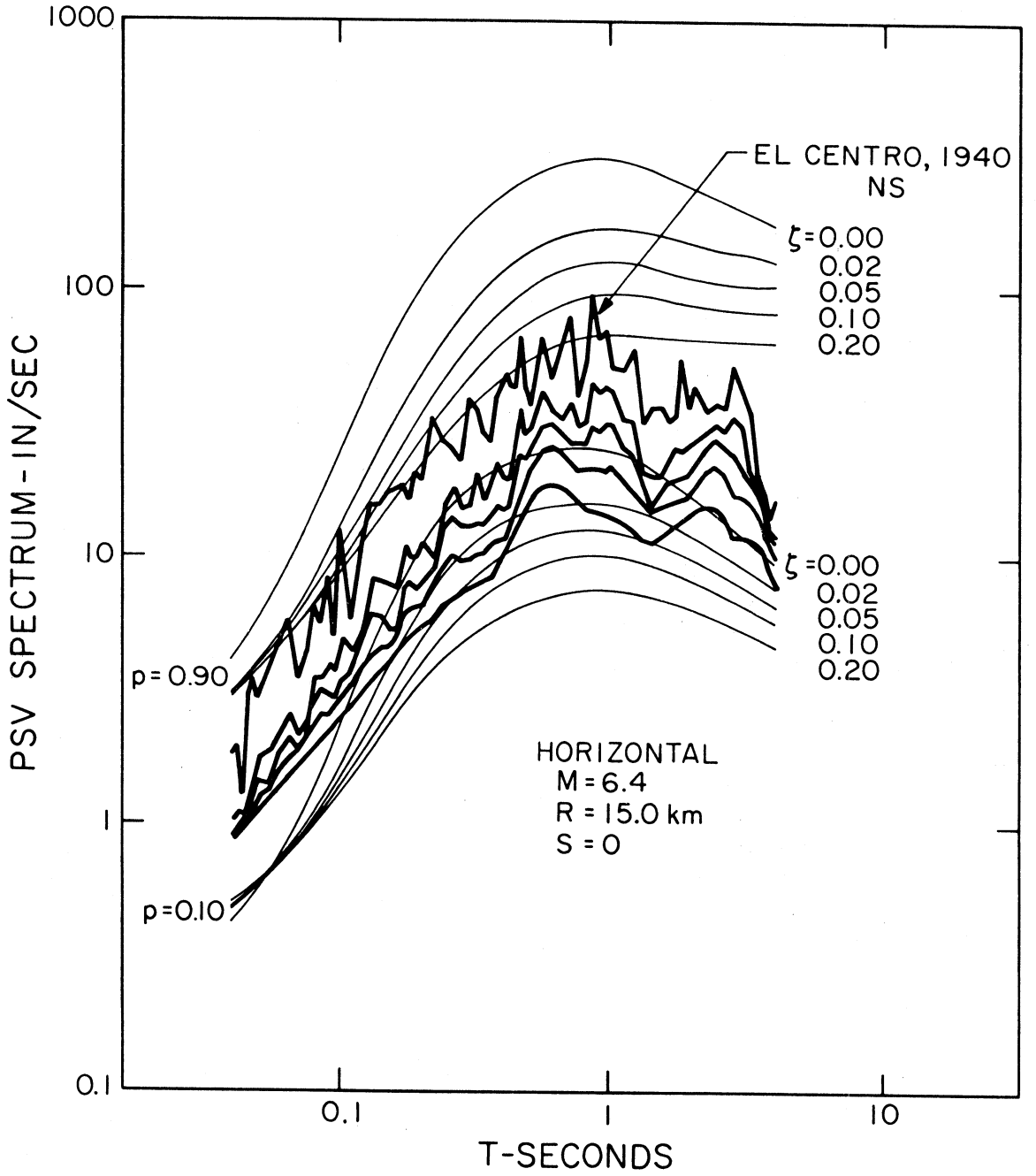
1000
100
10
1
0.1
PSV SPECTRUM-IN/SEC
EL CENTRO, 1940
NS
ζ=0.00
0.02
0.05
0.10
0.20
ζ=0.00
0.02
0.05
0.10
0.20
p=0.90
p=0.10
HORIZONTAL
M=6.4
R=15.0 km
S=0
0.1
1
10
T-SECONDS

FIGURE 28

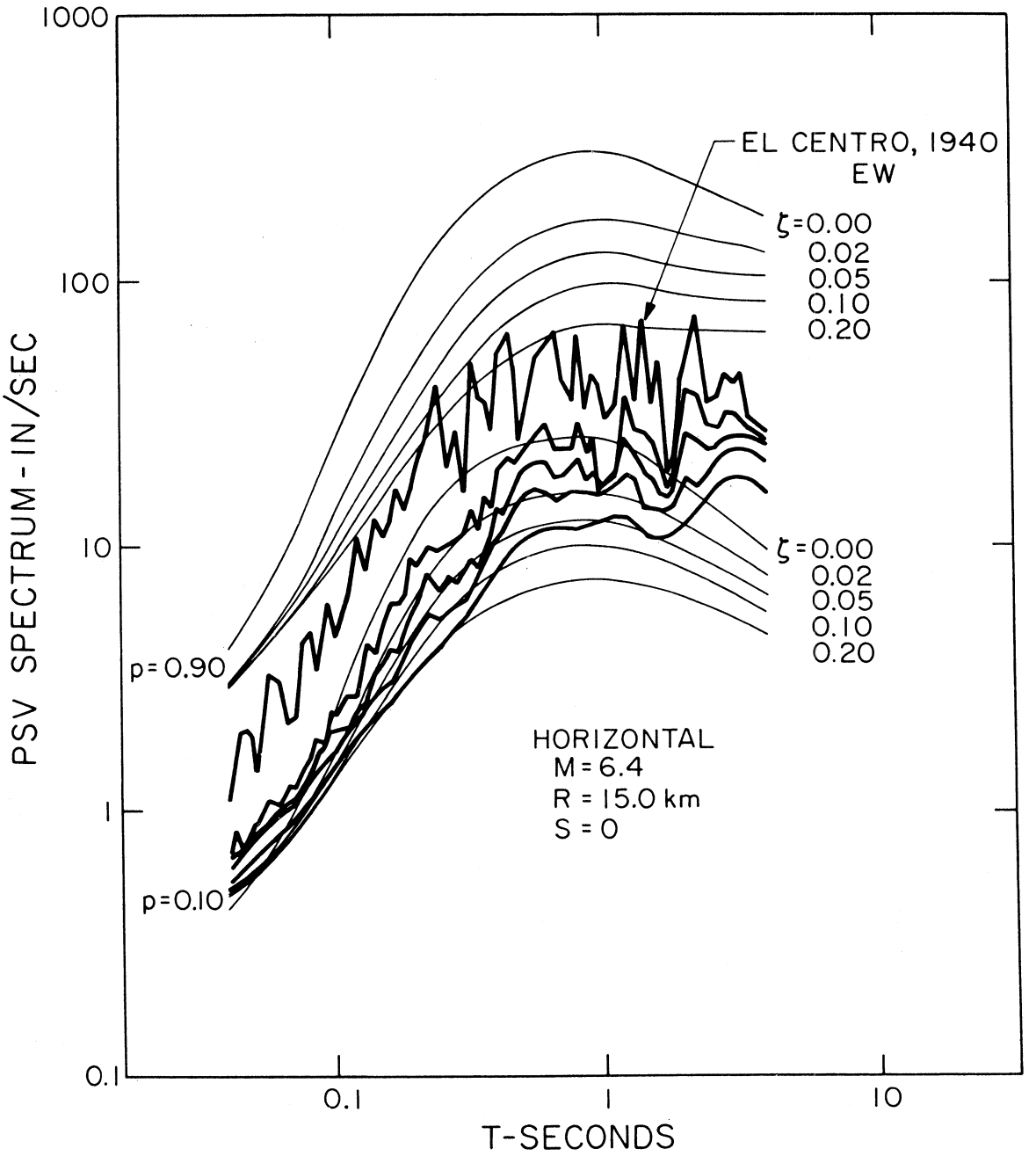
1000
100
10
1
0.1
PSV SPECTRUM - IN/SEC
EL CENTRO, 1940
EW
ζ=0.00
0.02
0.05
0.10
0.20
ζ=0.00
0.02
0.05
0.10
0.20
p=0.90
p=0.10
HORIZONTAL
M=6.4
R = 15.0 km
S = 0
0.1
1
10
T-SECONDS

FIGURE 29

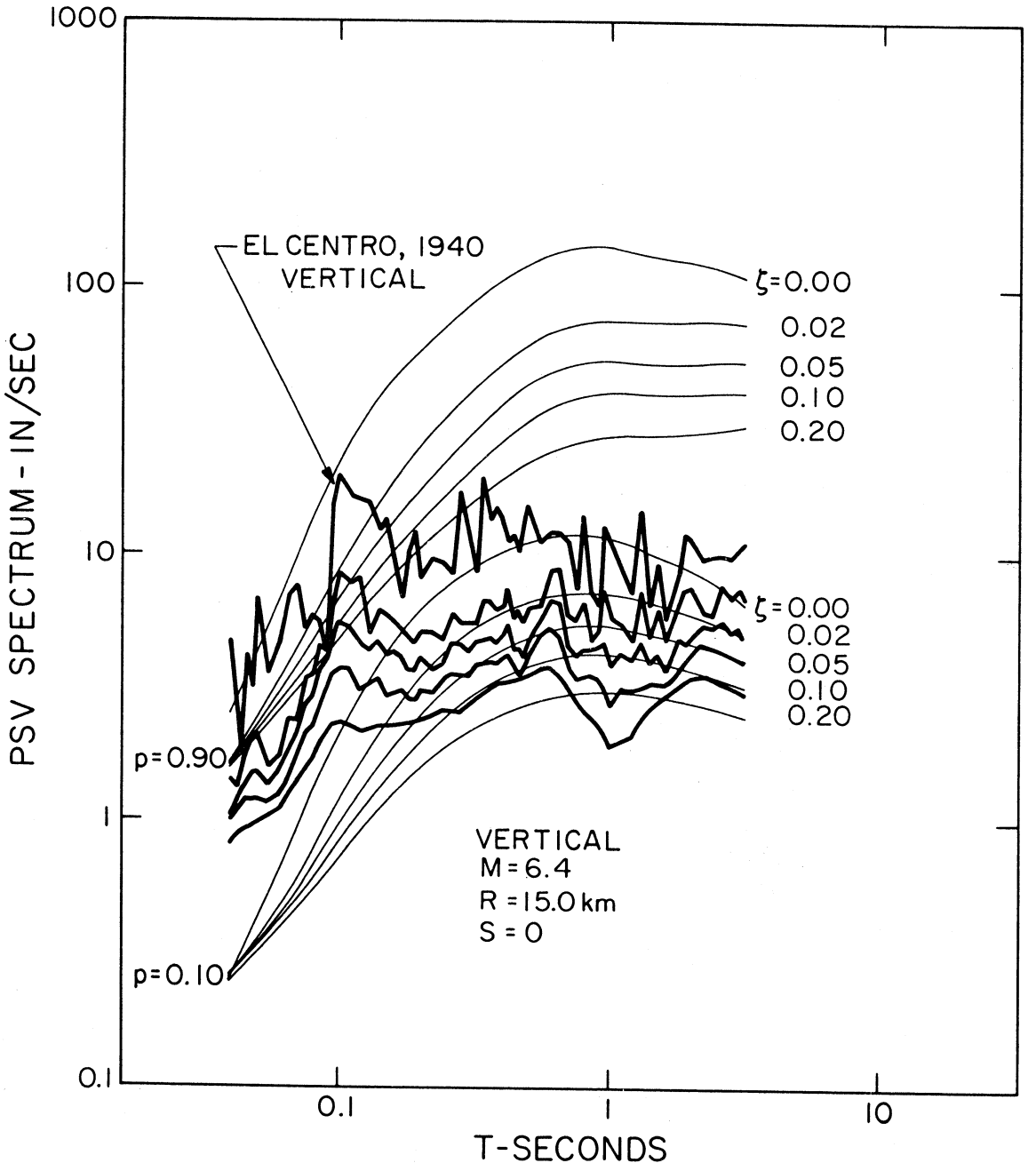
1000
100
10
1
0.1
PSV SPECTRUM - IN/SEC
EL CENTRO, 1940
VERTICAL
ζ=0.00
0.02
0.05
0.10
0.20
ζ=0.00
0.02
0.05
0.10
0.20
p=0.90
p=0.10
VERTICAL
M=6.4
R=15.0 km
S=0
0.1
1
10
T-SECONDS

FIGURE 30

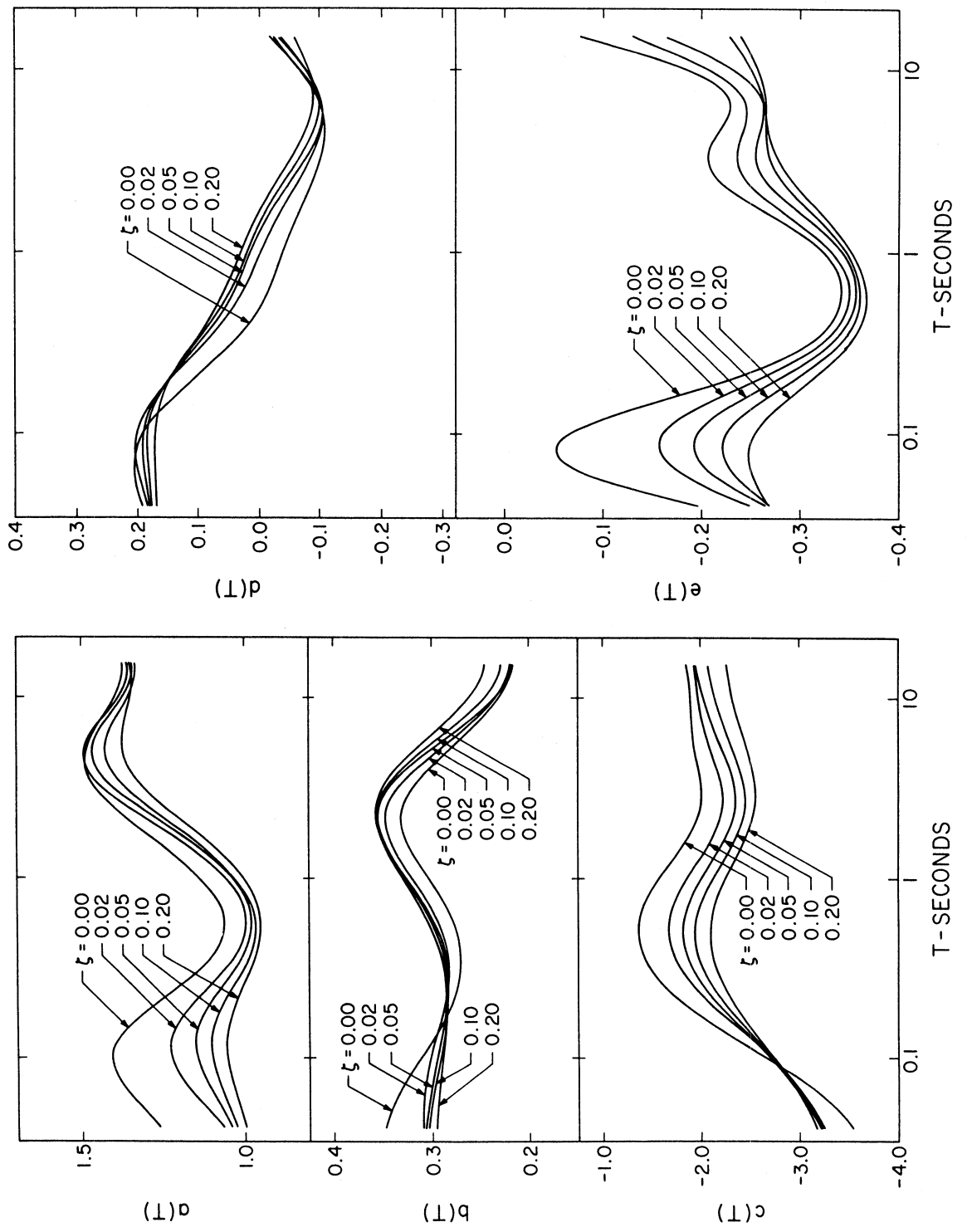

FIGURE 31

TABLE IV

Regression Parameters for Equation (2) and $\alpha(T)$, $\beta(T)$ and $N(T)^*$ at Eleven Selected Periods

$\log_{10}T$(sec)	-1.398	-1.171	-0.943	-0.716	-0.489	-0.261	-0.034	0.193	0.420	0.648	0.875
ζ = 0.0											
a(T)	1.262	1.376	1.400	1.274	1.120	1.061	1.126	1.271	1.428	1.493	1.440
b(T)	0.348	0.331	0.303	0.280	0.271	0.278	0.301	0.327	0.328	0.296	0.251
c(T)	-3.546	-3.129	-2.482	-1.858	-1.467	-1.370	-1.537	-1.829	-1.995	-1.995	-1.897
d(T)	0.193	0.206	0.180	0.114	0.043	-0.007	-0.034	-0.061	-0.090	-0.106	-0.091
e(T)	-0.197	-0.063	-0.090	-0.219	-0.313	-0.342	-0.331	-0.275	-0.214	-0.216	-0.224
α(T)	2.631	2.537	2.529	2.605	2.641	3.885	3.866	3.780	3.562	3.424	3.496
β(T)	-1.163	-1.134	-1.144	-1.182	-1.187	-2.456	-2.462	-2.454	-2.362	-2.284	-2.308
N(T)	2	2	2	2	2	1	1	1	1	1	1
ζ = 0.02											
a(T)	1.065	1.177	1.228	1.160	1.048	0.996	1.048	1.195	1.389	1.495	1.442
b(T)	0.310	0.307	0.298	0.287	0.283	0.293	0.317	0.343	0.344	0.307	0.256
c(T)	-3.276	-3.037	-2.606	-2.122	-1.775	-1.677	-1.823	-2.082	-2.216	-2.132	-2.006
d(T)	0.184	0.203	0.196	0.150	0.087	0.036	0.004	-0.028	-0.068	-0.100	-0.094
e(T)	-0.249	-0.168	-0.171	-0.251	-0.325	-0.350	-0.338	-0.290	-0.242	-0.241	-0.239
α(T)	2.612	2.574	2.572	2.642	3.642	3.841	3.773	3.713	3.558	3.450	3.483
β(T)	-1.167	-1.159	-1.171	-1.203	-1.200	-2.444	-2.419	-2.425	-2.367	-2.302	-2.296
N(T)	2	2	2	2	2	1	1	1	1	1	1
ζ = 0.05											
a(T)	1.041	1.109	1.151	1.107	1.021	0.979	1.027	1.165	1.354	1.467	1.425
b(T)	0.307	0.300	0.292	0.285	0.284	0.297	0.323	0.350	0.352	0.317	0.262
c(T)	-3.253	-2.996	-2.604	-2.189	-1.895	-1.821	-1.970	-2.217	-2.347	-2.256	-2.090
d(T)	0.180	0.191	0.188	0.152	0.097	0.049	0.020	-0.011	-0.056	-0.096	-0.098
e(T)	-0.265	-0.201	-0.205	-0.271	-0.334	-0.356	-0.348	-0.306	-0.261	-0.258	-0.258
α(T)	2.612	2.562	2.567	2.627	2.656	3.859	3.772	3.696	3.560	3.420	3.366
β(T)	-1.170	-1.149	-1.163	-1.202	-1.208	-2.457	-2.418	-2.414	-2.364	-2.280	-2.227
N(T)	2	2	2	2	2	1	1	1	1	1	1

TABLE IV (Continued)

ζ = 0.10

a(T)	1.026	1.074	1.103	1.068	0.996	0.996	1.021	1.150	1.320	1.427	1.399
b(T)	0.304	0.297	0.289	0.284	0.286	0.299	0.325	0.351	0.355	0.322	0.270
c(T)	-3.232	-2.983	-2.623	-2.256	-2.001	-1.943	-2.088	-2.322	-2.443	-2.357	-2.201
d(T)	0.177	0.183	0.181	0.152	0.103	0.056	0.026	-0.003	-0.045	-0.086	-0.093
e(T)	-0.270	-0.226	-0.234	-0.289	-0.343	-0.361	-0.351	-0.317	-0.278	-0.265	-0.264
α(T)	2.614	2.578	2.575	2.623	2.652	3.866	3.794	3.708	3.542	3.390	3.334
β(T)	-1.173	-1.156	-1.163	-1.194	-1.203	-2.460	-2.433	-2.416	-2.346	-2.259	-2.211
N(T)	2	2	2	2	2	1	1	1	1	1	1

ζ = 0.20

a(T)	0.997	1.035	1.055	1.028	0.976	0.952	0.993	1.110	1.269	1.370	1.369
b(T)	0.296	0.292	0.287	0.285	0.289	0.304	0.327	0.351	0.356	0.330	0.283
c(T)	-3.172	-2.955	-2.649	-2.345	-2.141	-2.098	-2.221	-2.423	-2.544	-2.495	-2.370
d(T)	0.169	0.171	0.169	0.148	0.107	0.065	0.036	0.007	-0.033	-0.072	-0.087
e(T)	-0.268	-0.247	-0.262	-0.308	-0.352	-0.367	-0.357	-0.326	-0.288	-0.269	-0.260
α(T)	2.593	2.586	2.601	2.628	2.639	3.855	3.770	3.686	3.552	3.394	3.319
β(T)	-1.166	-1.166	-1.180	-1.200	-1.200	-2.456	-2.412	-2.394	-2.348	-2.262	-2.204
N(T)	2	2	2	2	2	1	1	1	1	1	1

* See section entitled "Distribution of Spectral Amplitudes" for definition of α(T), β(T) and N(T).

analysis based on equation (2) and the data on PSV amplitudes. The functions a(T), b(T), .., e(T) have been computed at 91 periods for which PSV spectra are available (Trifunac and Lee, 1973) and then low-pass filtered along $\log_{10}T$ axis with an Ormsby filter. Figure 31 shows the resulting smoothed functions for ζ = 0.0, 0.02, 0.05, 0.10 and 0.20. Table IV presents the amplitudes of these functions and of $\alpha(T)$, $\beta(T)$ and N(T) (see the following section entitled, "Distribution of Spectral Amplitudes" for definition of $\alpha(T)$, $\beta(T)$ and N(T)) at eleven selected periods.

Equation (2) assumes linear dependence of PSV amplitudes on Modified Mercalli Intensity levels, I_{MM}. This assumption is the same as in several other related regression analyses which are all based on MMI as a scaling parameter. In this report, it should be noted again that there is no known direct physical basis which would support the assumption we use here that MMI levels can be assigned to a linear numerical scale ranging from 1 to 12. It appears, however, that the departures from such simple assignment, as judged from the available data, may not be significant (Trifunac, 1976b; Trifunac and Anderson, 1977). Several recent studies of the overall uncertainties in earthquake risk estimates (Anderson, 1978) have shown that the estimates of the uniform risk spectra of FS based on equation (2) lead to the distributions of estimated amplitudes which have smaller standard deviation than their counterparts based on equation (1). This suggests that from the practical viewpoint, the assumptions in equation (2) may not affect the final results in

risk calculations in a significant way.

Functions a(T), b(T), d(T), and e(T) are very similar to the corresponding functions in Figure 34 of Trifunac and Anderson (1977) which present similar correlations but for SA spectra. Functions c(T) differ, however, because $SA \approx \frac{2\pi}{T}$ PSV and because in the analysis of SA, the amplitudes were in units of g, the acceleration of gravity (9.81 m/sec^2, 386 in/sec^2) while in this report, all PSV amplitudes are in in/sec.

Figures 32 through 41 present PSV spectra plotted for the MMI levels ranging from 4 to 12, s=0 (dashed line) and s=2 (full lines), ζ = 0.0, 0.02, 0.05, 0.10 and 0.20 and for p = 0.50. Heavy lines for MMI in the range from 4 to 8 show approximately the range where equation (2) may apply. Outside this range, for MMI >8, essentially no data is now available and curves for MMI = 10 and 12 are only shown for completeness in presentation. Figures 32 through 41 also show the average and average plus one standard deviation of PSV spectrum amplitudes computed from digitization noise. For small MMI levels (4 and 6) PSV spectra intersect the spectra of digitization noise at periods typically longer than 1 to 2 sec. For small intensities and periods, the functions a(T) through e(T) in (2) are affected by the digitization noise and equation (2) ceases to predict accurately PSV amplitudes in this long period range. To illustrate this, the curves for MMI levels assigned to 4 and 6 in Figures 32 through 41 have been drawn only up to the periods where PSV spectra approach the amplitudes of noise spectra. Since a(T)

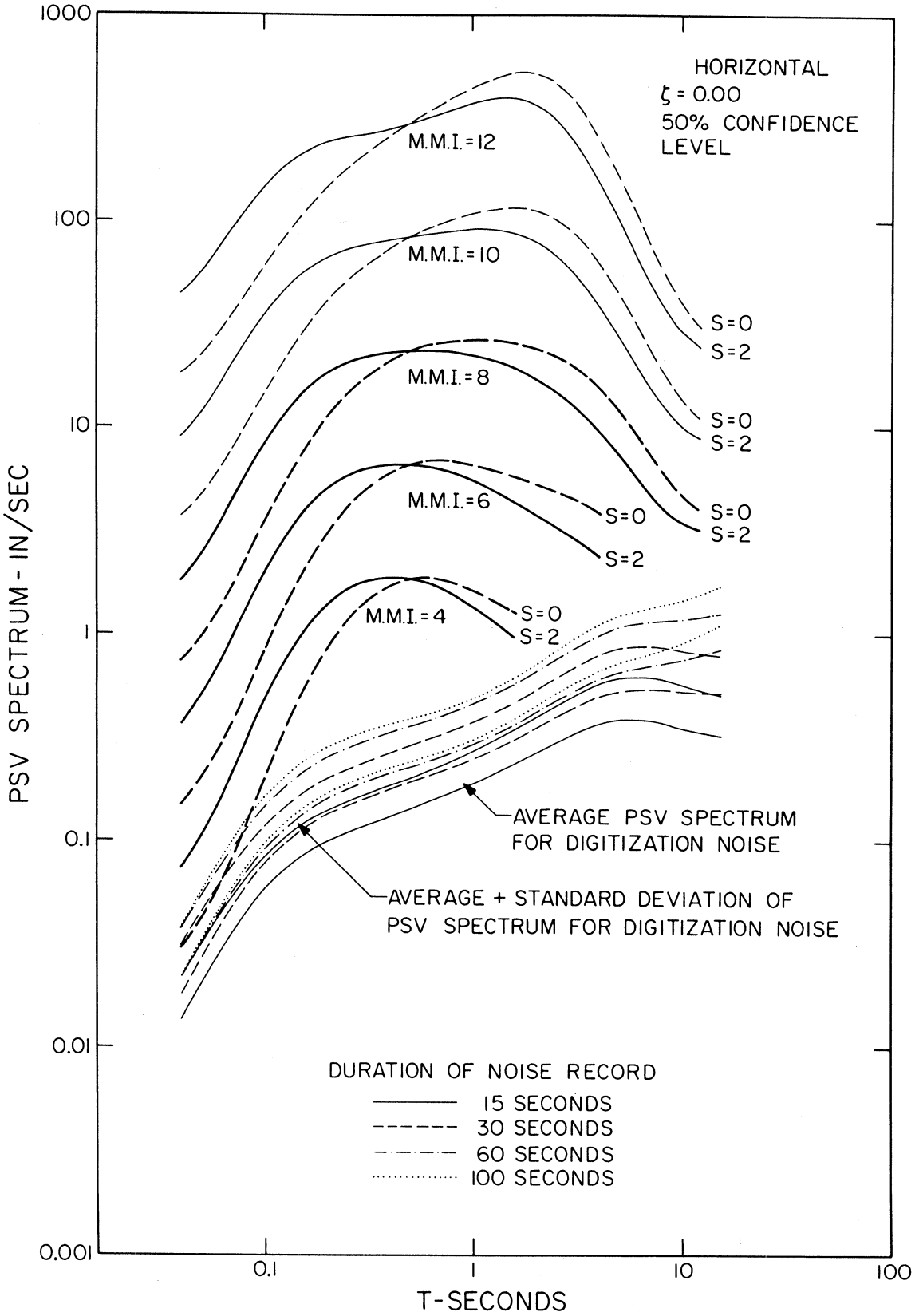
HORIZONTAL
ζ = 0.00
50% CONFIDENCE LEVEL
M.M.I. = 12
M.M.I. = 10
M.M.I. = 8
M.M.I. = 6
M.M.I. = 4
S=0
S=2
AVERAGE PSV SPECTRUM FOR DIGITIZATION NOISE
AVERAGE + STANDARD DEVIATION OF PSV SPECTRUM FOR DIGITIZATION NOISE
DURATION OF NOISE RECORD
15 SECONDS
30 SECONDS
60 SECONDS
100 SECONDS
PSV SPECTRUM - IN/SEC
T-SECONDS
1000
100
10
1
0.1
0.01
0.001
0.1
1
10
100

FIGURE 32

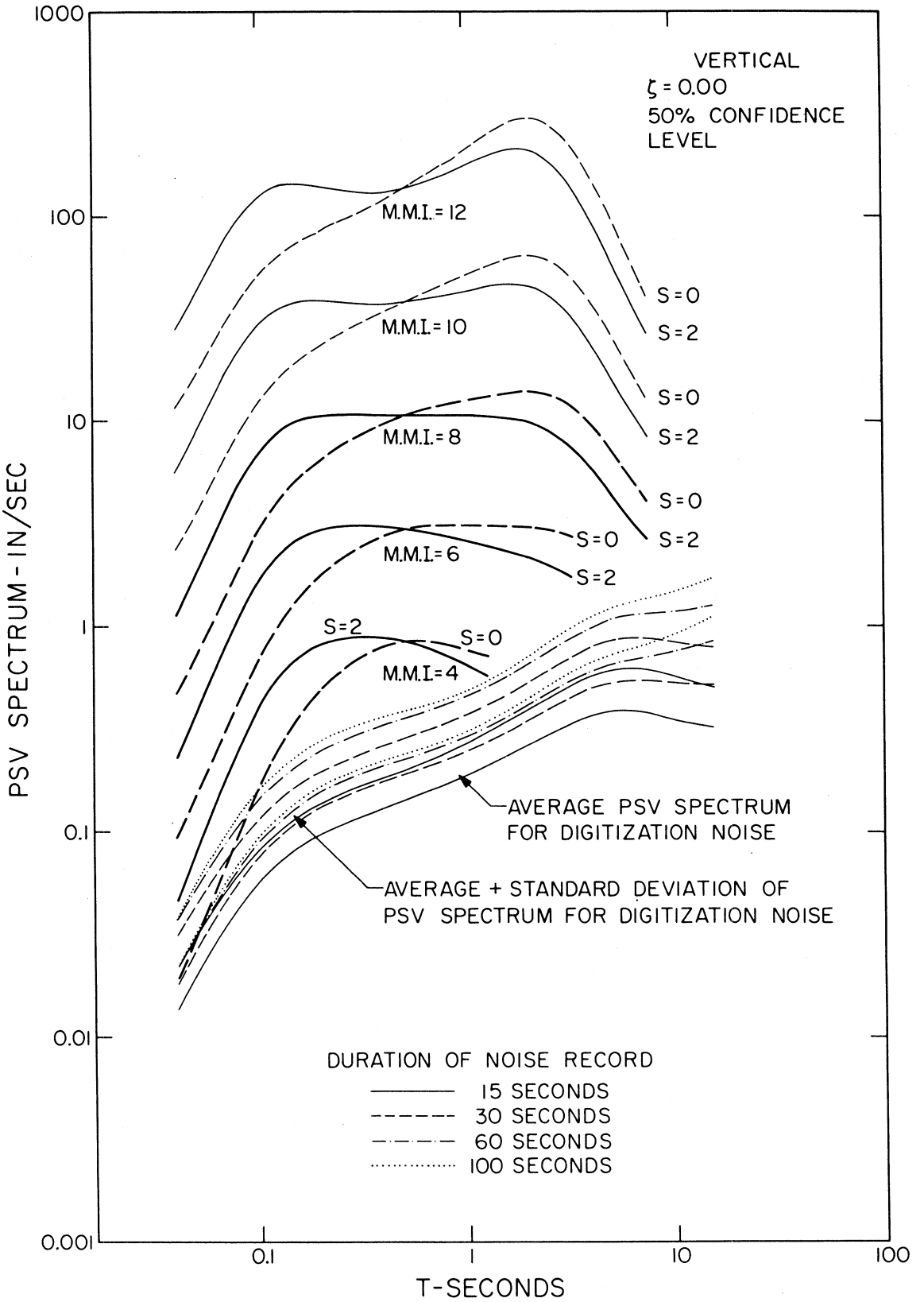
VERTICAL
ζ = 0.00
50% CONFIDENCE LEVEL
M.M.I. = 12
M.M.I. = 10
M.M.I. = 8
M.M.I. = 6
M.M.I. = 4
S = 0
S = 2
AVERAGE PSV SPECTRUM FOR DIGITIZATION NOISE
AVERAGE + STANDARD DEVIATION OF PSV SPECTRUM FOR DIGITIZATION NOISE
DURATION OF NOISE RECORD
15 SECONDS
30 SECONDS
60 SECONDS
100 SECONDS
PSV SPECTRUM - IN/SEC
T-SECONDS
1000
100
10
1
0.1
0.01
0.001
0.1
1
10
100

FIGURE 33

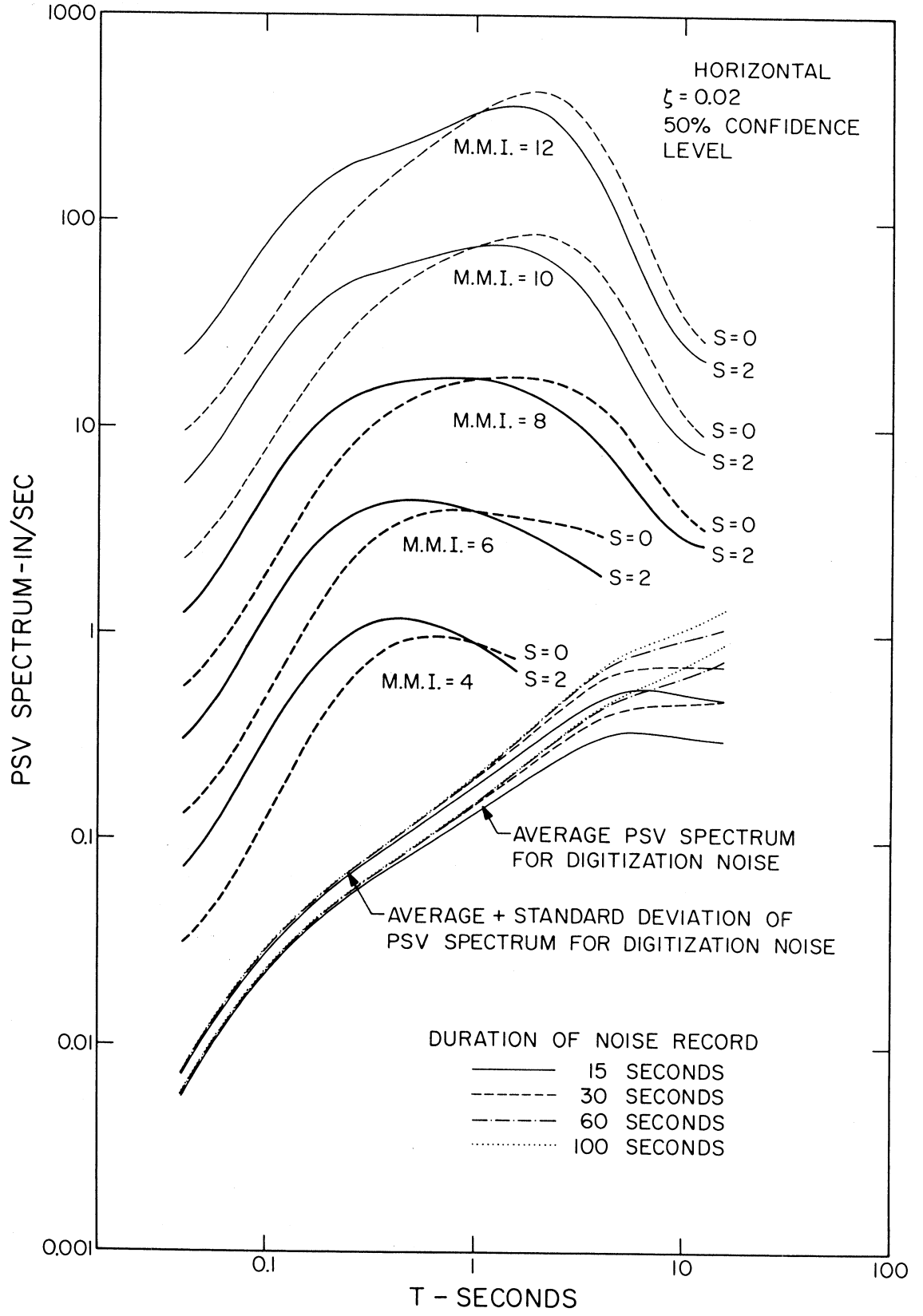
HORIZONTAL
ζ = 0.02
50% CONFIDENCE LEVEL
M.M.I. = 12
M.M.I. = 10
M.M.I. = 8
M.M.I. = 6
M.M.I. = 4
S = 0
S = 2
AVERAGE PSV SPECTRUM FOR DIGITIZATION NOISE
AVERAGE + STANDARD DEVIATION OF PSV SPECTRUM FOR DIGITIZATION NOISE
DURATION OF NOISE RECORD
15 SECONDS
30 SECONDS
60 SECONDS
100 SECONDS
PSV SPECTRUM-IN/SEC
T - SECONDS
1000
100
10
1
0.1
0.01
0.001
0.1
1
10
100

FIGURE 34

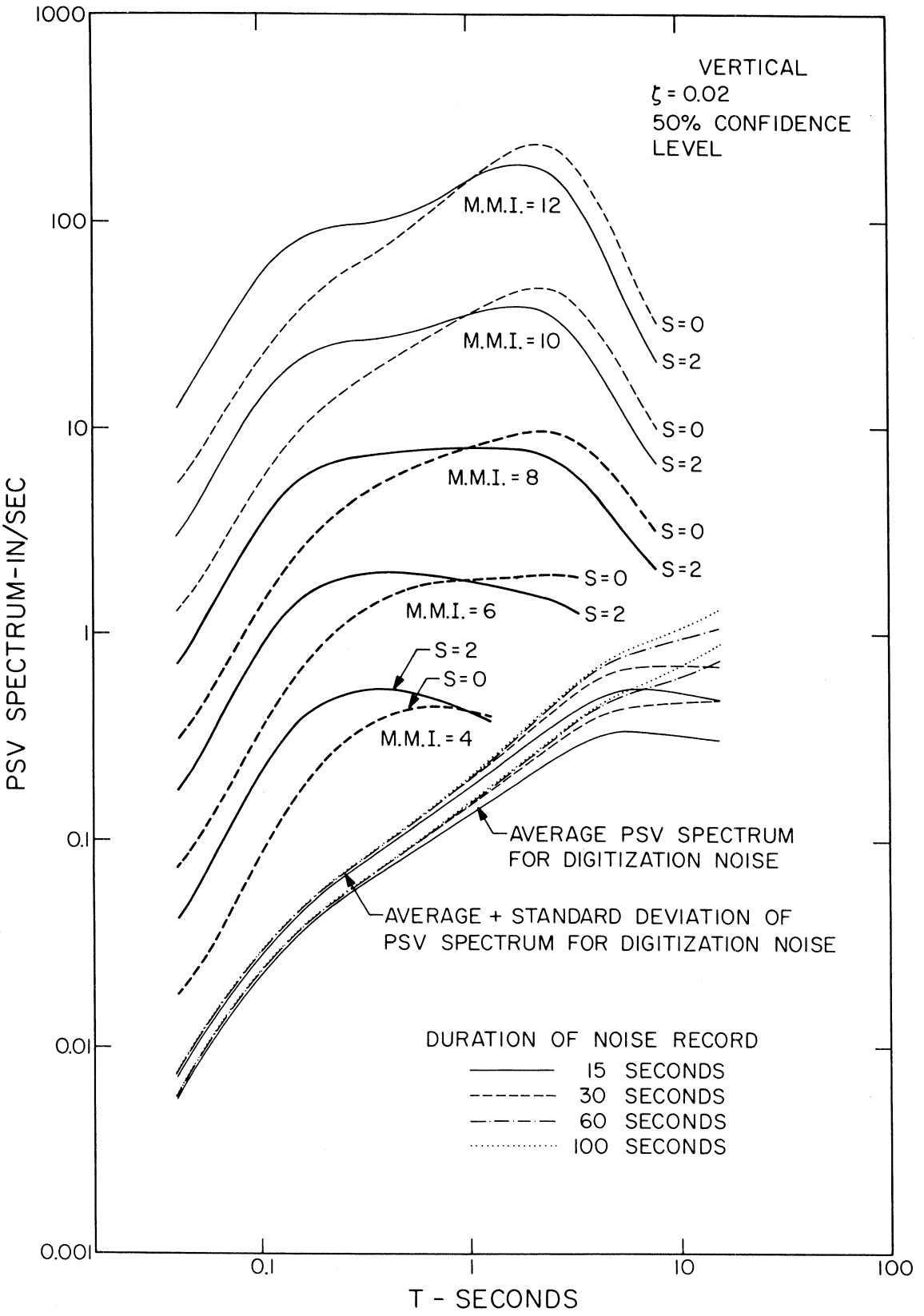
VERTICAL
ζ = 0.02
50% CONFIDENCE LEVEL
M.M.I. = 12
M.M.I. = 10
M.M.I. = 8
M.M.I. = 6
M.M.I. = 4
S = 0
S = 2
AVERAGE PSV SPECTRUM FOR DIGITIZATION NOISE
AVERAGE + STANDARD DEVIATION OF PSV SPECTRUM FOR DIGITIZATION NOISE
DURATION OF NOISE RECORD
15 SECONDS
30 SECONDS
60 SECONDS
100 SECONDS
PSV SPECTRUM-IN/SEC
T - SECONDS
1000
100
10
1
0.1
0.01
0.001
0.1
1
10
100

FIGURE 35

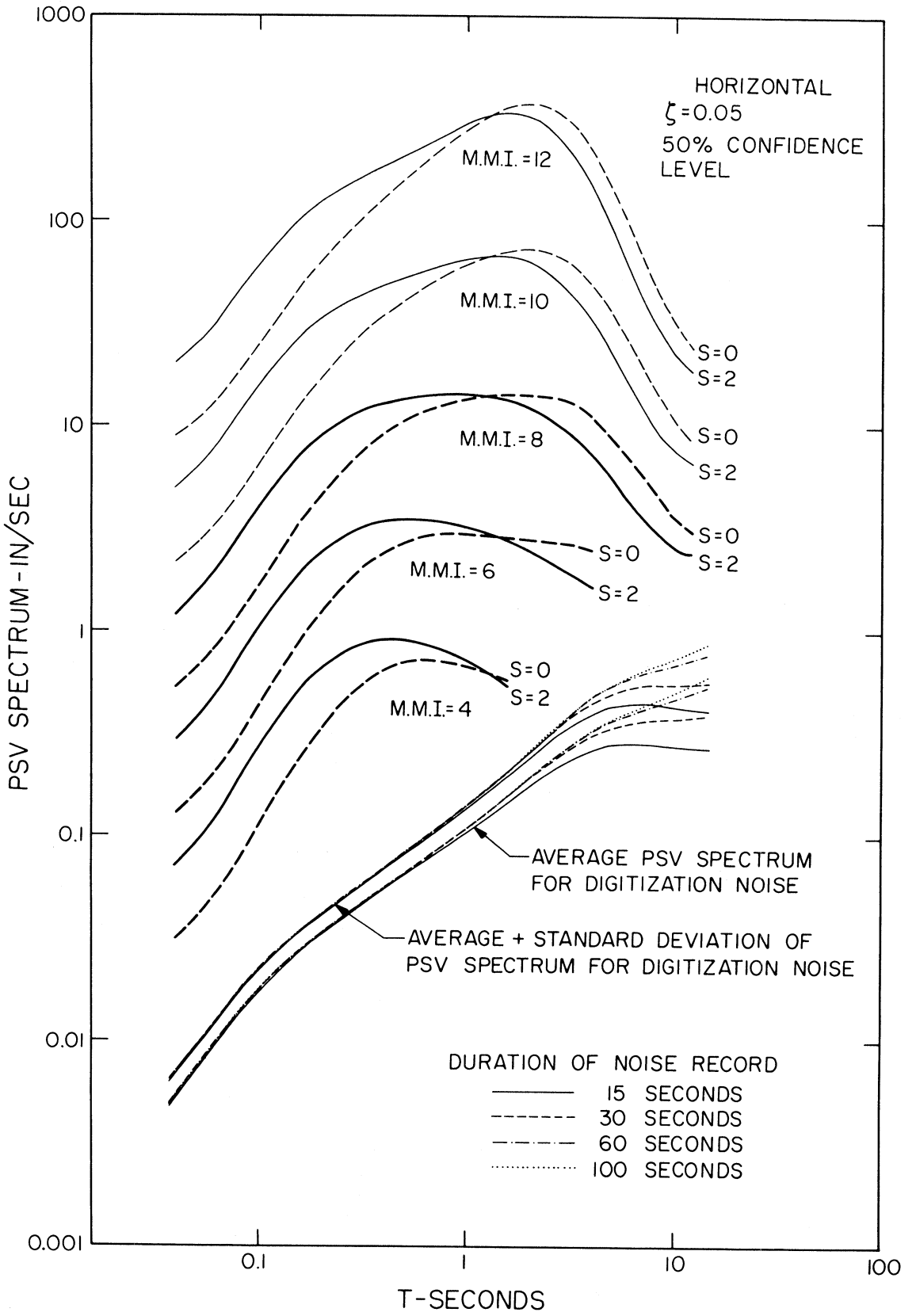
HORIZONTAL
ζ=0.05
50% CONFIDENCE LEVEL
M.M.I.=12
M.M.I.=10
M.M.I.=8
M.M.I.=6
M.M.I.=4
S=0
S=2
AVERAGE PSV SPECTRUM FOR DIGITIZATION NOISE
AVERAGE + STANDARD DEVIATION OF PSV SPECTRUM FOR DIGITIZATION NOISE
DURATION OF NOISE RECORD
15 SECONDS
30 SECONDS
60 SECONDS
100 SECONDS
PSV SPECTRUM-IN/SEC
T-SECONDS
1000
100
10
1
0.1
0.01
0.001
0.1
1
10
100

FIGURE 36

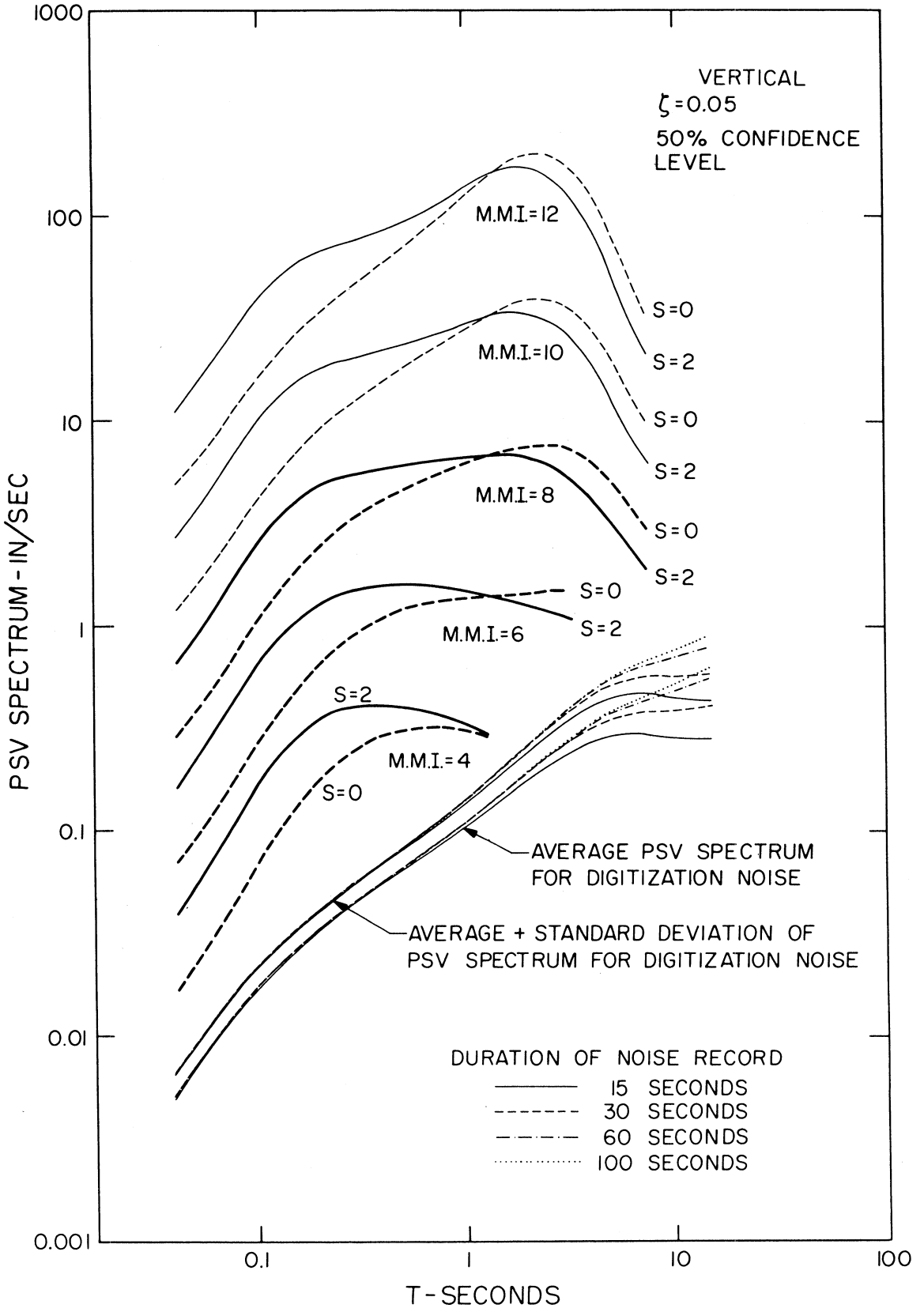
VERTICAL
ζ=0.05
50% CONFIDENCE LEVEL
M.M.I.=12
S=0
S=2
M.M.I.=10
S=0
S=2
M.M.I.=8
S=0
S=2
M.M.I.=6
S=0
S=2
M.M.I.=4
S=2
S=0
AVERAGE PSV SPECTRUM FOR DIGITIZATION NOISE
AVERAGE + STANDARD DEVIATION OF PSV SPECTRUM FOR DIGITIZATION NOISE
DURATION OF NOISE RECORD
15 SECONDS
30 SECONDS
60 SECONDS
100 SECONDS
PSV SPECTRUM - IN/SEC
1000
100
10
1
0.1
0.01
0.001
0.1
1
10
100
T-SECONDS

FIGURE 37

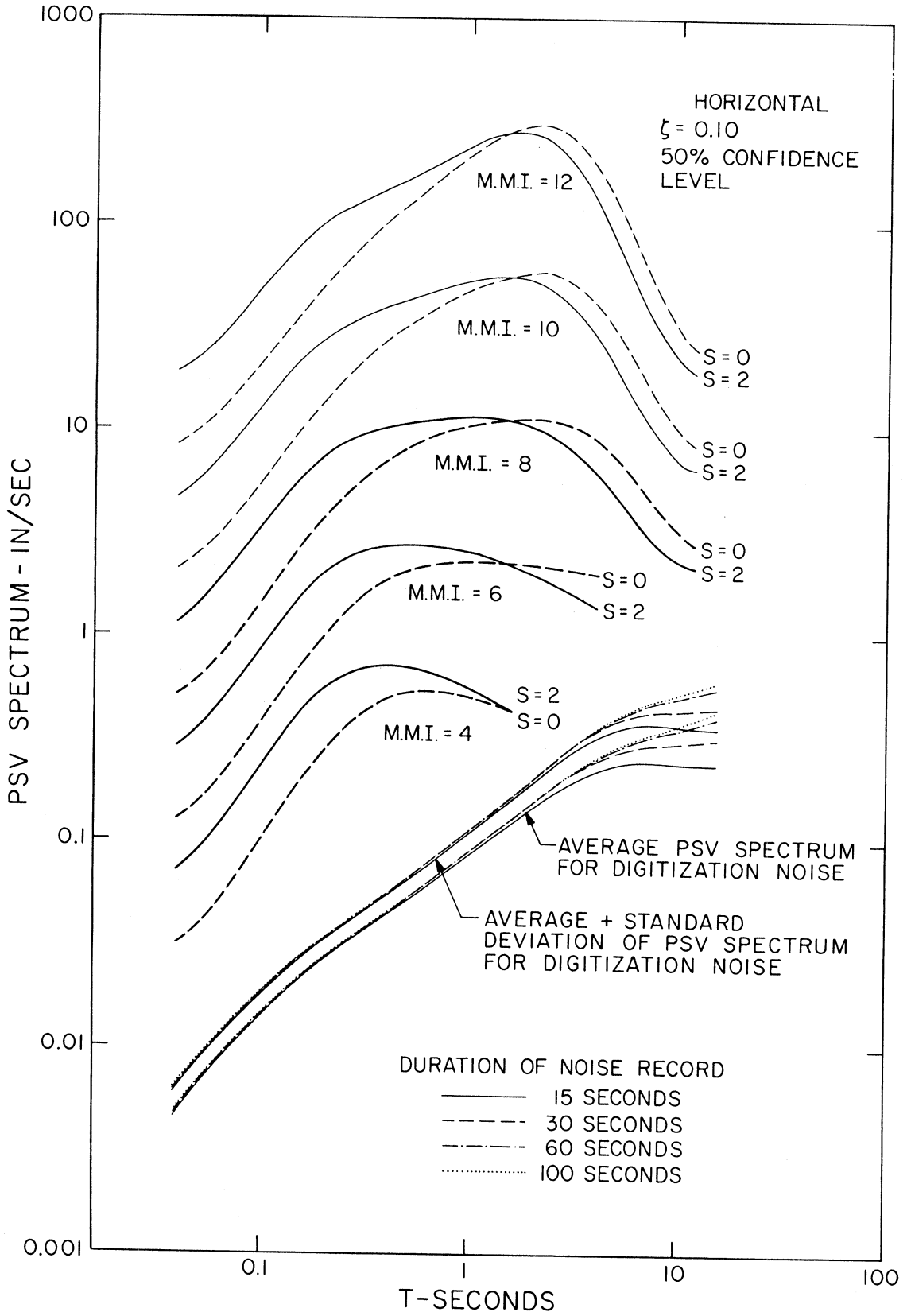
HORIZONTAL
ζ = 0.10
50% CONFIDENCE LEVEL
M.M.I. = 12
M.M.I. = 10
M.M.I. = 8
M.M.I. = 6
M.M.I. = 4
S = 0
S = 2
AVERAGE PSV SPECTRUM FOR DIGITIZATION NOISE
AVERAGE + STANDARD DEVIATION OF PSV SPECTRUM FOR DIGITIZATION NOISE
DURATION OF NOISE RECORD
15 SECONDS
30 SECONDS
60 SECONDS
100 SECONDS
PSV SPECTRUM - IN/SEC
T-SECONDS
1000
100
10
1
0.1
0.01
0.001
0.1
1
10
100

FIGURE 38

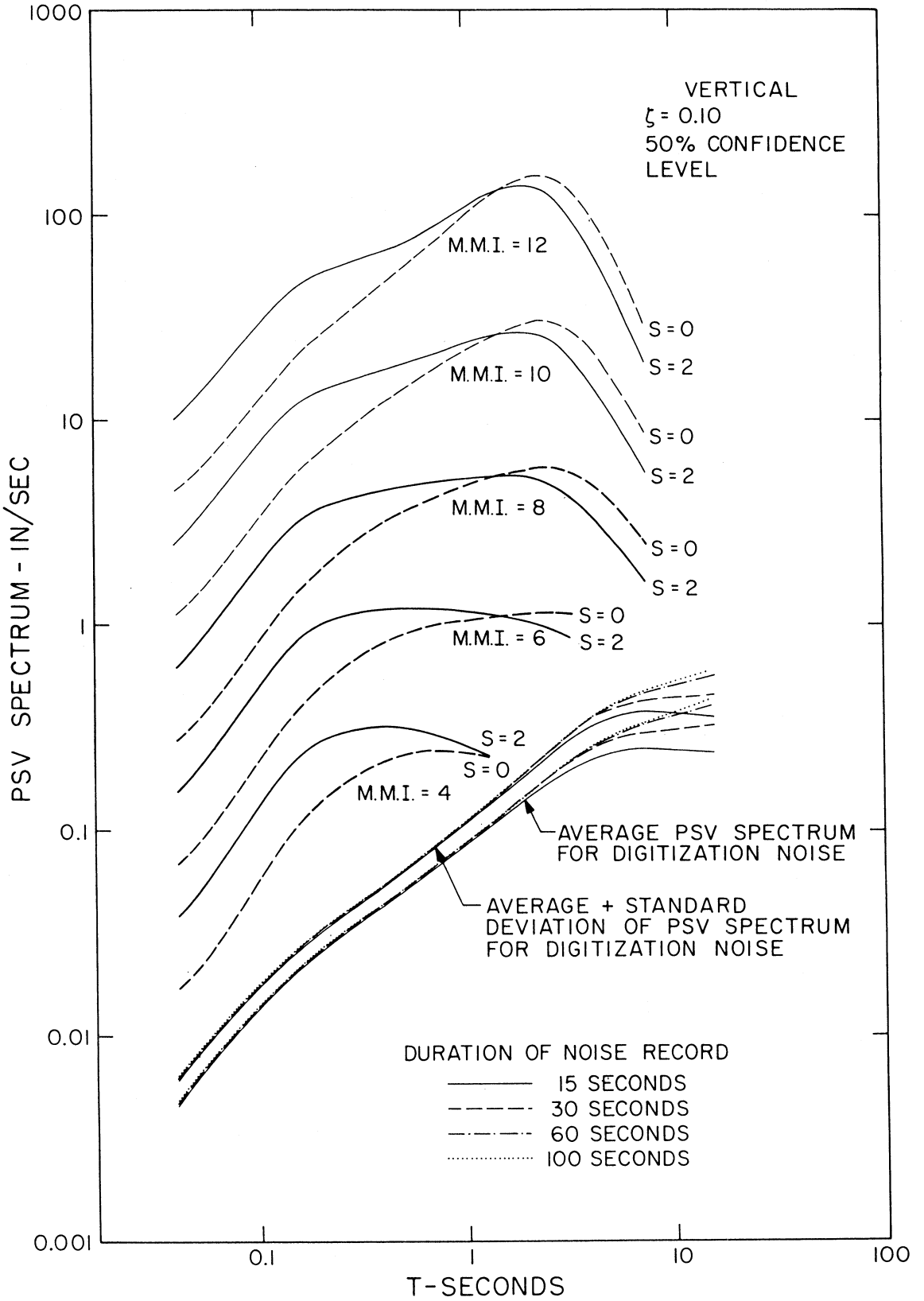
VERTICAL
ζ = 0.10
50% CONFIDENCE LEVEL
M.M.I. = 12
M.M.I. = 10
M.M.I. = 8
M.M.I. = 6
M.M.I. = 4
S = 0
S = 2
AVERAGE PSV SPECTRUM FOR DIGITIZATION NOISE
AVERAGE + STANDARD DEVIATION OF PSV SPECTRUM FOR DIGITIZATION NOISE
DURATION OF NOISE RECORD
15 SECONDS
30 SECONDS
60 SECONDS
100 SECONDS
PSV SPECTRUM - IN/SEC
T-SECONDS
1000
100
10
1
0.1
0.01
0.001
0.1
1
10
100

FIGURE 39

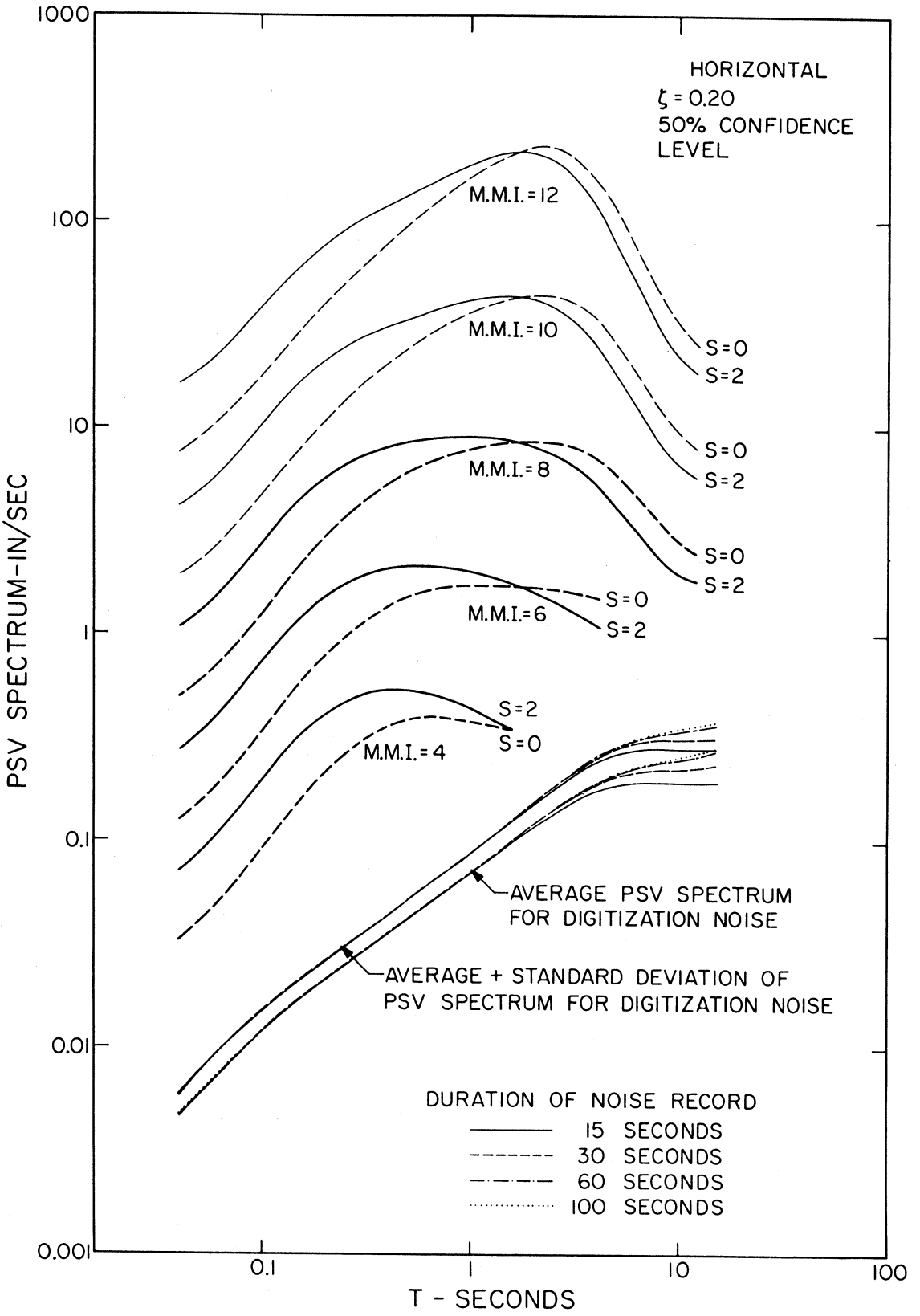
HORIZONTAL
ζ = 0.20
50% CONFIDENCE LEVEL
M.M.I. = 12
M.M.I. = 10
M.M.I. = 8
M.M.I. = 6
M.M.I. = 4
S=0
S=2
AVERAGE PSV SPECTRUM FOR DIGITIZATION NOISE
AVERAGE + STANDARD DEVIATION OF PSV SPECTRUM FOR DIGITIZATION NOISE
DURATION OF NOISE RECORD
15 SECONDS
30 SECONDS
60 SECONDS
100 SECONDS
PSV SPECTRUM-IN/SEC
T - SECONDS
1000
100
10
1
0.1
0.01
0.001
0.1
1
10
100

FIGURE 40

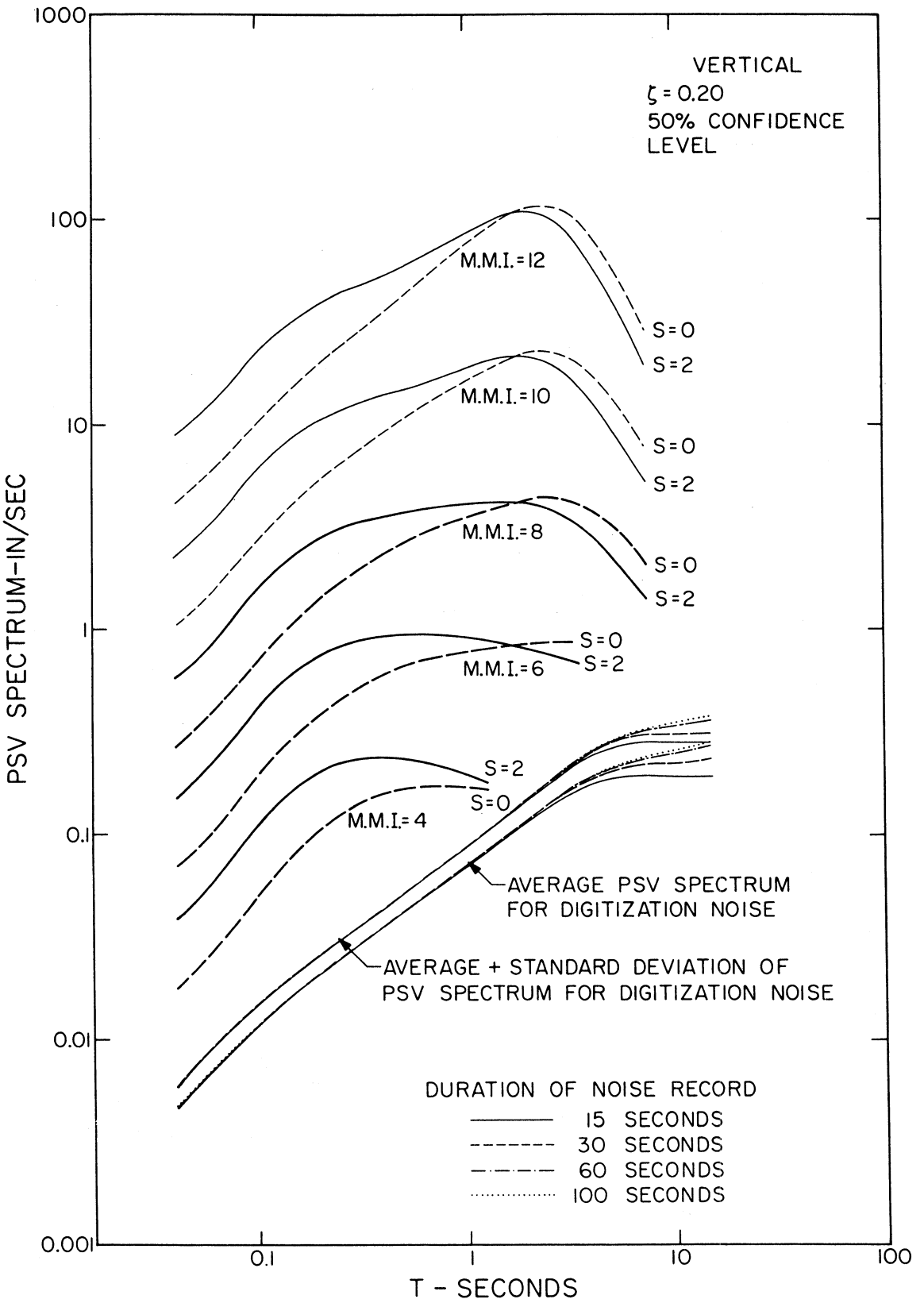
VERTICAL
ζ = 0.20
50% CONFIDENCE LEVEL
M.M.I. = 12
S = 0
S = 2
M.M.I. = 10
S = 0
S = 2
M.M.I. = 8
S = 0
S = 2
M.M.I. = 6
S = 0
S = 2
M.M.I. = 4
S = 2
S = 0
AVERAGE PSV SPECTRUM FOR DIGITIZATION NOISE
AVERAGE + STANDARD DEVIATION OF PSV SPECTRUM FOR DIGITIZATION NOISE
DURATION OF NOISE RECORD
15 SECONDS
30 SECONDS
60 SECONDS
100 SECONDS
PSV SPECTRUM-IN/SEC
1000
100
10
1
0.1
0.01
0.001
0.1
1
10
100
T - SECONDS

FIGURE 41

is between 1.3 and 1.5 in this period range the 80% confidence interval for PSV amplitudes covers approximately one order of magnitude and the period where a PSV spectrum for a chosen p will intersect the noise spectrum will clearly depend on p. The estimates based on equation (2) should then be considered only if the results are above the noise spectra.

Figures 42 through 47 present selected examples of the comparison of the PSV spectra computed from equation (2) and the spectra of recorded accelerations and illustrate the width of the 80% confidence interval for PSV amplitudes. PSV spectra of accelerations recorded at the Pacoima Dam site are in fair agreement with the extrapolated spectral amplitudes at MMI = 10. The amplitudes and the shapes of the PSV spectra for El Centro accelerograms, even though not inconsistent with the estimates based on equation (2) suggest that a more detailed scaling, perhaps involving a number of source mechanism parameters, may be required to describe PSV spectra in this case.

The data which is now available for scaling of any characteristic of strong ground motion in terms of MMI scale is perhaps marginally adequate to describe MMI levels V, VI and VII. Few data points that are available for MMI = IV and VIII suggest that various regression equations derived from data for MMI = V, VI and VII are most probably applicable to the whole range from MMI = IV to VIII. For greater intensities there are essentially no measurements and the lack of any known physical basis for extrapolation beyond MMI = VIII further limits our ability to develop some other inferences on how to scale PSV amplitudes in that range. In the two

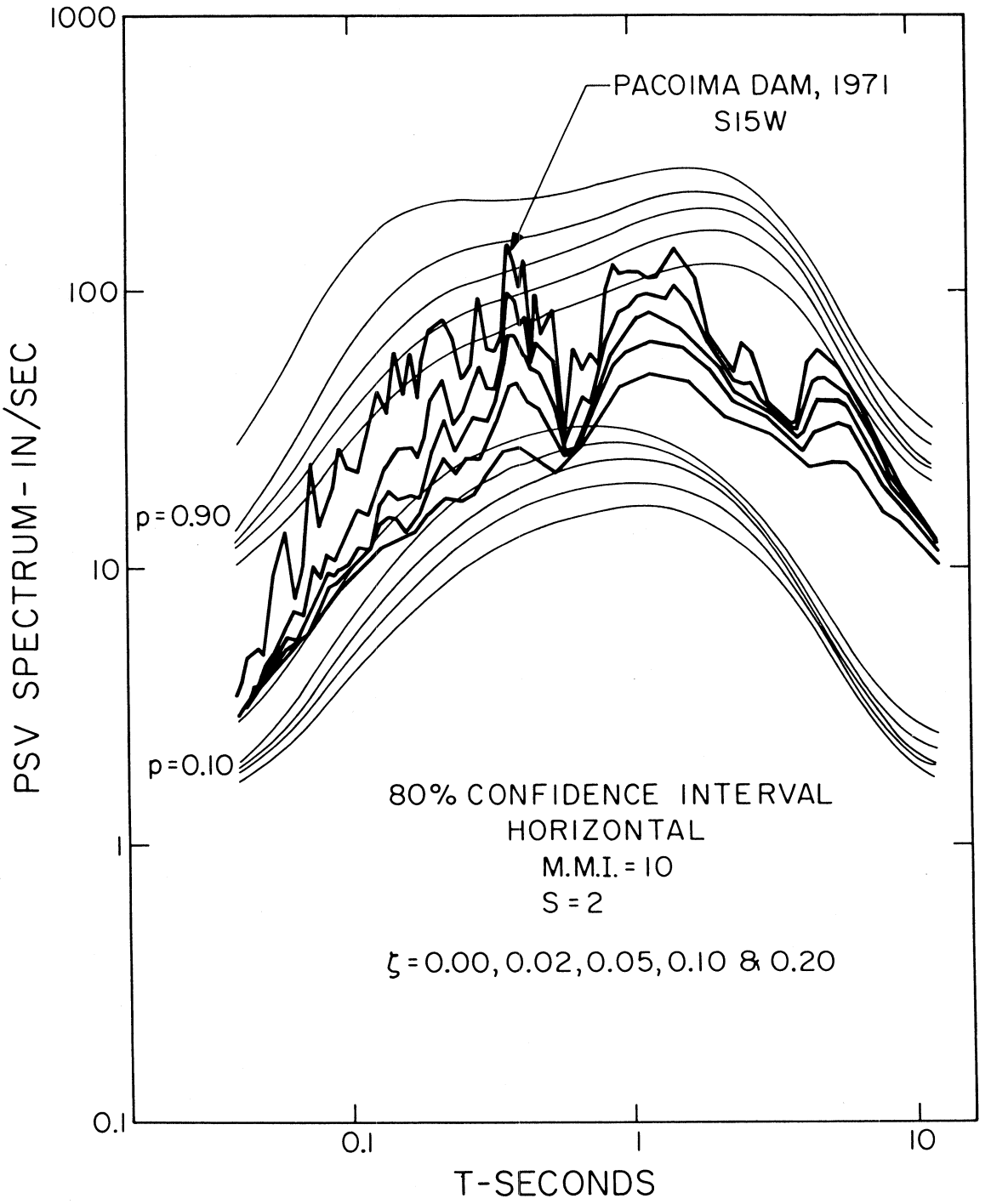
1000
100
10
1
0.1
PSV SPECTRUM - IN/SEC
PACOIMA DAM, 1971
S15W
p = 0.90
p = 0.10
80% CONFIDENCE INTERVAL
HORIZONTAL
M.M.I. = 10
S = 2
ζ = 0.00, 0.02, 0.05, 0.10 & 0.20
0.1
1
10
T-SECONDS

FIGURE 42

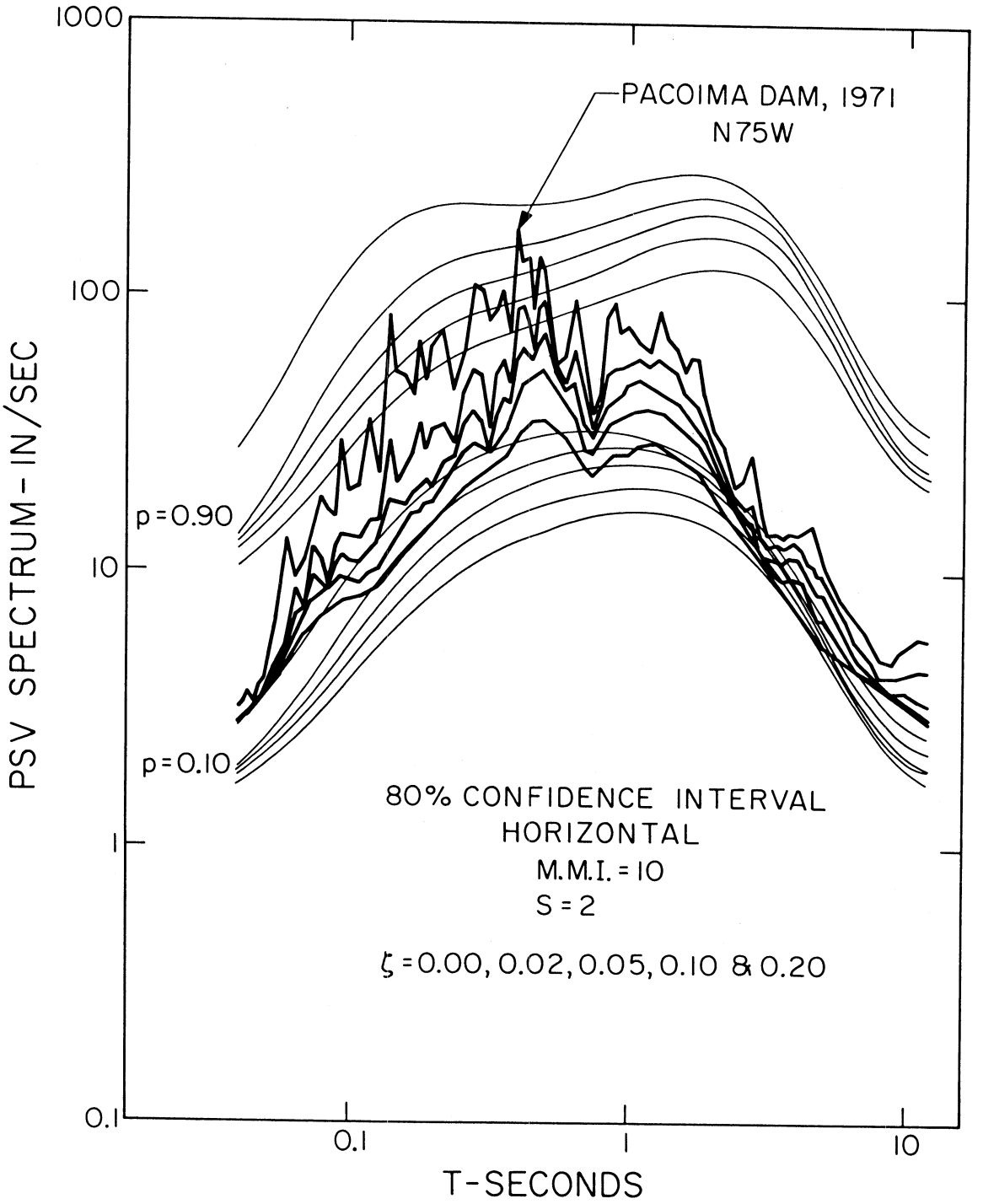
1000
100
10
1
0.1
PSV SPECTRUM - IN/SEC
PACOIMA DAM, 1971
N75W
p = 0.90
p = 0.10
80% CONFIDENCE INTERVAL
HORIZONTAL
M.M.I. = 10
S = 2
ζ = 0.00, 0.02, 0.05, 0.10 & 0.20
0.1
1
10
T-SECONDS

FIGURE 43

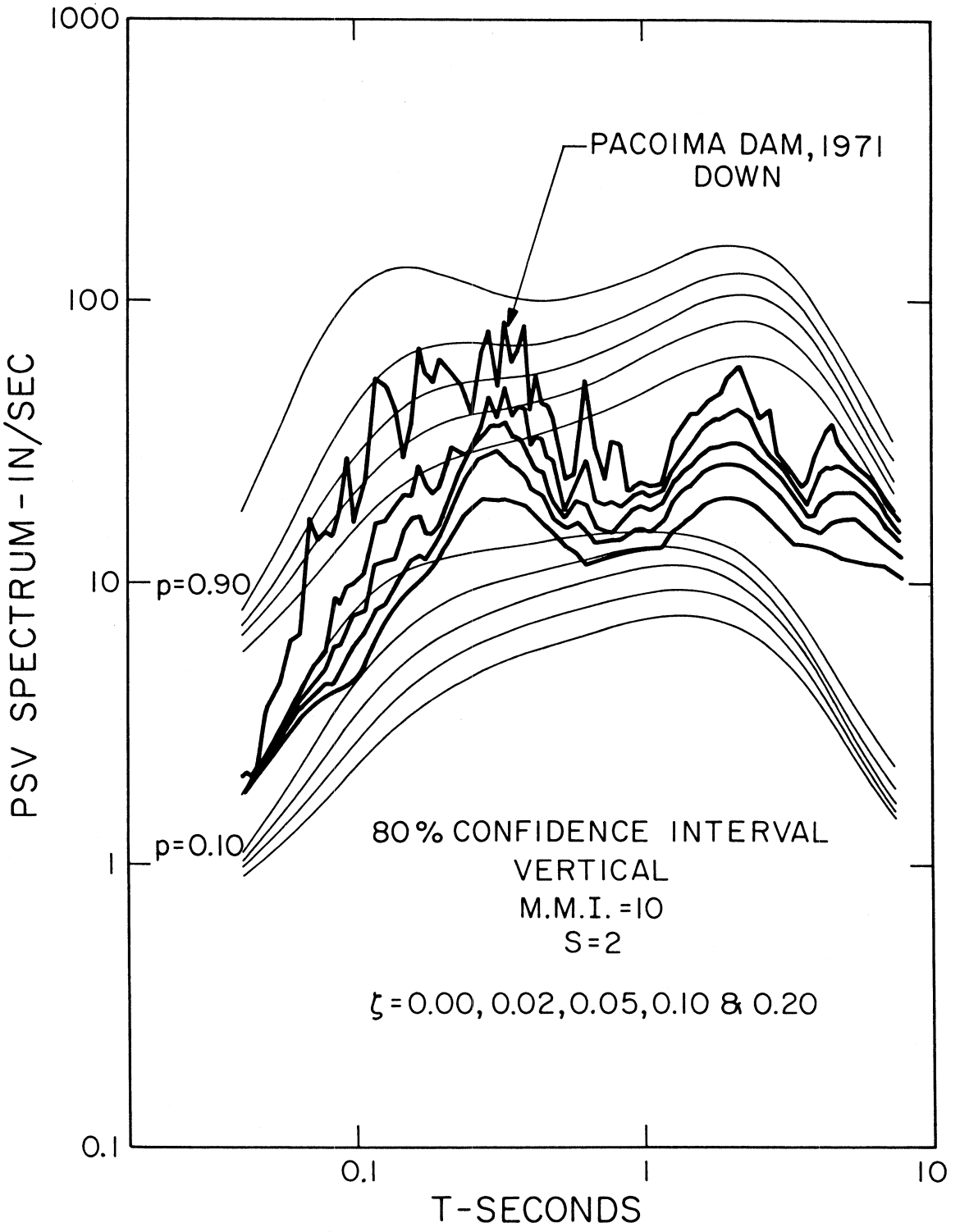
1000
100
10
1
0.1
PSV SPECTRUM - IN/SEC
PACOIMA DAM, 1971
DOWN
p=0.90
p=0.10
80% CONFIDENCE INTERVAL
VERTICAL
M.M.I. =10
S=2
ζ = 0.00, 0.02, 0.05, 0.10 & 0.20
0.1
1
10
T-SECONDS

FIGURE 44

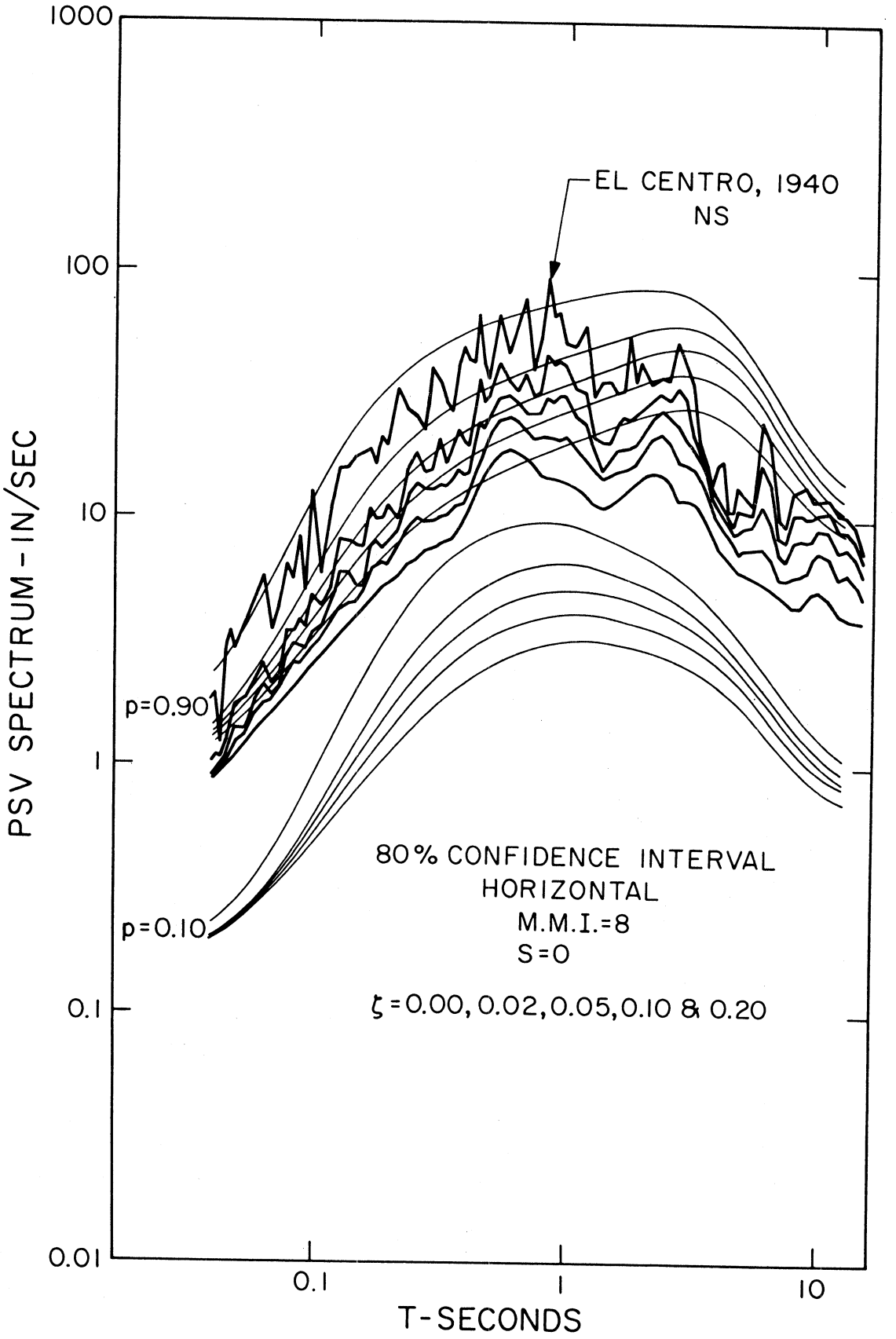
1000
100
10
1
0.1
0.01
PSV SPECTRUM - IN/SEC
EL CENTRO, 1940
NS
p=0.90
p=0.10
80% CONFIDENCE INTERVAL
HORIZONTAL
M.M.I.=8
S=0
ζ=0.00, 0.02, 0.05, 0.10 & 0.20
0.1
1
10
T-SECONDS

FIGURE 45

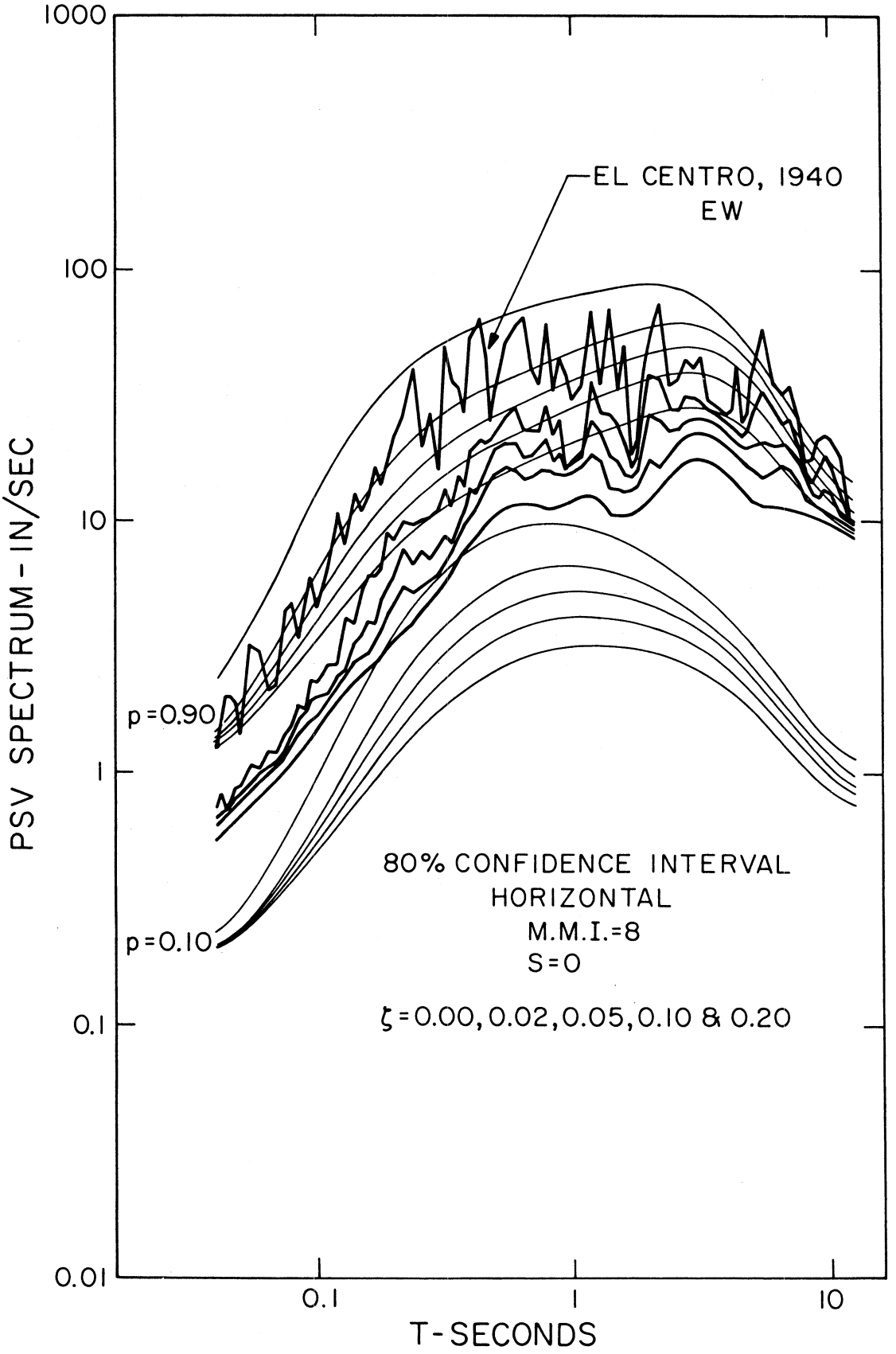
1000
100
10
1
0.1
0.01
PSV SPECTRUM - IN/SEC
EL CENTRO, 1940
EW
p=0.90
p=0.10
80% CONFIDENCE INTERVAL
HORIZONTAL
M.M.I.=8
S=0
ζ=0.00, 0.02, 0.05, 0.10 & 0.20
0.1
1
10
T-SECONDS

FIGURE 46

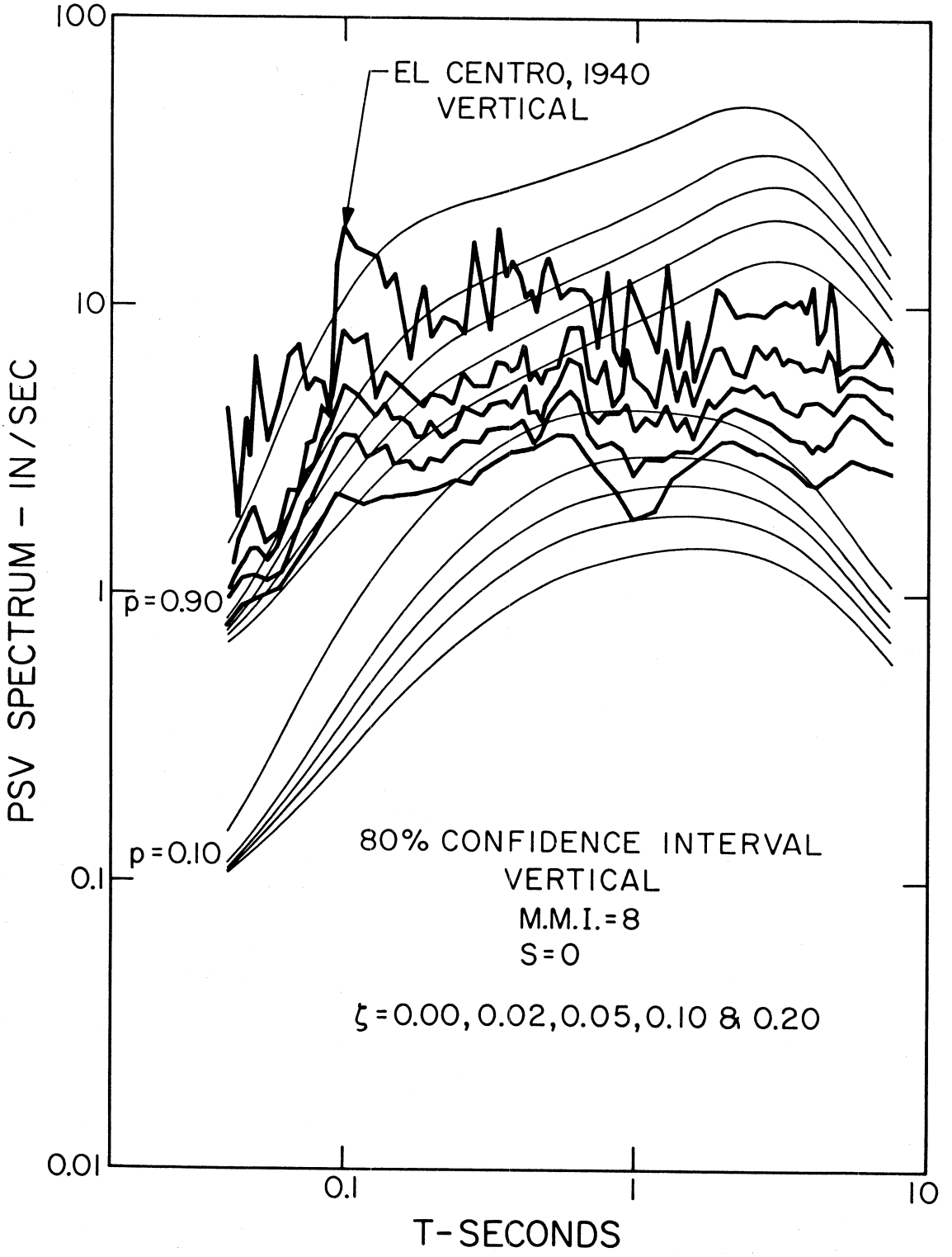
100
10
1
0.1
0.01
PSV SPECTRUM - IN/SEC
EL CENTRO, 1940
VERTICAL
p=0.90
p=0.10
80% CONFIDENCE INTERVAL
VERTICAL
M.M.I.=8
S=0
ζ=0.00, 0.02, 0.05, 0.10 & 0.20
0.1
1
10
T-SECONDS

FIGURE 47

related studies, we noted, however, that if the equation (2) has approximately correct slope b(T), and since it seems unlikely that the logarithms of PSV amplitudes change with I_{MM} more abruptly for $I_{MM} > 8$ than for $4 < I_{MM} < 8$, that a useful check may be to compare equations (1) and (2) for M = 8.5, R = 0 and for MMI = 12, respectively. Neither of these equations apply for these M, R, and MMI levels since there is no data there. However, the degree of extrapolation for equation (2) is considerably greater in going from the range $4 < I_{MM} < 8$ to $I_{MM} = 12$ than for equation (1) in going from $4 < M < 7$ to 8.5 and from $20 < R < 200$ to R = 0. Consequently, a check for consistency between equations (1) and (2) and especially for the slope b(T) in (2) is to compare the predicted amplitudes in the range for the largest possible levels of shaking. Such comparison is shown in Figures 48 and 49. It shows that the two regression models are not inconsistent for intermediate and long periods. For short periods, equation (2) either overestimates the PSV amplitudes or equation (1) underestimates them. These figures then suggest that the functional form in equation (2) when MMI levels are assigned to the linear numerical scale 1, 2, ... through 12 and where the $\log_{10}$PSV grows linearly with I_{MM} probably lead to a fair estimation of b(T). This further suggests that even if extrapolated to MMI = IX, and perhaps even X, equation (2) might still yield a useful estimate of possible spectral amplitudes.

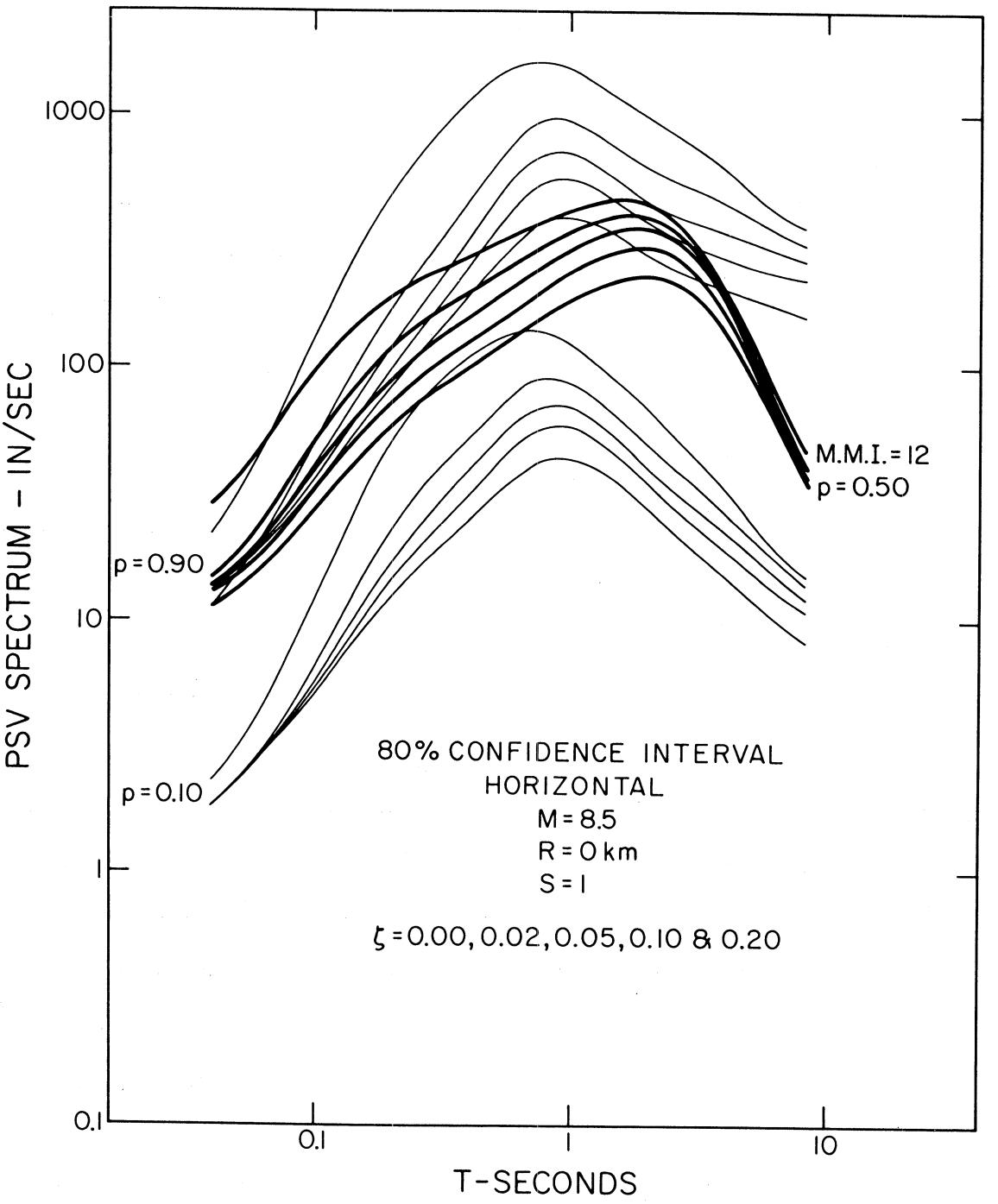
1000
100
10
1
0.1
PSV SPECTRUM - IN/SEC
M.M.I. = 12
p = 0.50
p = 0.90
p = 0.10
80% CONFIDENCE INTERVAL
HORIZONTAL
M = 8.5
R = 0 km
S = 1
ζ = 0.00, 0.02, 0.05, 0.10 & 0.20
0.1
1
10
T-SECONDS

FIGURE 48

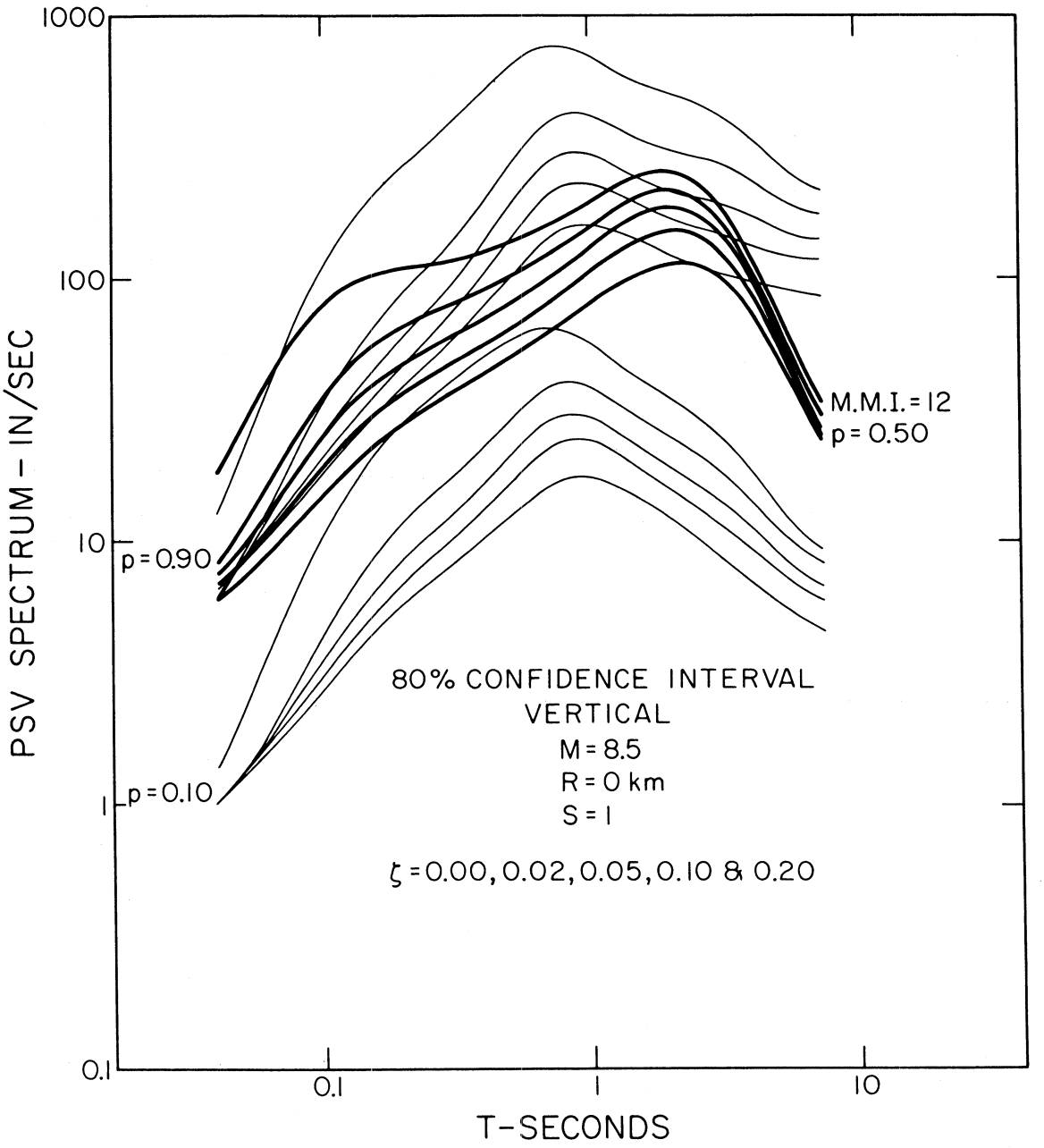
1000
100
10
1
0.1
PSV SPECTRUM - IN/SEC
p = 0.90
p = 0.10
M.M.I. = 12
p = 0.50
80% CONFIDENCE INTERVAL
VERTICAL
M = 8.5
R = 0 km
S = 1
ζ = 0.00, 0.02, 0.05, 0.10 & 0.20
0.1
1
10
T-SECONDS

FIGURE 49

DISTRIBUTION OF SPECTRAL AMPLITUDES

The regression analyses for equations (1) and (2) have been performed in terms of the variable p which was selected to approximate the probability of not exceeding the spectral amplitudes. In these equations, p is not a probability but for $0.1 \leq p \leq 0.9$ it is a linear approximation for the cumulative distribution of data with respect to equations (1) and (2). Figures 50 and 51 show how this approximation has been realized. In these figures, the actual cumulative distribution, p_a, of all available data with respect to equations (1) and (2) have been plotted for 9 values of p. Since this p represents a linear approximation to p_a and following the procedures suggested by Trifunac and Anderson (1977), in this section of the report, we will change the notation and use p_ℓ instead of p.

The amplitudes of p_a versus p_ℓ in Figures 50 and 51 have been computed by smoothing the computed distribution amplitudes for all available data points at 91 periods. These figures can then be used to find the actual distribution functions of data at any period or to interpolate a value of p_ℓ which would yield spectral amplitudes for (1) and (2) that correspond to the desired actual probability, p_a, of not being exceeded. However, for some applications in the computation of seismic risk, for example, it is useful to have continuous analytical relation between p_a and p_ℓ. The purpose of this section is to present such functional relationship.

It has been shown that the distribution of the logarithms of Fourier amplitude spectra can be approximated by a Gaussian distribution function (Anderson and Trifunac, 1978) and that the same assumption is

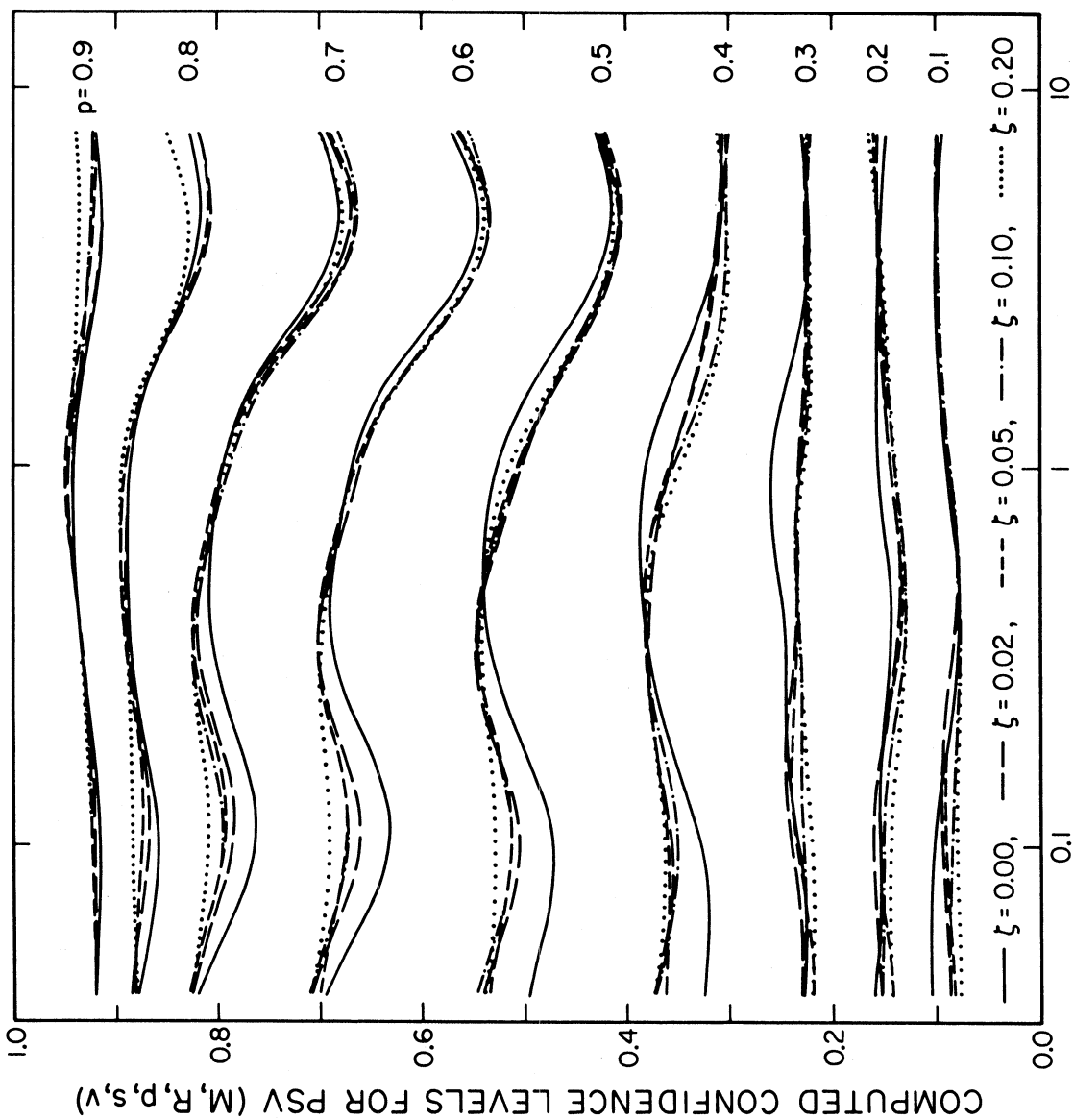
COMPUTED CONFIDENCE LEVELS FOR PSV (M,R,p,s,v)
0.0
0.2
0.4
0.6
0.8
1.0
0.1
1
10
T-SECONDS
p= 0.9
0.8
0.7
0.6
0.5
0.4
0.3
0.2
0.1
ζ = 0.00, ζ = 0.02, ζ = 0.05, ζ = 0.10, ζ = 0.20

FIGURE 50

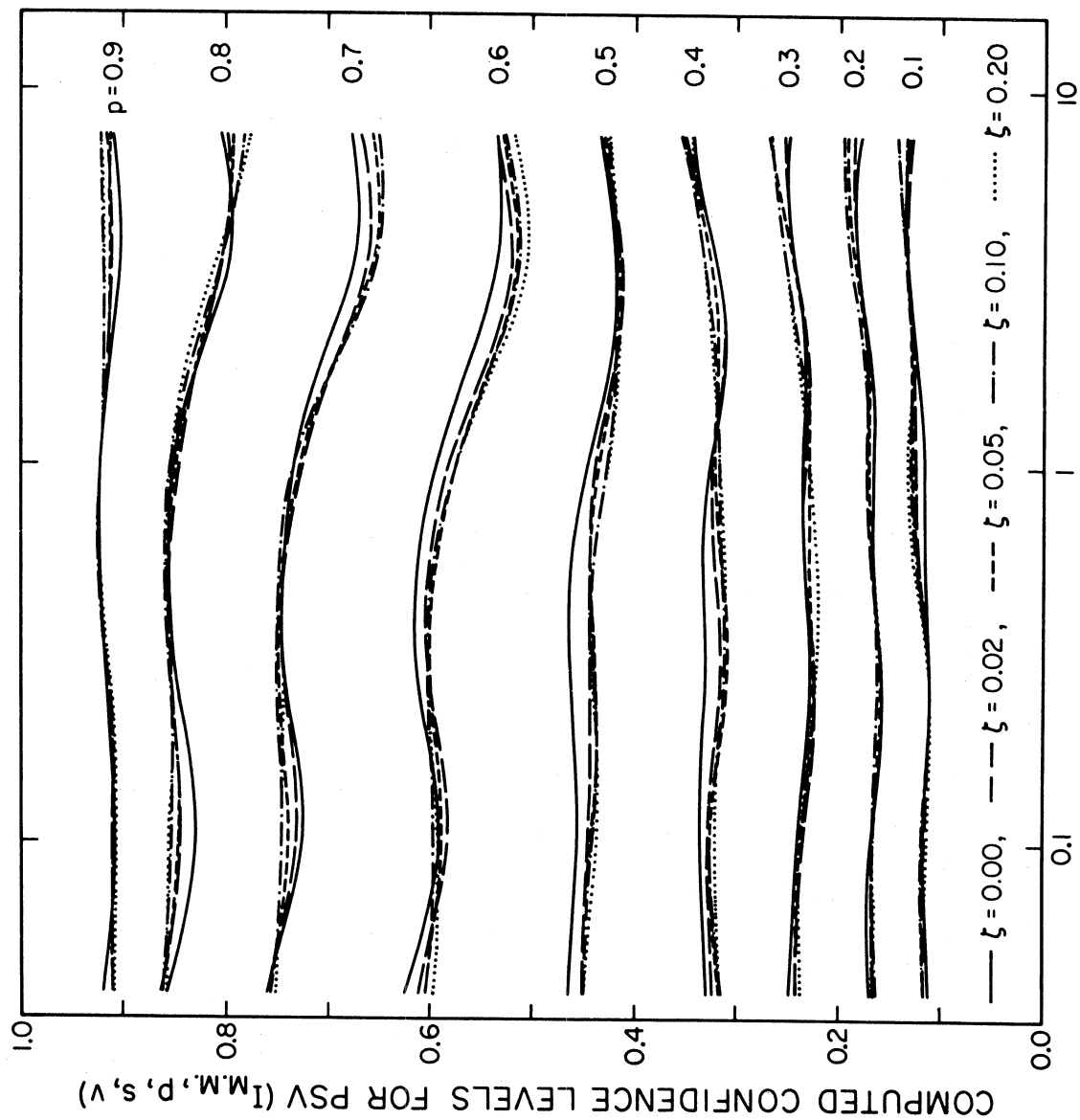
COMPUTED CONFIDENCE LEVELS FOR PSV ($I_{M.M.}$, p, s, v)
T-SECONDS
p = 0.9
0.8
0.7
0.6
0.5
0.4
0.3
0.2
0.1
0.0
1.0
0.1
1
10
ζ = 0.00, ζ = 0.02, ζ = 0.05, ζ = 0.10, ζ = 0.20

FIGURE 51

rejected with a high degree of confidence in similar descriptions of SA (Trifunac and Anderson, 1977). Consequently, to derive a meaningful analytical model for approximate description of spectral amplitudes, in this report we follow the steps proposed for SA spectra. In this approach, it is assumed that, since ζ is small, maxima of relative response follow the Rayleigh distribution. If N(T) is the number of response peaks occurring during the time interval that produces the spectrum amplitudes, then it can be shown (Trifunac and Anderson, 1977) that

$$p_a(T) = [1 - \exp(-e^{\alpha(T)p_\ell + \beta(T)})]^{N(T)} , \qquad (3)$$

where the values for $\alpha(T)$, $\beta(T)$ and N(T) can be chosen on the basis of data in Figures 50 and 51. It can be shown that $\alpha(T)$, $\beta(T)$ and N(T) should depend at least on M or I_{MM}, R, s, and v, and that (3) formally gives the distribution of amplitudes for a single event or a group of events which all have the same parameters. Therefore, (3) may not apply for the entire data set represented in Figures 50 and 51. The calculation of Trifunac and Anderson (1977) and the subsequent results in this report suggest, however, that (3) does represent a useful analytical approximation for the relationship between p_a and p_ℓ. Subsequent Kolmogorov-Smirnov (K-S) and χ^2 tests further suggest that (3) has the capability to describe the data on p_a versus p_ℓ.

To avoid difficult nonlinear fitting procedures we have calculated the values of $\alpha(T)$ and $\beta(T)$ for different values of N(T) ranging from 1 to 1000 and plotted the intervals of N where the χ^2 (Figure 52) and K-S (Figure 53) tests suggest the acceptance of equation (3) at the 95% confidence level. In Figures 52 and 53 the best values of N are

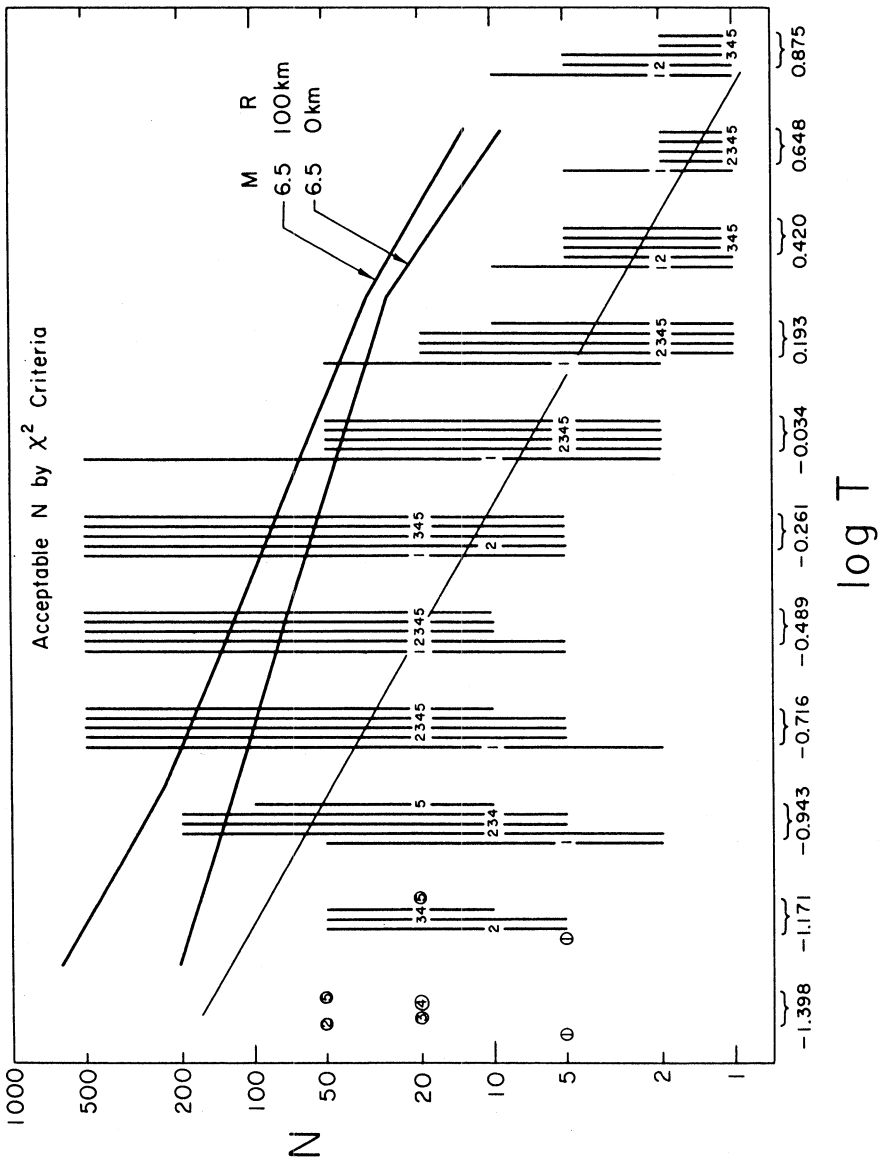

FIGURE 52

Summary of the results of the statistical χ^2 test for distribution of form (3) relating p_a and p_ℓ for the regression of $\log_{10}$[PSV] as a function of p_ℓ, M, R, s, and v. For each of 11 periods, we have plotted an integer (1-5) at the value of N which leads to the smallest value of χ^2. The vertical line shows the range of N which leads to a value of the χ^2 statistic which is small enough that the corresponding distribution is not rejected at the 95% confidence level. Where the integer (1-5) is circled, the best value of χ^2 is rejected. The integers 1-5 refer to the value of damping: 1 for ζ = 0.0; 2 for ζ = 0.02; 3 for ζ = 0.05; 4 for ζ = 0.10; and 5 for ζ = 0.20.

The values of N which might be expected from the results of Trifunac and Westermo (1976a) for a magnitude 6.5 earthquake at 0 km and 100 km are shown. For reasons described in the text, we chose the value of N to be integers approximately equal to the straight line through the data, which has the equation N = 6.5/T.

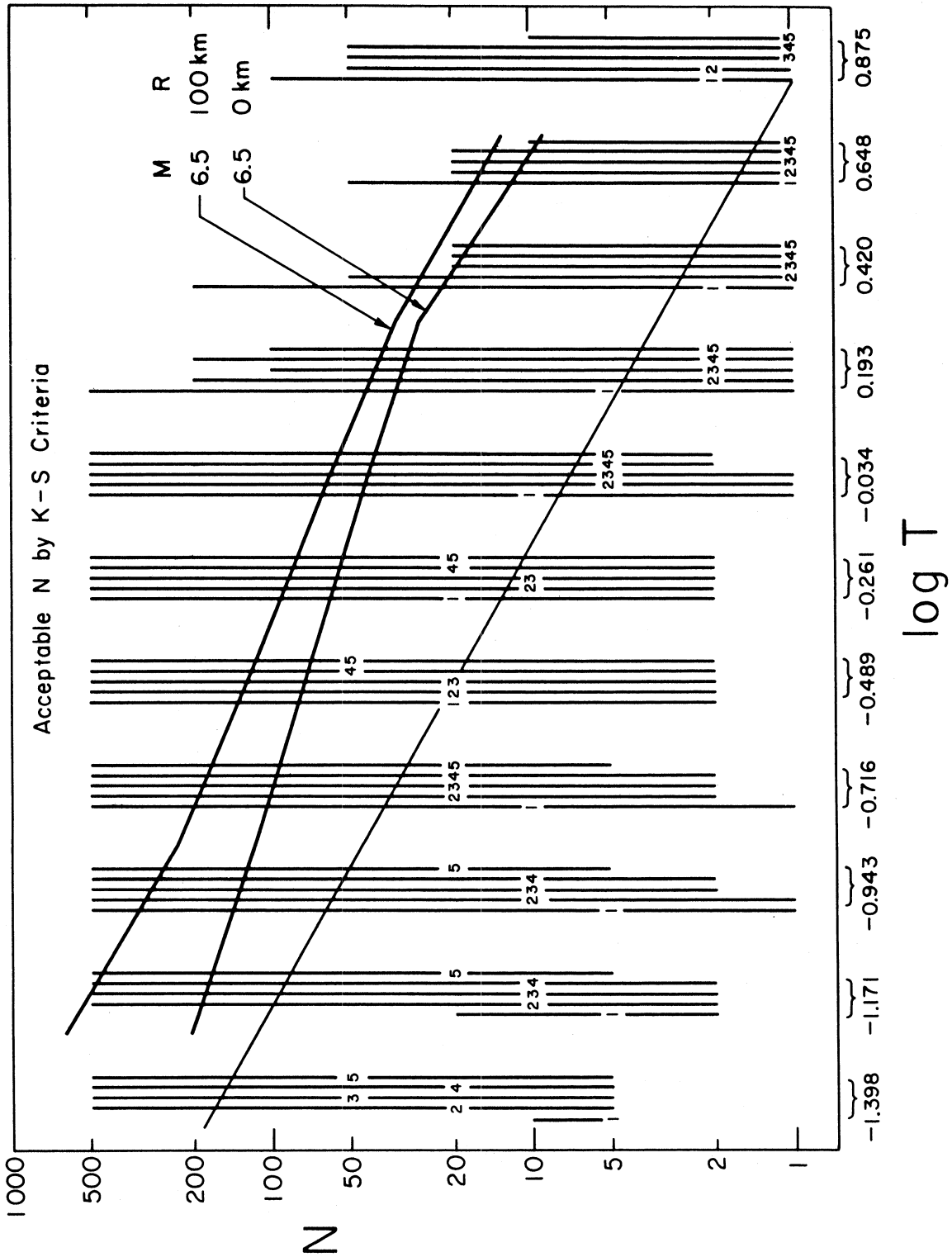

FIGURE 53

Results of the Kolmogorov-Smirnov statistical test to determine which values of N are acceptable to fit the data of p_a vs. p_ℓ for the regression of PSV with magnitude and distance. Other symbols are as in Figure 52.

indicated with numbers 1-5 which also identify the corresponding fractions of critical damping, 1: $\zeta = 0.0$; 2: $\zeta = 0.02$; 3: $\zeta = 0.05$; 4: $\zeta = 0.10$; and 5: $\zeta = 0.20$.

The best values of N(T) in Figures 52 and 53 decrease with increasing period, in agreement with what one would expect if N(T) is twice the duration of strong shaking divided by T. However, the best values of N(T) are considerably smaller than the values of N that would result from the above relation with D computed from the frequency dependent empirical scaling relations for D in terms of magnitude and epicentral distance (Trifunac and Westermo, 1976a). Examples of N computed in this way are shown in Figures 52 and 53 for M = 6.5, and R = 0 and 100 km. The definition of duration in Trifunac and Westermo (1976a,b) is based on the time interval during which 90% of "energy" of strong shaking is recorded at a station. The best value of N in (3) appears to be more sensitive to a shorter time interval which contributes significantly to the maximum response amplitude only. These differences may also result because of the assumption that the theory based on stationary time series can be used to derive (3), as well as because of considerable contributions to the computed durations from processing and recording noise (Trifunac and Westermo, 1976a,b) for long and short frequencies. Since the object of this report is merely to derive a useful analytical approximation for p_a versus p_ℓ and of a form which does not violate a number of simple physical principles which are expected to govern this relationship, we select the approximate relationship $N(T) = 6.5/T$.

With N = greatest integer [6.5/T] and N = 1 when $6.5/T < 1$, the best values of $\alpha(T)$ and $\beta(T)$ have been calculated and plotted in

Figure 54. This figure also presents the mean and standard deviation of the p_a versus p_ℓ distribution and the computed χ^2 and the largest K-S difference versus T for the chosen $\alpha(T)$, $\beta(T)$, and N(T), and for ζ ranging from 0.0 to 0.20. It is seen from this figure that at the 95% confidence level, equation (3) leads to p_a which is not acceptable only for $\zeta = 0.0$ and for short periods $T < 0.1$ sec. For longer periods and higher damping, p_a is accepted at the 95% confidence level.

Figures 55 and 56 present the values of permissible N(T) when equation (3) is applied to the data scaled in terms of MMI. Again, those values of N for which χ^2 and K-S differences are smallest have been designated with numbers 1-5 where 1 corresponds to $\zeta = 0.00$ and 5 to $\zeta = 0.20$, respectively. In contrast with Figures 52 and 53, but similar to Figures 60 and 61 in Trifunac and Anderson (1977), Figures 55 and 56 show that N, computed from $N = 2D/T$, when D comes from Trifunac and Westermo (1976b) and for MMI levels V, VI and VII, is much greater than required by χ^2 and K-S tests. The reasons for this are similar to those mentioned earlier for data in Figures 52 and 53, but may also be related to the fact that the MMI is a function of both the amplitude of shaking and of the duration as discussed by Trifunac and Anderson (1977).

We chose $N(T) = 2$ for $T \leq .4$ sec and $N = 1$ for $T > .4$ sec. With these values of N(T) functions $\alpha(T)$ and $\beta(T)$ and the resulting $\mu(T)$ and $\sigma(T)$ are as shown in Figure 57 and Table IV. The bottom part of Figure 51 then shows that except for some long periods, equation (3) can be accepted with 95% confidence level. The corresponding K-S test suggests that the model in equation (3) is acceptable for all T and ζ.

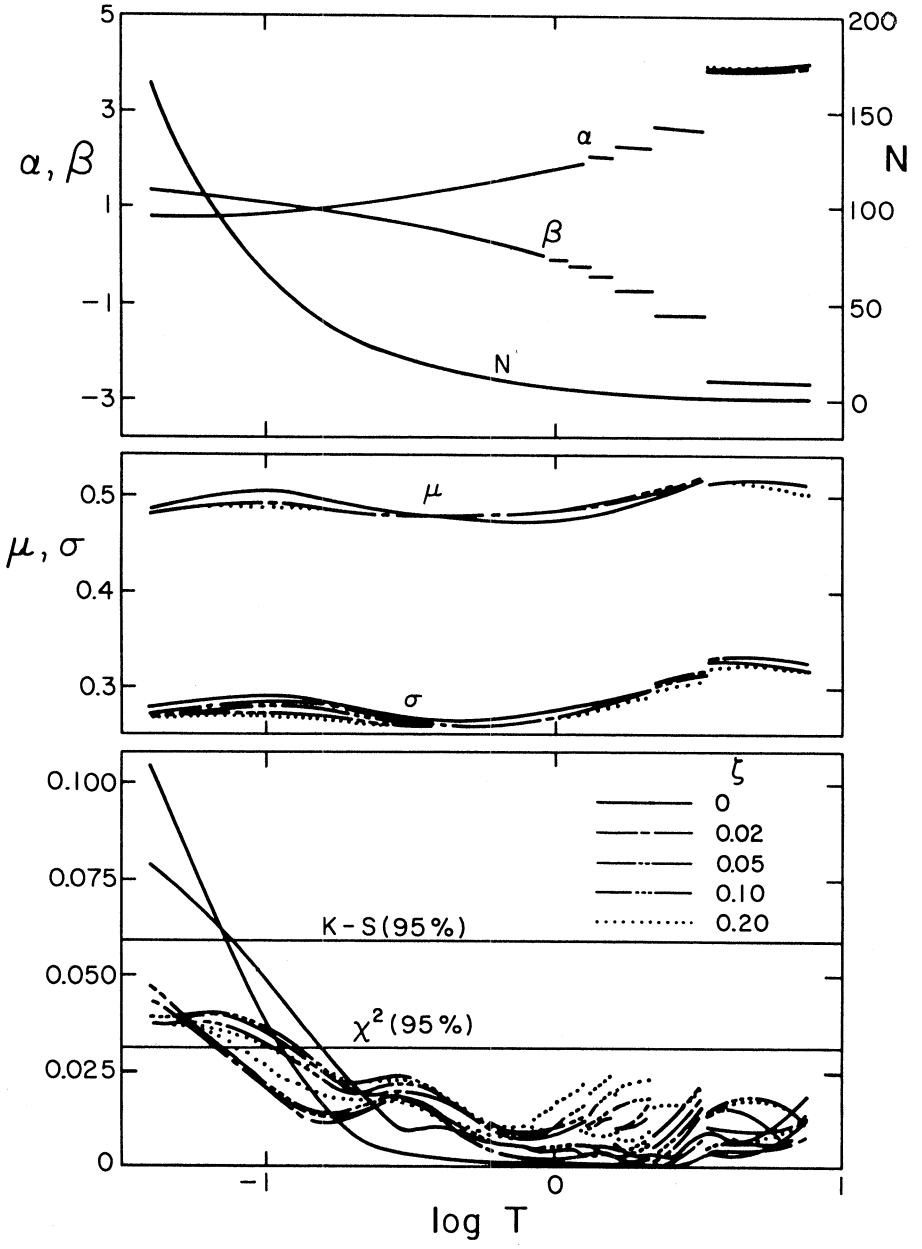

FIGURE 54

Parameters for one set of distributions (3) which approximately give p_a as a function of p_ℓ. The upper curves give α, β, and N (equation (3)). N is quantized, but the individual integers cannot be illustrated on this scale, so N is drawn as a continuous line.

The central section gives the parameters μ and σ derived from α, β, and N using equations (6) through (9) in Trifunac and Anderson (1977). The lower section shows the statistical quality of fit by the Kolmogorov-Smirnov and the χ^2 criteria. The χ^2 test can be recognized by its smaller amplitudes for periods in the central portion of the graph. The levels marked K-S (95%) and χ^2 (95%) are those which, if exceeded, lead to rejection of the assumed distribution at that frequency. The five lines are for the five values of damping, as indicated.

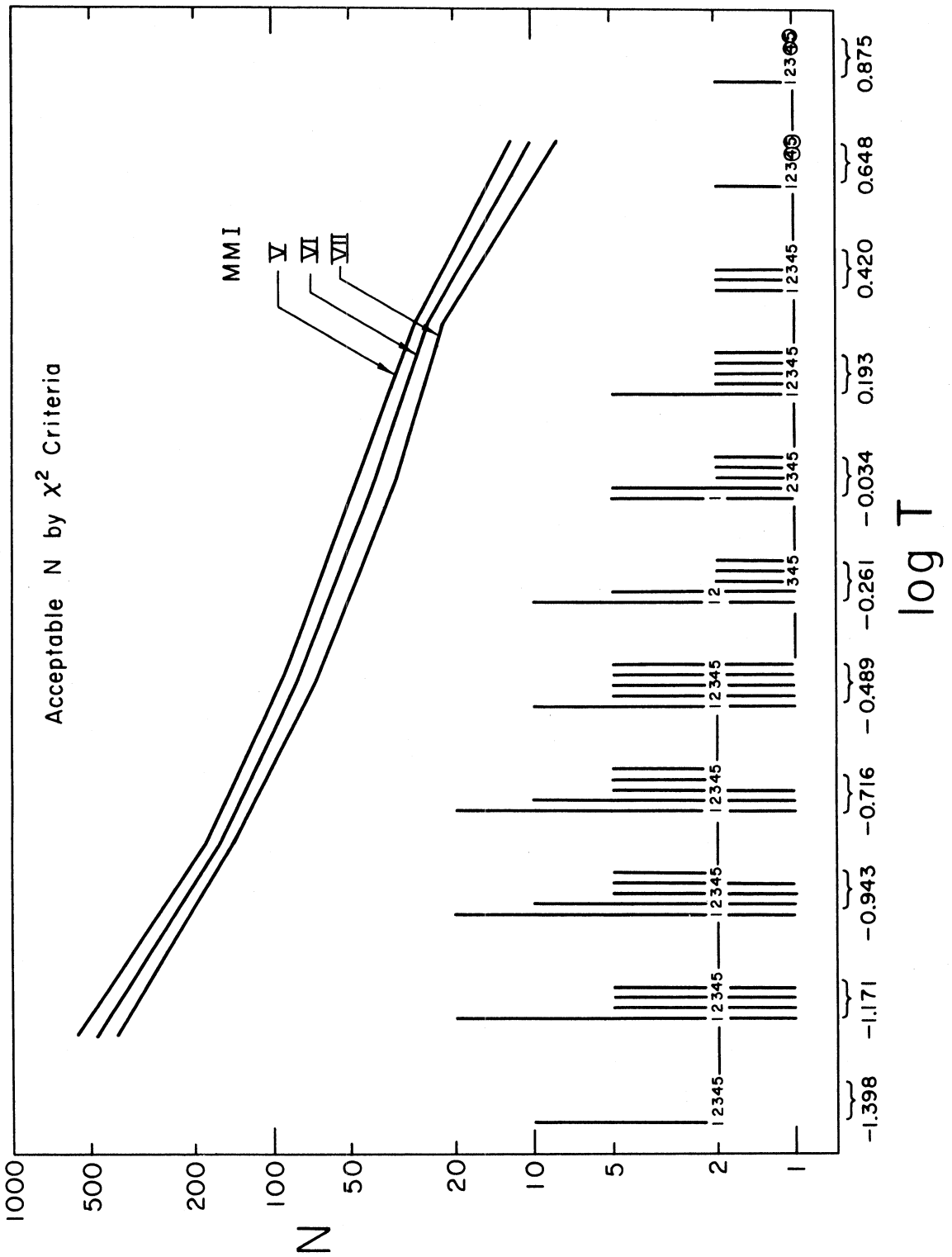

FIGURE 55

Results of the χ^2 statistical test to determine which values of N are acceptable to fit the data of p_a vs. p_{ℓ} for the regression of PSV with Modified Mercalli Intensity. The upper lines show those N which might be expected on the basis of results of Trifunac and Westermo (1976b) for intensity V, VI and VII shaking. For the later regression, we chose the N indicated by the light line. Other symbols are as in Figure 52.

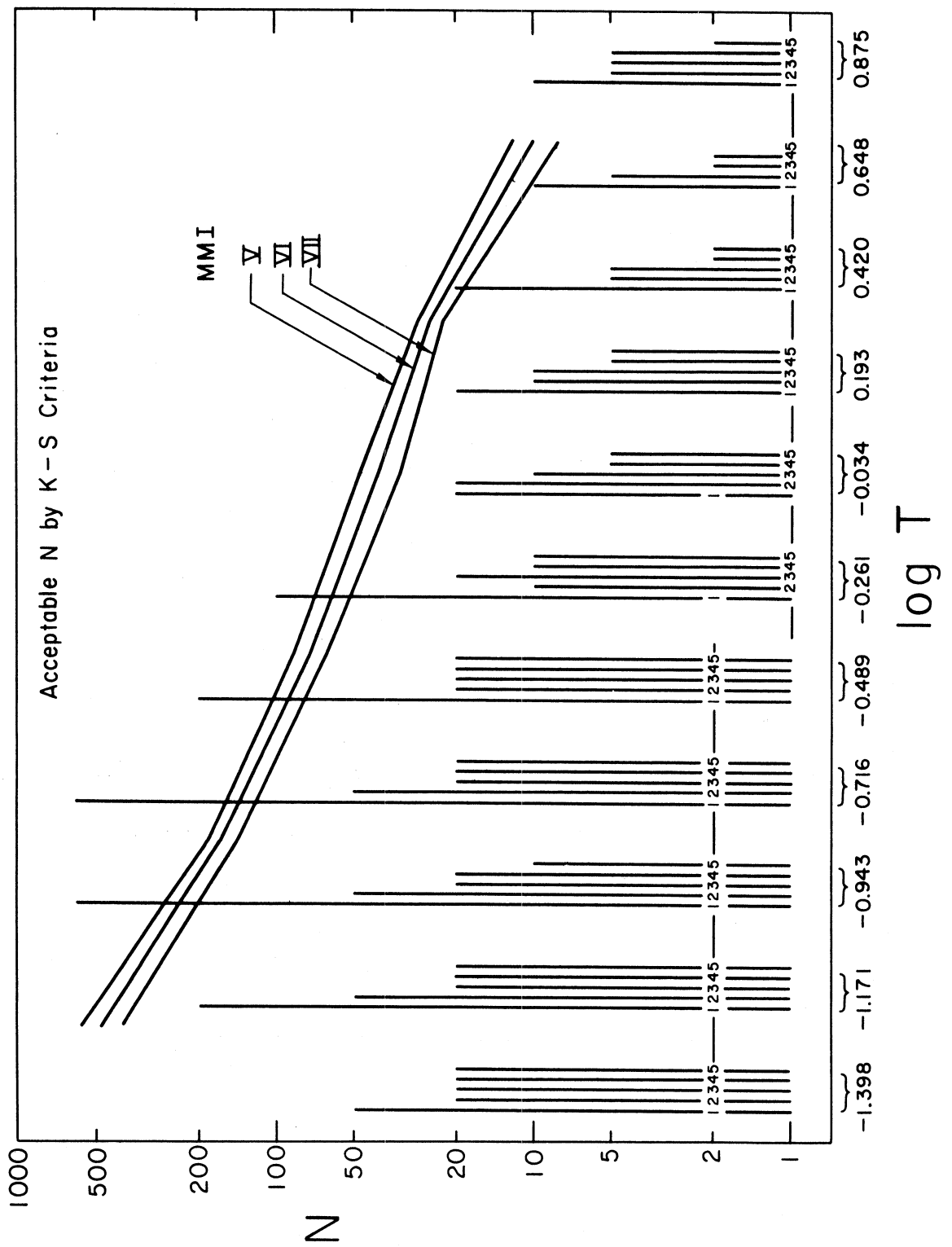

FIGURE 56

Equivalent of Figure 55, except that it shows the results of the Kolmogorov-Smirnov test.

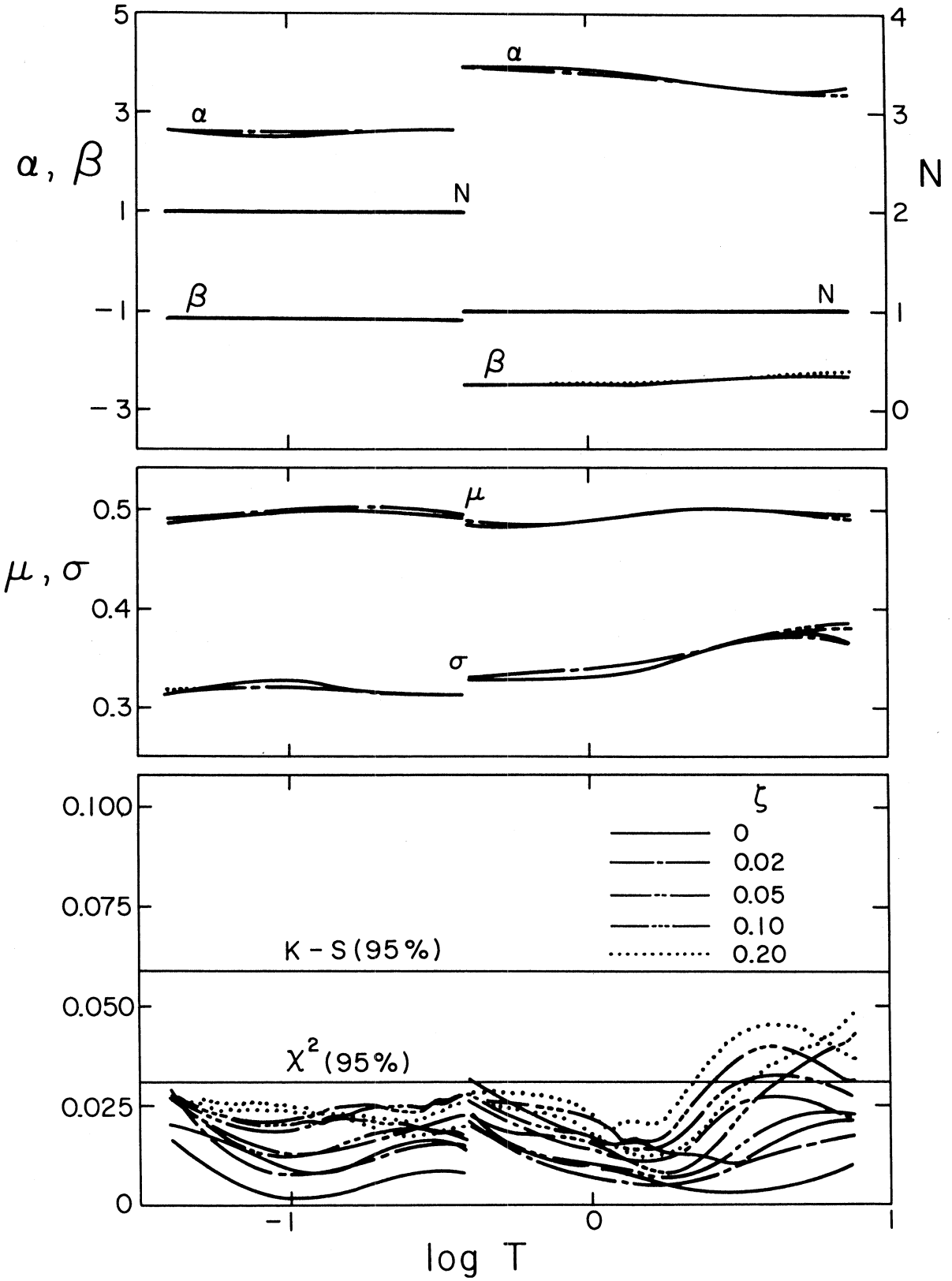

FIGURE 57

Equivalent of Figure 54 for the regression of PSV with intensity

CONCLUSIONS

In this report, we have presented two regression analyses which result in empirical scaling relationships for PSV spectrum amplitudes in terms of either (a) magnitude, M, epicentral distance, R, or (b) MMI at a site. These models have also considered the direction of ground motion for which PSV is calculated, i.e., horizontal (v=0) or vertical (v=1) components, geologic site conditions at the recording station (s=0 for alluvium, s=2 for basement rocks and s=1 for intermediate sites) as well as the distribution of all data about the assumed empirical models.

The data, the method of analysis and the results of this work in many respects duplicate what we presented earlier for scaling of SA spectra (Trifunac and Anderson, 1977). For this reason, the discussions in this report have been kept as brief as possible to reduce unnecessary repetition and to summarize the main results as quickly and as directly as possible. Some repetition, however, could not be avoided since it would have resulted in an incomplete and not a self-contained report. We noted at a number of places in the text, that a more detailed discussion can be found elsewhere. To a reader who is interested in considerable detail, we suggest to study our earlier report on SA spectra (Trifunac and Anderson, 1977) first and then to turn to this report. Mutatis mutandis virtually all details of our earlier report apply here as well.

Essentially all assumptions and regression results in this report are consistent with our earlier findings about Fourier amplitude spectra (Trifunac, 1976,78) and SA spectra (Trifunac and Anderson, 1977). These are:

1. The rate of growth of spectral amplitudes decreases with increasing magnitude.
2. Spectral amplitudes at high frequencies tend to be higher on basement rock sites (s=2) than on alluvium sites (s=0). This trend is consistent in all empirical models studied, so far, but the differences in spectral amplitudes seem not to be significant at high frequencies. At long periods, this trend is reversed and becomes significant.
3. The differences in amplitudes of horizontal versus vertical PSV spectra depend on the period T and cannot be approximated by a constant.
4. The scatter of PSV spectrum amplitudes about the regression model (1) in terms of earthquake magnitude, M, and epicentral distance, R, is not smaller than the scatter of the same amplitudes about the empirical model (2) in terms of MMI.
5. The distribution of PSV spectrum amplitudes about the two regression models (1) and (2) is not inconsistent with the assumed Rayleigh distribution of the peaks of response amplitudes.
6. For the largest possible levels of strong shaking and well outside the range where equations (1) and (2) apply, we found that these two empirical models are consistent.

Finally, it should be noted that, as for other related models, the results of this report should be considered as preliminary since when more abundant and complete data becomes available, it will be possible to develop better, more detailed and more complete empirical scaling methods. In the meantime, the models presented here may serve as an interim basis for estimation of PSV amplitudes and for known or assumed

parameters describing the strong shaking. In deriving these models we made every effort possible to select a model and a method which are most closely related to the physics of the problem. The lack of detailed knowledge on many of these processes and the limited number of data points available have obviously limited our success at the very onset. The large standard deviation of the distributions about the models proposed here reflect these uncertainties. The reader should therefore keep in mind these limitations while using the models presented here.

ACKNOWLEDGEMENTS

This research has been supported in part by a grant from the National Science Foundation and by a contract from the Nuclear Regulatory Commission.

REFERENCES

Anderson, J.G. (1978). Uniform Risk Fourier Amplitude Spectra Derived from Intensity Statistics on Earthquake Occurrence, (in preparation).

Anderson, J.G., and M.D. Trifunac (1978). Uniform Risk Functionals for Characterization of Strong Earthquake Ground Motion, Bull. Seism. Soc. Amer., 68, 205-218.

Housner, G.W. (1970). Design Spectrum, Chapter 5 in Earthquake Engineering, edited by R.L. Wiegel, Prentice Hall.

Hudson, D.E., M.D. Trifunac and A.G. Brady (1972). Strong Motion Accelerograms, III, Response Spectra, Earthquake Eng. Res. Lab., EERL 72-80, Calif. Inst. of Tech., Pasadena.

Newmark, N.M., and E. Rosenblueth (1971). Fundamentals of Earthquake Engineerings, Prentice Hall, New Jersey.

Richter, C.F. (1958). Elementary Seismology, Freeman, San Francisco.

Seed, H.B., C. Ugas, and J. Lysmer (1974). Site Dependent Spectra for Earthquake Resistant Design, Earthquake Eng. Res. Center, EERC 74-12, University of California, Berkeley.

Trifunac, M.D. (1973). Analysis of Strong Earthquake Ground Motion for Prediction of Response Spectra, International J. of Earthquake Eng. and Struct. Dyn., Vol. 2, No. 1, 59-69.

Trifunac, M.D. (1976a). Preliminary Empirical Model for Scaling Fourier Amplitude Spectra of Strong Ground Acceleration in Terms of Earthquake Magnitude, Source to Station Distance and Recording Site Conditions, Bull. Seism. Soc. Amer., 66, 1343-1373.

Trifunac, M.D. (1976b). A Note on the Range of Peak Amplitudes of Recorded Accelerations, Velocities, and Displacements with Respect to the Modified Mercalli Intensity, Earthquake Notes, Vol. 47, 9-24.

Trifunac, M.D. (1977a). Forecasting the Spectral Amplitudes of Strong Earthquake Ground Motion, Sixth World Conf. Earthquake Eng., New Delhi, India.

Trifunac, M.D. (1977b). Uniformly Processed Strong Earthquake Ground Accelerations in the Western United States of America for the Period From 1933 to 1971: Pseudo Relative Velocity Spectra and Processing Noise, Dept. of Civil Eng., Report No. CE 77-04, U.S.C, Los Angeles.

Trifunac, M.D. (1978a). Preliminary Empirical Model for Scaling Fourier Amplitude Spectra of Strong Ground Acceleration in Terms of Modified Mercalli Intensity and Recording Site Conditions, Int. J. Earthquake Eng. and Struct. Dyn., (in press).

Trifunac, M.D. (1978b). Uniformly Processed Strong Earthquake Ground Accelerations in the Western United States of America for the Period from 1933 to 1971: Pseudo Relative Velocity Spectra and Processing Noise, Dept. of Civil Eng., Report No. CE 77-04, U.S.C., Los Angeles.

Trifunac, M.D., and J.G. Anderson (1977). Preliminary Empirical Models for Scaling Absolute Acceleration Spectra, Dept. of Civil Eng., Report No. CE 77-03, U.S.C., Los Angeles.

Trifunac, M.D., and A.G. Brady (1975). On the Correlation of Seismic Intensity Scales with the Peaks of Recorded Strong Ground Motion, Bull. Seism. Soc. Amer., 66, 139-162.

Trifunac, M.D., and A.G. Brady (1976). Correlations of Peak Acceleration, Velocity and Displacement with Earthquake Magnitude, Distance and Site Conditions, International J. of Earthquake Eng. and Structural Dynamics, Vol. 4, 455-471.

Trifunac, M.D., and J.N. Brune (1970). Complexity of Energy Release During the Imperial Valley, California, Earthquake of 1940, Bull. Seism. Soc. Amer., 60, 137-160.

Trifunac, M.D., and V.W. Lee (1973). Routine Computer Processing of Strong Motion Accelerograms, Earthquake Eng. Res. Lab., EERL 73-02, Calif. Inst. of Tech., Pasadena.

Trifunac, M.D., and B.D. Westermo (1976a). Dependence of Duration of Strong Earthquake Ground Motion on Magnitude, Epicentral Distance, Geologic Conditions at the Recording Station and Frequency of Motion, Dept. of Civil Eng., Report No. 76-02, U.S.C., Los Angeles.

Trifunac, M.D., and B.D. Westermo (1976b). Correlation of Frequency Dependent Duration of Strong Earthquake Ground Motion with the Modified Mercalli Intensity and the Geologic Conditions at the Recording Stations, Dept. of Civil Eng., Report No. 76-03, U.S.C., Los Angeles.